NAME OF AUTHOR.....Mr. A. Y. Kandeil.....

TITLE OF THESIS......"On the Compaction of Metal Powders with

Particular Reference to Densification

Hardening"

UNIVERSITY......McMaster University.....

DEGREE FOR WHICH THESIS WAS PRESENTED...Master of Engineering

YEAR THIS DEGREE GRANTED....1975.....

(Signed)..........................

PERMANENT ADDRESS:

1830 Main W. #.201
HAMILTON - ONTARIO
....

DATED...21/11/1974....19

NL-91 (10-68)

INFORMATION TO USERS

THIS DISSERTATION HAS BEEN
MICROFILMED EXACTLY AS RECEIVED

This copy was produced from a micro-
fiche copy of the original document.
The quality of the copy is heavily
dependent upon the quality of the
original thesis submitted for
microfilming. Every effort has
been made to ensure the highest
quality of reproduction possible.

PLEASE NOTE: Some pages may have
indistinct print. Filmed as
received.

Canadian Theses Division
Cataloguing Branch
National Library of Canada
Ottawa, Canada   K1A 0N4

AVIS AUX USAGERS

LA THESE A ETE MICROFILMEE
TELLE QUE NOUS L'AVONS RECUE

Cette copie a été faite à partir
d'une microfiche du document
original. La qualité de la copie
dépend grandement de la qualité
de la thèse soumise pour le
microfilmage. Nous avons tout
fait pour assurer une qualité
supérieure de reproduction.

NOTA BENE: La qualité d'impression
de certaines pages peut laisser à
désirer. Microfilmée telle que
nous l'avons reçue.

Division des thèses canadiennes
Direction du catalogage
Bibliothèque nationale du Canada
Ottawa, Canada   K1A 0N4

ON THE COMPACTION OF METAL POWDERS

WITH PARTICULAR REFERENCE TO

DENSIFICATION HARDENING

ON THE COMPACTION OF METAL POWDERS

WITH PARTICULAR REFERENCE TO.

DENSIFICATION HARDENING

By

ABD EL RAZEK YOUSSEF KANDEIL, B.Sc., Mech.Eng.

A Thesis

Submitted to

The School of Graduate Studies

in Partial Fulfilment of the Requirements

for the degree

Master of Engineering

McMaster University

November, 1975

MASTER OF ENGINEERING (1975)   McMASTER UNIVERSITY
                                   Hamilton, Ontario.

TITLE: On·the Compaction of Metal Powders with Particular
                  Reference to Densification Hardening.

AUTHOR: Abd El Razek Youssef Kandeil, B.Sc., Alexandria
                                                        University

SUPERVISOR: Professors, M.C. deMalherbe, M.A. Dokainish

NUMBER OF PAGES: xiii, 164

SCOPE AND CONTENTS: The purpose of this work was to examine the

process of isostatic compaction of metal powders and the related phenomenon

of densification hardening.

The relationships between density, hardness and compacting

pressure, for different commercial powders, have been obtained. Data result-

ing from the experimental study of isostatic compaction was applied to tests

conducted on die compacts, enabling the density and pressure distributions to

be examined by simple hardness measurements. The compacts were produced

in a range of compacting dies, designed especially for this purpose.

Results of density determination and metallographic examination

of a series of atomized aluminum, copper, lead and reduced iron powder

compacts are presented. From these results it is concluded that extensive

plastic deformation occurs even during the initial stage of compaction.

It has been shown that density and hardness are uniform within

compacts produced by the isostatic method, while the die compacts showed

remarkable variation of hardness and density within the samples. The results indicate the higher efficiency of the isostatic compaction method as compared to the die method.

A method for isostatic pressure measuring and recording, utilizing the expansion of the pressure vessel, is described.

ACKNOWLEDGEMENTS

TABLE OF CONTENTS

LIST OF ILLUSTRATIONS

LIST OF TABLES

1 INTRODUCTION

Powder metallurgy, one of the earliest technologies to appear in the evolution of man, was used by the ancient Egyptians to fabricate implements from sponge iron [1]. Applications of the more recent past were mostly confined to either highly specialized materials such as molybdenum and tungsten, or alternatively to powders used for the fabrication of low-cost cold pressed and sintered parts. Products of the latter variety have found increasing application allowing close control of tolerances, low scrap losses, complex shape designs, and good reproducibility.

The advent of improved atomization techniques for complex alloys has allowed the metallurgical advantages of powder processing over conventional casting and ingot-conversion techniques to be more fully exploited. These advantages are mostly a direct result of the more rapid cooling rate observed in a small metal particle as compared to that in an ingot. The solidification of a large piece of metal leads to a variety of structural flaws, both on a macro and micro scale. It is the uniformity and homogeneity of the microstructure that lends to the powder product desirable mechanical properties with a high degree of reproducibility.

In spite of the long history and increasing application of these processes the basic phenomena of powder compaction are still not well understood. This thesis is concerned with some aspects of the cold compaction

process in both isostatic and die pressing equipment with particular regard to information which may be derived from hardness tests on the resulting compacts. Pressure-density-hardness data obtained from isostatically pressed samples, are used to derive pressure and density distributions from hardness measurements on open and closed die compacts. The results illustrate the feasibility of this technique and facilitate a comparison of the two processes.

The experimental portion of this program was carried out on newly commissioned equipment.

2   LITERATURE SURVEY

2.1   GENERAL

Powder metallurgy is the technology of converting metals in powder form into useful shapes or components. Most commonly the materials are compacted in mechanical or hydraulic die presses at room temperature, although the use of the isostatic compacting process is becoming more widespread. Other powder consolidation techniques such as hot isostatic pressing, isostatic extrusion, roll compacting and high energy rate methods are also used. The green compacts pressed by these methods are normally sintered to produce parts of high strength and density.

The above techniques possess a number of advantages allowing production of complex shapes with tight tolerances and good surface finish in a wide range of materials with relatively low labour and scrap costs. Some parts requiring porosity such as certain filters and self lubricating bearings can only be produced by powder metallurgy.

Major powder metallurgy materials in commercial use today include the following metals: iron, aluminum, bronze, steel, nickel-steel, copper-steel, nickel-silver, stainless steel, brass and tungsten. The characteristics of metal powders are quite different from those of metals in more massive forms.

Other materials which are currently being formed by isostatic pressing include plastics, ceramic materials, carbon, refractory metals,

nuclear materials, in fact almost any material which can be produced in powder form. The applications are as varied as the materials, ranging from nuclear fuel elements and ablative ceramic nose cones, to the widely known glazed clay sewer pipes and television tubes.

For the majority of components manufactured by the powder metallurgy route the principal stages involved during manufacture are:

1. Powder preparation and mixing

2. Consolidation of the powder

3. Sintering of the compact

Powders may be broadly classified into either metallic or non-metallic. The behavioral patterns during compaction of powders may be quite different due to differences, primarily in:

a. Mechanical properties e.g. hardness, plastic behaviour and rates of work hardening.

b. Chemical bonding between particles.

c. Surface effects, e.g. friction, adhesion, adsorbed layers.

Other but equally important factors, not wholly connected with intrinsic powder properties, which influence consolidation are particle packing, interparticle friction, transmission forces and bonding between particles.

d. Geometric factors e.g. size, shape, surface area and distribution of the powder particles.

e.   The use of additives or lubricants with the powder.

f.   Mode of compaction e.g. whether pressing is applied uni-

directionally or, hydrostatically.

Isostatic pressing is a means of forming compacts from powdered

material by the application of a uniform pressure on all surfaces of an elasto-

meric form or mould.   As a basic process it dates back to 1913 when the

Westinghouse Lamp Co. was granted a U.S. Patent [2].   Its utilization, how-

ever, in routine production processes is extremely new since there have been

recent advances in metallurgical technology and high-pressure techniques, which

have made it possible to design economical pressure vessels and pressure

generators for this process.   In fact, we are just now witnessing the transition

from a laboratory to a production tool.

The reasons for isostatic pressing are manifold.   In some cases isostatic

pressing is the only feasible way to make a compact of the materials.   In

others it permits the manufacture of complex shapes with little waste of

expensive raw material and/or minimum costly machining processes.   Still other

reasons include improved dimensional control of compacts, more uniform density,

hi;her 'green strength', and the elimination of expensive mechanical presses.

The basic isostatic pressing process can be carried out with extremely

simple equipment.   A rubber or other flexible elastomeric mould is used.   This

mould is geometrically similar to the desired shape, but enlarged by an amount

which is determined by the compressibility of the material.   This explains the

complexity of shapes which can be isostatically pressed. Configurations are limited only by the imagination of the designer and the ability to remove the compact from the elastic mould.

A normal wet-bag mould consists of an elastic mould, mostly of rubber with a rigid metal support. The mould is filled with powdered material and then sealed. It is placed, with the support, into a pressure vessel filled with fluid, a mixture of water and rust inhibitor. After undergoing a cycle of pressurization the mould is removed. The powder will have been compacted in the sealed mould. In many applications it is necessary to remove substantial quantities of air prior to starting compaction. This is accomplished by evacuating the mould, using conventional vacuum pump equipment. After compression the compact is removed from the mould and will be substantially the same shape as the mould, but reduced in size.

Equipment for carrying out this process, generally referred to as the 'wet-bag process', consists of a pressure vessel of a size sufficient to contain the assembled elastomeric tooling, a pumping system to develop the required pressure and a control system. The controls are generally manually operated.

In a paper by Gripshover [3], a comparison is presented between conventional and hydrostatic pressing of metal powders. The uniaxial die pressing is shown as exhibiting some limitations for the process engineer; (1) the geometry of the piece in question must be such that closed die pressing is possible, (2) the length-to-diameter ratio of the compact is very limited,

normally to a maximum value of between 1.5 and 1, (3) the density of die

pressings is not uniform, and (4) die cost may be excessive for certain

geometries, short runs of parts, and hard or abrasive powders.

The limitations discussed above indicate why other powder-metallurgy

processes such as hydrostatic pressing are important. The limitation of geometry

in die pressing is rather obvious. The prime consideration must be ejection

from the die after pressing. The limitation on the length-to-diameter ratio

results from the inability to transmit the applied pressure through the powder

column because of frictional losses among the powder, punch, or die wall.

Fracturing and severe density gradients are often the results in these cases.

Density gradients are a problem because they lead to non-uniform dimensions

and properties throughout the final structure. This is especially true in large

pressings where small differences in density may result in large dimensional

differences after sintering.

The limitations of conventional die pressing can often be overcome by

applying hydrostatic pressing techniques. Illustrations are provided in reference

[3] which graphically demonstrate the basic differences between die and hydro-

static-pressing methods as well as their relative effects on the resulting micro-

structures, dimensional tolerances and properties. Figure (1) presents a

schematic comparison of hydrostatic and die pressing. The significant differences

are that no die is required in hydrostatic pressing and pressure application is

omnidirectional. Because of these two basic differences, any geometry can

be prepared by hydrostatic pressing. Since die friction is eliminated, large length-to-diameter ratios can be pressed without failure, and uniform density can be achieved throughout the pressing. Hydrostatic pressing is particularly well suited for large components and those having high surface area-to-volume ratios such as hollow cylinders and cones. In such components, substantial, input-materials savings can be achieved when compared with many other fabrication approaches.

Hydrostatic pressing is not without its limitations. In general, only one surface can be pressed to finish size in complex pressings; some finish machining will be required on the other surfaces. Further, the production rates of components made by hydrostatic pressings are generally lower than those for conventional pressing and that naturally implies increased cost. Future applications of both processes will expand rapidly. The introduction of automated equipment may make hydrostatic pressing more competitive for smaller components. As part size increases, however, press capability for die pressing will become a severe limitation and hydrostatic pressing will become an important manufacturing process.

As a first step towards the overall study of compaction and irrespective of the material type, considerations should be made of the initial packing and formation of the powder particles which are not subjected to any application of pressure.

The initial or loose stacking of a powder depends on its physical

characteristics and the features of the die geometry. This initial stacking

will greatly influence the degree of compressibility of the powder. A loosely

packed powder mass will in many cases consist of randomly arranged particles

which are either irregular in shape or varied in size or possibly both [4].

The porosity of this loose mass, expressed as a space fraction not occupied by

particulate material, of the total volume of the powder mass may be well

defined geometrically and easily measurable, though the pore size distribution

even for mono sized and uniformly shaped particles may be less readily

measurable. Even more difficult to assess is the specific surface of the powder

particles which is a measure of the ratio of internal surface to the bulk volume.

In practice powder consists of a finite size distribution and calcula-

tions have been made based on introducing smaller particles into the inter-

stices of a system of larger particles without increasing the overall volume of

the bed. A review was published by P.J. James [4], discussing the pertinent

factors concerned with the consolidation of powders.

Beddow [5] indicated that particle rearrangement is an important

factor during the early stages of compaction of a metal powder, particle

attrition, fracture, and deformation must also play an important role in the

process.

In one of the first important studies concerning metal powders

reported in the literature the experimenters observed the compaction behaviour

of spherical copper powder in a steel die. It was noted that the initial

volume change, i.e. at the commencement of pressing was relatively much

greater than the volume changes occurring towards the end of the pressing

operation. The curve of volume change versus compaction pressure was divided

into two sections corresponding to the so called initial and second stages of

compaction. It was reasoned that the primary mode of particle movement dur-

ing the initial stage of compaction is one of rearrangement of individual par-

ticles into a more dense packing order, while the second stage corresponds to

densification primarily resulting from particle deformation.

The green strength of a cold-pressed powder compact is an important

property, since most industrial processes necessitate a certain amount of handling

before hot sintering. In 1973 Stromgren, Astrom, and Easterling [6] published

a paper discussing the effect of interparticle contact area on the strength of

cold-pressed aluminum powder compacts. Their measurements of the tensile

strength of spherical cold-pressed aluminum powder, pressed to various densities

up to the theoretical maximum, indicated that compaction is a two-stage process.

At some high, intermediate pressure, interparticle sliding occurs in a way which

does not itself increase densification but facilitates further deformation. They

suggested that the pressure at which this sliding takes place is dependent on

the work-hardening rate of the powder as well as the powder size and morphology.

It was also concluded that the strength of a green compact is dependent

upon the interparticle metallic contacts made during compaction. However,

the green strength was well below that of wrought aluminum, probably

due to the presence of broken-up oxides, which act as stress-concentrators at the interparticle boundaries.

2.2 PRESSURE-DENSITY RELATIONSHIPS

One of the most important problems of the theory and practice of pressing powders is the establishment of the relationship between the compacting pressure and density of the compact. Usually, this relationship is expressed in the form of a polytropic, exponential, or logarithmic equation.

In all, some tens of pressing equations have been proposed by various authors, although a few of them can be reduced to the same form of expression [7]. The majority of these equations were obtained as a result of mathematical processing of experimental data and can therefore be expected to describe, more or less accurately, the pressing of similar powders under the same conditions.

Most of these equations have been discussed fully in a recent review [8]. This work covers low pressure isostatic compaction, die compaction and other related areas. The author concluded that the compaction process may be considered as consisting of several different stages in which different compacting mechanisms operate, though the limits of the stages need not be well defined, and more than one mechanism may be operative at any instant. Also, they suggest that the harder or stronger the powder particle, the lower the compression for a given pressure, or the higher the ultimate porosity. They further concluded that the effect of particle geometry on the actual value of the density is generally as follows: Mixed sizes of particles give a higher apparent density

as the smaller particles fill the voids between larger ones, and uniform particles

tend to produce the same apparent density if their surface development is the

same. A higher apparent density generally produces a higher density for a

given pressure and powder type, but this has not been confirmed for many powder

types and mixtures of sizes and geometries.

It was suggested in [8] that among many and varied formulae that have

been proposed relating compaction pressure and density, only three main types

seem worthy of consideration. Initially, the polytropic type due to Balshin [9],

which appears to give good agreement with experimental data for certain

materials in the first and second stages of compaction. It does not, however,

give good agreement at high pressures. The second relationship is the one in-

cluding the equations due to Shapiro and Kolthoff [10], Konopicky [11],

Torre [12], Heckel [13] and Kunin and Yurchenko [14] which may be written:

$$\ln \left(\frac{1}{1-D}\right) = KP + A \qquad (1)$$

where:

D = relative density of compact
K, A = constants
P = compacting pressure

Hewitt et al [8] observed that while equation (1) appears to give good agree-

ment with experimental data in the second stage of compaction, it overestimates

the experimentally determined density at high pressures. They suggested that,

this phenomena was a result of the effects of work hardening.

In 1961, Heckel [15] developed a method of obtaining density-pressure relationships from very low compaction pressure up to about 7700 bar. The method was designed to eliminate the shortcomings of earlier techniques of density measurements. He used the fact that the linear movement of the punch during a single die compaction could be used to calculate the change in volume of the powder as a function of pressure. He tested the accuracy of his method by compacting various grades of iron, copper, nickel, tungsten and steel (SAE 4630) powders. It was concluded that the initial curved region of a plot of $\ln (\frac{1}{1-D})$ vs P is associated with the densification which takes place by a mechanism of individual particle movement in the absence of interparticle bonding. It was also found that the transition from curved to linear behaviour in the powders used, corresponded closely with the minimum pressure necessary to form a coherent compact. Therefore it was concluded that the densification represented by the linear region of a plot of $\ln (\frac{1}{1-D})$ vs P occurred by plastic deformation of the compact after an appreciable amount of interparticle bonding had taken place.

In a second paper, published in 1962, Heckel [16] modified equation (1) and suggested that densification of powders could be analyzed as a three-stage process in terms of the expression:

$$\ln (\frac{1}{1-D}) = KP + \ln (\frac{1}{1-D_o}) + B \qquad (2)$$

where:

D_o : relative density of loose powder at zero pressure

B : increases from 0 at P = 0 to a constant value at the end

of the second stage of compaction. He defined the first stage of compaction as the filling of the die and the density here is indicated by D_0. It can be shown that D_0 is primarily a function of the geometry of the powder particles, decreasing with increasing particle size. The second stage is characterized by individual particle movement and rearrangement at low pressures before inter-particle bonding becomes appreciable. The third stage is characterized by the proportionality of the rate of change of density with pressure and the void fraction of the compact. Also, he made a correlation between K and the yield strength of the metals investigated. He approximated the relation by:

$$K = \frac{1}{3\sigma}$$

(3)

where σ is the yield strength of the material.

The expression relating pressure and density of the compact was further developed by Heckel [16], when he noted that increases in D_0 were almost always accompanied by decreases in B. In general he found that:

$$\ln \left(\frac{1}{1-D_0}\right) + B = A$$

(4)

was approximately constant for many powders. He normalized density-pressure data for different powders to a common set of axes by plotting relative density D against reduced pressure $\frac{P}{3\sigma}$.

In 1963 Shapiro [17] published a detailed study of the compressibility of powders. He investigated different types of powders, ranging from plastic to brittle, to determine their compressibility and the mechanism by which

compaction was achieved. He kept the particle size fairly uniform both within

a sample and between different powders. He concluded that powder compaction

takes place via plastic deformation for plastic type powders, or via fragmenta-

tion for brittle powders, or via a combination of the two. Shapiro suggested

that, for plastic materials within a pressure range up to 6200 bar, the pressure-

porosity relationship could be expressed by equation (1), while for other

materials, two terms of the general equation,

$$H = \sum_i a_i \, e^{-K_i P} \tag{5}$$

are required.

In 1963 Kunin and Yurchenko [14] proposed a formula relating

compacting pressure and density of the compact. They compacted bismuth,

cadmium, copper, tin, zinc, iron, aluminum (dust), graphite, sulfur, and rock

salt as well as the K-18-2 compacting powder, at pressures ranging between 0

and 3300 bar. Powders were compacted in a universal testing machine and

density was determined by hydrostatic weighing. They examined the effect of

pressure on the coefficient of compaction and it was possible to divide schemat-

ically the whole densification process into three regions of compacting. The

first region is characterized by the particles being brought closer together and

densified without undergoing deformation. The second region was characterized

by the particles undergoing brittle and plastic deformation and flowing past one

another. In the third stage, bulk compression of the resultant compact body

takes place.

In 1964 a further paper published by Kunin and Yurchenko [17], compared their pressing equation to those proposed by Balshin, Konopicky, Torre, and polytropic equations of the type

$$P \ D^n = C \tag{6}$$

where: n, c are constants

They concluded that not a single one of the existing pressing equations encompasses completely the entire range of pressures and densities, and they regarded the selection of one or another formula as an empirical determination for each powder and compacting condition.

In 1964 Greenspan [18] isostatically compacted beryllium, iron, copper and aluminum powders using pressures up to 11200 bar. He observed that the order of easiest pressing for the materials investigated was aluminum, copper, iron and beryllium and that the end point porosities (at 9400 bar) were of the order of 1%, 4.2%, 7.4% and 8.6% respectively. He expressed the porosity-pressure data in terms of equation (1) suggested by Shapiro [10] and others i.e. as a plot of $\ln \left(\frac{1}{1-D}\right)$ vs pressures and observed that the results were represented closely by two straight line segments. Greenspan [18] suggested that strain hardening effects might be important with respect to the change point. He showed the influence of strain hardening by interjecting a stress annealing operation on the pressing cycle; beryllium compacts initially pressed to 8.0 – 9.5% porosity, stress annealed and pressed again at the same pressure

were densified further to a porosity of 2.7 - 3.3%. He repeated the entire cycle and produced further densification to about 1 - 1.6% porosity.

In 1967 Savin and Ukhina [19] proposed an analysis of the results of pressing various nickel powders with the use of the equations of Balshin [20], Lipson [21] and Kunin and Yurchenko [17]. He found that compaction of different nickel powders during pressing in the 290 - 4900 bar range could not be described by any one of the investigated equations of pressing.

Meerson, Islankina, Mel'nikov and Gol'dman [22] investigated the hydrostatic compaction of stainless steel powder. They compared their experimental results with compaction in both single and double acting dies. They observed that to produce compacts of a given relative density, the pressure used in hydrostatic compaction is about 1.5 to 2 times lower than that required with a double action press and as much as 3 times lower than with a single acting press.

In 1974 Tomlinson, Hewitt and Venter [23] published a paper describing compaction work performed at very high pressures (up to 40000 bar). They presented pressure-density results and hardness measurements for a hard nickel-base superalloy together with scanning electron micrographs of the compacted particles. The compaction was performed in a single-acting piston-cylinder arrangement and a continuous pressure-density curve was determined using the method proposed by Heckel [13]. Even at 40000 bar the powder reached only 94% of its theoretical density, and was not sufficiently consolidated to permit

any but the most delicate handling.

They observed that the compact expands when ejected from the die because of elastic recovery. By compacting iron and copper to 40000 bar and by direct measurement of the diameters of these materials, they found that there was a nearly linear variation of the diameters of these compacts with pressure up to a point where the hardness of the compact was no longer increasing. They explained this as, when the pressure is raised, the yield strength of the powder increased as evidenced by the increase in hardness, and so the amount of elastic recovery increases. Also, they observed that micro and macro examination of the compacts revealed little evidence of interparticle bonding, and what little green strength was developed was primarily due to shearing at the edges of the compact due to motion within the die.

Comparing the hardness of the powder after compaction with those obtained by isostatic compaction, they suggested that at relatively low pressures (14000 bar), isostatic compaction may be 50 to 100% more efficient than die compaction, but at much higher pressures (40000 bar) the two methods are very similar. However scattered values were obtained in this investigation and it seems that these efficiency values depend upon the properties of powder and the compacting condition.

They plotted the density data as $\ln(\frac{1}{1-D})$ versus pressure and they found that this plotting qualitatively confirmed a recent theory that the transition from stage 1 to stage 2 compaction occurred when the compaction pressure

exceeded the current flow stress of the powder, i.e. when plastic deformation became homogeneous instead of local.

In 1973 Beddow [5] determined the pressure-density curves for three copper powders using a small hydraulic compaction device. He concluded that the value of the tap density can be used to indicate the end of the initial stage of compaction of a metal powder. He suggested also, to re-examine the concept that particles mainly tend to relocate in the powder mass during the low pressure portion of the compaction process.

In 1973 Hewitt, Wallace and deMalherbe [24] modified Torre's model of a hollow sphere subjected to external pressure to cover strain-hardening of the material and they accurately predicted the compaction behaviour in the second stage of compaction. However, they concluded that the strain-hardening characteristics of the material do not cause the curvature observed in the third stage of compaction. They found that the $\ln\left(\frac{1}{1-D}\right)$ vs pressure curve for Atomet 28 iron powder exhibits the three characteristic regions observed by other investigators for a variety of materials. They observed a rapid increase in $\ln\left(\frac{1}{1-D}\right)$ with pressure in the first region (0 to $\sim$2800 bar), from 2800 to 10000 bar there was an almost linear variation, while above 10000 bar the slope decreased rapidly.

Hewitt, Wallace and deMalherbe [25] reviewed some opinions on the role of plastic deformation in powder compaction. They presented results of mechanical testing, metallographic examination, and x-ray-diffraction analyses

of some atomized iron powder compacts, together with some metallographic examination of compacted spherical high-temperature, high-strength alloy powders.

They observed that extensive plastic deformation can take place during the first stage of powder compaction. Also, they concluded that plastic deformation always occurs during consolidation, though it does not always cause consolidation. They suggested that consolidation is a result of both mechanical interlocking and associated frictional welding due to surface shear deformation caused by asymmetrical loading. Thus, it was difficult to achieve consolidation in spherical powders even after considerable plastic deformation. They concluded that transition from stage 1 to stage 2 of compaction occurs when the pressure exceeds the bulk yield stress of the material, i.e. when plastic flow becomes homogeneous instead of local. Thus, any model of compaction assuming homogeneous plastic flow can become valid only at the beginning of stage 2.

In 1974 Bondarenko, Dzhamarov, and Baidenko [7] published a discussion of the application of theoretical pressing equations to the hydrostatic densification of hard-alloy mixtures. They utilized some of the pressing equations proposed by various authors to describe the densification behaviour of VK 15 hard-alloy mixtures without a plasticizer and with a 0.75 wt % addition of synthetic rubber. Pressing was performed in a hydrostatic apparatus over the presssure range 300-1200 bar. They concluded that the equation of Bal'shin afford the most accurate descriptions of the compaction of hard-alloy mixtures.

It can be seen that no single formula which has been proposed to describe the pressure–density relationship for powders appears to give satisfactory agreement with experiment for all pressures and all materials. It should also be noted that there exists virtually no theoretical justification for any of these formulae. There would thus appear to be considerable scope for future work in the analysis of the compaction process.

2.3   PRESSURE AND DENSITY DISTRIBUTION IN DIE COMPACTION

In 1947 Kamm, Steinberg, and Wulff [26] were the first to investigate quantitatively the distribution of density in powder compact as a function of pressure, height, and diameter of the die etc. They used a deformable lead grid within the powder in order to ascertain the density gradients in cold pressed metal powders. They pressed the compact in cylindrical dies and the ejected compact was radiographed. From the radiograph, density and deformation from point to point was readily measured. Strain and stress trajectories were also determined. Their experiments were carried out using carbonyl iron powder (type L, General Aniline and Film Co.), and pressures of 2250, 5500, 6750 and 9000 bar were used.

They concluded that the use of a deformable lead grid within powdered-metal compacts gave very satisfactory results for the measurement of density distribution. Also, they observed that the densest part of a compact pressed from one side is at the outer circumference at the top (near the movable

plunger), and the least dense part was at the bottom (near the immovable plunger) at the outer circumference. Frequently the density on the axis of a cylindrical compact was less at the top than at the bottom. Also, they concluded that friction on the side walls of the die was a controlling factor in the irregularity of the density distribution, hence, side-wall lubrication would appear to be of greater importance than interparticle lubrication.

. In 1949 another paper was published by Kamm et al [27] further developing the lead grid method described in their previous paper. They found that circular-hole grids could be more accurately made and, when deformed within the powder, more readily measured and analyzed. They repeated most of the former work and new results including the effect of lubrication, compact height, pressure, and speed of pressing were obtained.

They observed the importance of adequate lubrication in achieving maximum average density and uniformity of density distribution in metal powder compacts. For relatively hard powders such as nickel and iron the speed of pressing, pressing from both sides and vacuum pressing, appeared relatively unimportant as compared to adequate die wall lubrication in obtaining maximum density and uniformity of density. For softer powders they observed that simultaneous pressing from both ends did serve a useful purpose in achieving a more uniform density distribution especially in the pressing of longer compacts. Also, they concluded that the harder metals such as iron and nickel were less sensitive to pressing speed change than the softer ones such as tin.

Their results on vacuum pressing indicated that not much could be gained by this technique in the pressing of relatively hard powders such as nickel. In the pressing of copper powders a higher density was achieved by pressing in a vacuum but not enough to warrant the added complexity of the method in industrial operation.

They concluded also that there was no lateral movement of powder during compression in a cylindrical die and that the powders travelled straight downward while being plastically deformed. A slight lateral movement was found however in compacts pressed at very high pressure without lubricant.

The lead grid method has one serious shortcoming; namely, that it does not permit the determination of deformation and density immediately adjacent to the die wall.

In 1956 Kuczynski and Zaplatynskyj [28] published a technical note describing a new method which makes it possible to determine the density distribution in green powder compacts with the same accuracy as the lead-grid method but which is far simpler and faster and requires only standard laboratory equipment. Instead of using a lead grid, the hardness at selected points of the sectioned compact was determined. The relationship between hardness and density was found by measuring hardness and densities of thin compacts, assuming that, in such compacts, the density for all practical purposes was constant throughout. They tested the method on a Plast nickel powder, grade FIA-A20 and the results obtained confirmed the findings of Kamm, et al [26,27] mentioned previously.

In 1969 Zhdanovich [29] was able to establish a theoretical formula of the distribution of pressure and density in the single and double-ended pressing of axially-symmetric compacts. He considered an axially-symmetric problem and solved the equilibrium differential equation which applied with many simplifying assumptions. He plotted data which represented experimentally determined values of median density in cross sections of axially-symmetric compacts from iron and copper powders and he claimed that the calculated results were in excellent agreement with the experimental data.

In 1970 Radomysel'skii and Pechentkovskii [30] discussed the effect of pressing tool design on density distribution in bushing-type sintered parts. They designed a die set such that the displacements of its working elements could be recorded as a function of pressing load. They carried out their experiments on a reduced iron powder with an apparent density of 1.56 g/cm^3. They determined the compact density and its distribution over the height by the technique of hydrostatic weighing of both the actual compacts and of ring specimens machined from them. By analyzing the results they observed certain fundamental differences in the densities of parts pressed by the different processes. It was suggested pressing by some specific processes to obtain the best density distribution over the compact height. Also, they suggested some processes for automatic die sets. They concluded that, when both the core rod and die were floating, this gave the least satisfactory results, the compact acquiring a density gradient of about 17%, between the layers located under

the punches and the layer halfway along the height of the part. When the die

and core rod moved relative to each other, the density gradient was reduced

by more than half and the mean compact density substantially increased. Also,

they concluded that the relationship between the mean compact density and the

compaction pressure was dependant upon the pressing process employed.

In 1970 Fedorchenko, Kovynev and Polukhin [31] studied the pressures

exerted on the working parts of die sets by means of pin sensors. Pressing was

performed in a die set into the side wall of which were inserted a spiral line

of pins, provided with strain gauges, for measuring lateral pressures. Similar

measuring pins with strain gauges were fitted into the upper and lower punches.

They presented diagrams of pressure distribution on working parts of die sets in

the pressing of compacts from copper, iron, and Stalinite powders. For copper

compacts they found that the maximum pressure for the upper punch was located

in the region of the upper corner of the compact cross section; while on the

lower punch, the maximum values of pressure were found in the central zone.

The pressure diagram for the pressing of the copper powder was in agreement

with experimental data, obtained by a photo elastic technique, on stresses

generated in the working parts of die sets [32] and also with the theoretical

findings of Zhdanovich [29].

They suggested that the non-uniformity of pressure distribution on the

working parts must be linked with the characteristics of compact formation from

a powder mass. The powder begins to resist deformation from the initial instant

of load application. From experimental results they concluded that the compaction pressure was transmitted through a powder mass which was being pressed, but had not yet been compacted, and reached the lower punch. Finally, it was concluded that there was an urgent need to study the processes taking place within powders undergoing compaction.

In 1970 Meerson, Rasskazov and Chulkov [33] described a technique for studying the pressing process with the aid of resistance strain gauges. Pressing was performed on a GRM-1 testing machine in a die set provided with resistance gauges bonded to the punch and the die cylinder for recording relevant stresses. They determined coefficients of lateral pressure and the external friction of powder against the die walls during pressing. They concluded that, for ductile metals, the coefficient of lateral pressure (f) was not constant. For low-ductility metals such as tungsten, and brittle materials, (f) increased slightly at low pressures, but above ~ 2100 bar it becomes virtually constant.

The coefficient of lateral pressure for a fine-grained, oxidized powder of most metals is slightly less than that for a coarser, unoxidized powder. They related this to the increased interparticle friction. Also, the use of inactive lubricant, whether applied to the die set walls or, in the form of a thin layer to particles with a well-developed, uneven surface, has no effect on the value of (f). Finally they concluded that the coefficient of external friction (μ) diminishes with a rise in pressure at low compaction pressures, but

remains constant at high pressures (above 1400 - 2100 bar for low ductility and brittle materials).

In 1970 Vinogradov [34] measured the lateral pressure in compaction. He used Ni, Al, W, Fe, Cr, and Ti powders and their mixtures, with or without graphite additions. From these experiments, he established that the co-efficient of lateral pressure was independent of density at low degrees of densification and proportional to density in the second stage of pressing, while in the third stage it sharply increases.

In 1970 Fedorchenko, Kovynev, and Polukhin [32] employed the strain measurement technique for studying the stressed state of the die set in the press-ing of iron, copper, and Stalinite powders. Pressing was performed in a 2 PG-250 hydraulic press. The pressing load in all experiments was constant at 4200 bar.

From their experimental analysis, they concluded that, with a decrease in the powder fill height in the die, the pressure on the lower punch increases, but the character of the pressure distribution remains unchanged. Also, the pressures on the lower punch depend on the resistance of the particles in the mass being pressed to plastic deformation. The pressing of metal powders was visualized as a process consisting of two basic stages.

1. Deformation of a free-flowing mass, during which a pattern of non-uniform density is established and the behaviour of the material is governed by pressure distribution laws characteristic

of granular media.

2. Deformation of a compact having a non-uniform density distribution over its cross section and exhibiting increasingly the properties of a continuous, non-porous metal.

In 1970 Katashinskii and Rukhailo [35] developed a new technique for the investigation of shear strains in free-flowing materials, permitting direct recording of slip plane formation by x-ray radiography. They concluded that metal powder deformation in an open volume gives rise to the formation of three characteristic zones within the compact. These zones correspond to different modes of powder deformation namely ejection, shear strain and densification.
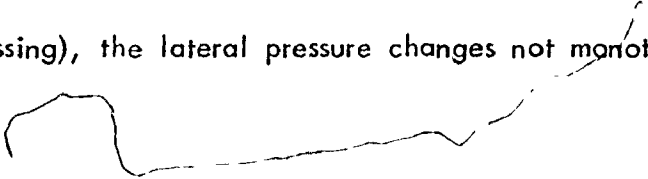
In 1971 Fischmeister, Aren, and Easterling [36] reported observations on plane-strain upsetting, between unlubricated flat punches, of powder performs of varying density. Macroscopic deformation behaviour was characterized by the pressure/strain relationship and by the ratio of lateral to vertical flow. Densification was studied as a function of strain and pressure. Also, the density distribution in typical forgings was charted by means of hardness measurements.

They found a significant difference in deformation behaviour between porous and dense preforms. It was also observed that densification was most rapid in the initial stage of deformation, where, in consequence, lateral flow is almost absent. The pressure/strain relationship for porous preforms does not follow a normal strain-hardening law.

In 1972 Wakatsuki, Ichinose and Aoki [37] published a paper providing notes on compressible gasket and bridgman-anvil type high pressure apparatus. They analyzed the squeezing process of a disc-shaped gasket, between Bridgman-anvils, on the basis of a very simple model for equilibrium of plastic flow in the gasket. They concluded that the behaviour of the disc and pressure distribution depend essentially on the thickness of the disc. A normalized characteristic thickness, $\dfrac{h_c}{2a}$, may be defined as a quantity inherent in the material of the disc, where h_c is a critical value at which the flow region occurs just at the center and a is the radius of the anvil face. Pressure in the disc becomes more and more concentrated at the center as the initial thickness of the disc, h_i, is increased in the range $h_i < h_c$. But the concentration ceases to grow when h_i exceeds h_c.

In 1972 Meerson, Ivensen, Sapronov, and Vissarionov [38] discussed the different techniques which have been proposed for evaluating the lateral pressure exerted by powder during compaction and suggested a method for the experimental determination of the lateral pressure. They used a composite cylindrical die whose walls were assembled from separate rings. The lateral pressure was measured by the deformation of the individual rings forming the body of the die which, in turn, was measured by wire resistance strain gauges fixed to the outer wall of each ring.

They concluded that with increasing distance from the upper, pressing punch (in single-ended pressing), the lateral pressure changes not monotonically,

but according to a more complex law, which, in the case of tungsten carbide-cobalt mixtures, depends on the amount of the ductile metal (cobalt). The presence of cobalt facilitates relative displacement of the carbide particles and increases the friction of the powder on the die wall. The combined action of these factors determines the character of the vertical and lateral pressure distributions along the height of the mass being pressed.

In 1972 a paper has been published by Roman, Perel'man, and Doroshkevich [39] discussing the problems of stress and, consequently, density distribution in powder pressing. They provided an illustration of the distribution of density in a cylindrical compact pressed from a copper-nickel powder mixture. They observed that density was less at the surface of the pressing punch than at some distance from it.

In 1973 Shulishova and Shcherbak [40] described a new method for the quantitative and qualitative study of density distribution in compaction processes by filling the pores of a part made by a powder metallurgy process with a fluorescent substance and then placing the part under an ultraviolet light source. The distribution of the intensity of the resultant luminescence corresponds to the distribution of porosity in the part.

They applied this method to study the vertical density distribution on the surface of a specimen produced by the single-action compaction of a reduced iron powder. A fine magnesium arsenate powder containing $Li_2 O_3$ addition was rubbed into the surface of the specimen, and the resultant

luminescence was photographed. The distribution of the degree of blackening of the film was determined with a spectrometer. This degree of blackening of the film was proportional to the porosity of specimens and inversely proportional to their densities. Their results agreed with those obtained by other investigators for the same case.

In 1973 Vlasyuk, Klimenko, Radomysel'skii, Spuskanyuk, and Chernyi [41] investigated the process of isostatic pressing at different pressures in the range of 5000 - 25000 bar for powder mixtures having compositions corresponding to those of R18 and R25 high-speed steels. In their isostatic pressing experiments use was made, in addition to uncompacted powder mixtures, of preforms of approximately 40% residual porosity pressed in steel dies.

The results of these experiments showed that, specimens isostatically pressed from powder were denser than specimens prepared by the isostatic densification of prepressed compacts. This was referred to the uneven densification of the powder pressed in steel dies. The resultant compacts had a denser outer layer composed of work-hardened particles, which reduced the effectiveness of a subsequent isostatic compression operation. Even in this case, however, better results were obtained than in the case of compression in steel dies.

In 1975 Aren [42] discussed the optimization of preform shape in the powder forging of a linear gear profile. He studied the influence of tooth height versus total height of the preforms on the location of remaining porosity in the forgings, the risk of cracking and tendency for folding. Also, he

studied the densification during different stages of forging iron powder, up to 94% relative density, by Brinell-hardness testing. Specimens were annealed at 550° for 30 minutes before hardness testing in order to cancel out residual effects of work hardening. He referred to the hardness increase with an increase in compacting pressure and resulting densification as the process of densification hardening.

From these measurements, he concluded that densification progresses quickly in the vertical direction, but only slowly in the lateral direction, producing a strongly non-uniform densification pattern, which results in crack formation in zones exposed to tensile stresses. The cracks close again towards the end of the forging stroke where die filling is completed. He suggested some limits for the optimum ratio of tooth-to-base heights which provide the most homogenous densification.

Further ideas on the concept of densification hardening are found in Chapter 4.

3 ISOSTATIC COMPACTION

3.1 ISOSTATIC PRESS

The isostatic compaction unit used in this investigation was an Auto-clave Engineers research type press, capable of providing working pressures up to about 4000 bar. The press has a working chamber size of 100 mm I.D. x 550 mm length. The vessel body is of single cylinder construction and designed to operate elastically at its rated pressure.

The press is powered by a 200 psi (1318 bar), two stage air compressor. The reservoir was filled with a mixture of 64 parts of water and one part of Hydrolubric #2 oil, which is the presurizing medium. The schematic piping system of the press is shown in Figure 2. The isostatic fluid is pressurized by an air driven piston pump, 1, which is controlled by the solenoid valve 2. Fluid is drawn through a system of one way valves from the reservoir, 3, through the pump to the pressure vessel, 4. For safety reasons air may be bled from the system via the shut-off valve, 5. Maximum pressure control is possible by limit switches in the pressure gauge, 6, which are connected to the solenoid valve 2. A safety rupture disc, 7, rated at 5000 bar is also included in the circuit. Pressure is released via valve 8 and excess fluid returned to the reservoir. The pressure vessel closure is of the pin type, with pneumatic removal and location of the main closure, 9.

3.2 PRESSURE MEASURING AND RECORDING SYSTEM

3.2.1 Introduction

Since rates of increase and decrease of pressure in the pressure vessel during a compaction process can affect the densification of compacts; it was desirable to develop a measuring and recording device for their detection.

Since most pressure vessels designed to operate below about 7000 bar respond elastically to load with negligible creep or hysteresis, measurement of the expansion of the pressure vessel should provide a linear correlation with pressure. Strain gauges applied to the cylinder to measure this expansion were initially considered but were rejected in favour of the system described in section 3.2.2. This system measures the mean radial displacement on any section of a prismatic pressure vessel and has the following advantages:

. 1. Longterm reliability under the conditions experienced on the isostatic pressure vessel in question, i.e. vibration and the intermittent presence of a surface layer of liquid.

2. Mobility - the unit is simply and rapidly installed on any section of of the pressure vessel.

3. Sensitivity and output - the transducer has a large primary output of 600 mV at 4000 bar on the pressure vessel in question.

4. Accuracy - since the instrument measures a mean strain over a section of the vessel, manufacturing imperfections in such parameters as roundness and concentricity have reduced effect on the gauge in terms of absolute calibration.

3.2.2   Description

The extensometer utilizes a displacement transducer, Hewlett Packard type 7DCDT which requires 6 volts D.C. exitation and has a linear output of 1.34 volts per mm over a range of 1.25 mm. The principle of operation of the transducer is adequately documented elsewhere [43]. The transducer is mounted in the fixture F, shown in Figure 3(a), to which is clamped a length of steel cable. This cable encircles the section of the pressure vessel under observation, where it is located by the five carriers C, Figure 3(b). The system is tensioned by the adjusting turnbuckle T, which applies an initial tension to the extension springs. An external view of the system mounted on the central part of the pressure vessel is shown in Figure 4.

In operation, the radial displacement of the pressure vessel is transferred to the measuring system via the carriers. This displacement causes an extension of the steel cable and spring system. Since the steel cable has a high stiffness compared to the two springs, the majority of the extension is accommodated in this area, where it is detected by the transducer. Friction is minimized by the use of roller bearings on both the carriers and in the sliding mechanism of the fixture F.

The cable was 1/16 inch aircraft cable with an elasticity of 860 Kgf/mm [44]. The springs were one inch long with a spring constant of 1.0 Kgf/mm

3.2.3 Use and Calibration

The instrument was initially calibrated against the bourdon gauge of the isostatic press. The results are shown in Figure 5. They indicate that both instruments are linear above about 500 bar, but does not show which is responsible for the nonlinearity at low pressures. It is expected however that this error may be attributed to backlash in the bourdon mechanism.

To investigate the calibration of the device, the strain over the central portion of the pressure vessel was determined experimentally and compared with a theoretical solution.

Since the solution due to Lame is a widely used basis for vessel design [45], it was applied to this case to predict a radial displacement for the central section of the cylinder. The calculated value is 6.29×10^{-7} mm/bar. The value obtained experimentally over the central portion of the cylinder was approximately 6.583×10^{-7} mm/bar. This difference is greater than that which could be attributed to the expected experimental error.

Since the Lame solution cannot allow for the strengthening effect of the non loaded end sections of the vessel, some discrepancy was inevitable. It was expected, however, that the extra support from the ends of the vessel would reduce the strains in the central portion to values below those predicted by the Lame solution. This difference in results may be due to deviation from the plane strain condition inherent in the Lame solution as a result of the end conditions.

Displacement at different cross sections of the pressure vessel were measured at various pressures and the corresponding displacements for a 1 Ksi pressure increase are given in Table 1 and plotted in Figure 6.

Since the maximum displacement is observed on the central portion of the pressure vessel, the measuring device was mounted there for measuring and recording of the pressurizing cycles used in subsequent experiments.

3.3 DESCRIPTION OF POWDERS

Four types of powder were selected as being representative of a wide range of particle geometries and mechanical properties. The powders were:

1. Alcoa grade 1202 atomized aluminum powder, supplied by the Aluminum Company of Canada, Figure 7.

2. Atomet 28 Iron powder, a product of Amax Metal Powders Ltd., Figure 8.

3. C-3 Copper powder obtained from Canada Metal Company, Figure 9, and

4. L-4 Lead powder also produced by Canada Metal Company, Figure 10.

Chemical and screen analysis as supplied by the manufacturers of these powders are given in Tables 2 to 5.

3.4 COMPACTION BAGS

It was originally intended to make the required compaction bags for

holding the powder during compaction. Flexane 80, a room temperature curing urethane produced by Devcon Canada, Limited Company, was poured into an aluminum mould machined for this purpose. The aluminum mould was coated with a thin layer of grease before pouring to allow release of the rubber bag after drying. An external view of the aluminum mould is given in Figure 11.

It was, however, difficult to obtain bags without imperfections in this manner and as a result the compaction bags used in this investigation were commercially produced urethane and latex bags manufactured by Trexler Rubber Company of Ravenna, Ohio.

Fourteen bags were used in the experiments. Dimensions of these bags and the weights of the various powders used in each are summarized in Table 6. Urethane 50 has a hardness of 50 on the Shore A durometer scale, while Urethane 70 has a hardness of 70.

The procedures described in the next three sections were carried out for all compacts produced in the isostatic pressing experiments.

3.5 PACKING PROCEDURE

The use of vibration methods to obtain increased and more uniform densities during the packing of loose powder materials has become common [46]. By subjecting powders to such vibrational forces, each particle is set into motion and seeks a more favourable location for packing. This process increases the tap or pre-pressed density of the bulk-powder and thus reduces the

amount of particle deformation necessary for attainment of a high final density after compaction.

For all following experiments a rubber compaction bag was filled with a measured weight of powder and gently vibrated until no further reduction in volume occurred (approximately 2 minutes). The bag was sealed with a cylindrical rubber bung. Finally the bag and bung were clamped using a rubber band to prevent any initial fluid leakage into the bag.

Since the lead powder was much softer than the other three powders, it was necessary to use a perforated metal tube to support the bag in the pressurizing medium while compaction was taking place. All other procedures were as above.

3.6 PRESSURIZING PROCEDURE

A filled compaction bag was placed on the carrier platten. The bag and carrier were inserted into the pressure vessel. The compressor was switched "on" and the compressor control valve was adjusted to provide compressed air up to 100 psi (7 bar) slightly higher than the operating pressure of the Haskel pump. The cover of the press was replaced by means of the pneumatic control valve and the closure pin was inserted. The shut-off valve was opened and the pressure release valve closed. The pump switch was turned to the "on" position.

When the hydraulic fluid filled the sight glass, the shut-off valve was closed and the pump switch was turned "off" simultaneously. The pump switch

was maintained in the "off" position until the inlet air pressure reached 90 psi (6.2 bar) at which time the pump switch was turned "on". This was done to ensure a consistent pressing rate for the samples. The air regulator valve of the press was adjusted to 90 psi to allow the Haskel pump to provide a hydraulic pressure up to 4000 bar [47]. When the required pressure was reached, the pump switch was switched off and full pressure was maintained for 20 seconds. Pressure was then released slowly by opening the pressure release valve.

When the pressure reached zero psi, the shut-off valve was opened and the pressure release valve was closed to prevent draining of the hydraulic fluid from the pressure vessel to the reservoir.

The closure pin and the cover were removed. The carrier and bag were removed and the compact extracted. The pressurizing and depressurizing rates were recorded by means of the pressure measuring and recording system described in Section 3.2. Both rates were approximately 1200 bar/minute for all samples.

3.7 MACHINING OF SAMPLES

In order to allow accurate size measurements for density determinations, it was necessary to machine the samples to accurate cylinders. It was difficult to obtain a good surface finish with Al, Fe and Cu when machining samples on a lathe without the use of appropriate coolants. Since the rough surface finish of specimens can affect the accuracy of density determinations, PLASTAL TOOL

coolant was used and a good surface finish was obtained. Figure 12 shows

four aluminum samples all compacted to 2060 bar, two machined without and

two with lubricant. The improved surface finish when using a lubricant is

evident.

Since specimens compacted from powders exhibit a high degree of

porosity, coolant fluids can permeate the specimen producing an error in the

density calculations. To overcome this difficulty, specimens were washed

using alcohol and dried for two hours in air to enable the alcohol to evaporate,

then heated for a further half hour in a furnace at 200°F to evaporate the

remaining alcohol. By applying this technique to a preweighed sample,

(soaked in coolant but not machined), it was found that the change in weight

due to unremoved coolant after washing was less than 1/2%.

3.8   DENSITY VARIATION ALONG COMPACT LENGTH

To examine the variation of density along the length of a compact,

five specimens were machined from an aluminum sample compacted at 2070

bar in mould #1. All the specimens had dimensions of 20 mm diameter and

10 mm length $\pm$ .02 mm.

The results are presented in Table 7. The maximum difference in

density detected was .36% of the theoretical density (2.700 g/cm^3). This is

within the experimental error of the measurements. Thus while variation of

density along an isostatic compact has been detected [41], no significant

variation has been observed in this study.

3.9 DENSITY VARIATION ACROSS COMPACT DIAMETER

To detect any variation of density across the diameter of a compact, four specimens were machined from an aluminum sample compacted at 690 bar in mould #1. The specimens had diameters of 12.66, 19.1, 31.78 and 44.88 mm, while the nominal length was kept constant at about 13 mm. The density was calculated for each sample by weighing and measuring its dimensions.

The results are shown in Table 8. It may be concluded that no significant variation in density exists across the isostatically compacted samples.

3.10 EFFECT OF TOOLING

3.10.1 Introduction

It is often observed for isostatic compacts that, when the mould is opened, compacts are found to be severely damaged. This type of damage has been discussed by Bloor, Brett and Popper [48]. They attribute this type of damage to stresses which arise from movement of the tool during the pressing cycle. It is conceivable that these stresses could affect the final density of the compact. Since these stresses can be affected by the tool geometry and material properties, it was decided to study the effect of tool diameter, thickness and material.

A selection of bags from among those described in Table 6 were

chosen to study each effect independently. The particular bags used for each study are given in the following sections. Aluminum powder was used for all experiments in the study of tooling. Reasons for this choice are the following:

- aluminum has an intermediate hardness compared with the other metals studied.

- aluminum may be compacted over a wide pressure range.

- the powder is relatively inexpensive.

- aluminum compacts are easy to machine.

3.10.2 Mould Diameter

Two moulds with different internal diameters but the same wall thickness of Latex, Urethane 50 and Urethane 70 were used. These moulds are numbers 3 to 8 in Table 6. The small and large mould of each pair were filled with aluminum powder. These were compacted simultaneously in order to eliminate any variation in compacting pressure between them. Three pairs of compacts were produced at the following pressures: 1034, 2070 and 3100 bar.

One specimen was machined from each compact. All the specimens had a length of 20 mm, one from each pair having 20 mm diameter and the second 43 mm diameter. These specimens were accurately weighed and measured to determine their individual densities.

The results are shown in Table 9. It can be seen that diameter has no significant effect on compact density over the range of pressure studied.

3.10.3 Mould Thickness

Two sets of moulds of urethane 50 and urethane 70 were used. Each set had a range of three different thicknesses. The thicknesses used were 5 mm, 10 mm and 15 mm for both sets of moulds. Internal diameter and length of all moulds were maintained constant. These moulds are numbers 9 to 15 in Table 6.

To eliminate any variation in the compacting pressure between each set of bags all three bags were placed together in the press. The complete set of experiments for both urethane 50 and 70 was repeated at pressures of 1034, 2070 and 3100 bar, to detect any effect of thickness on the compact at the different pressures. One specimen was machined from each compact. Each specimen was weighed and measured and its density calculated. The results are given in Table 10. It can be seen that there is no significant effect on density of the mould wall thickness.

3.10.4 Tool Material

Since three different mould materials were used to detect the effect of tool diameter and thickness, the results obtained by the experiments described in the two previous sections are sufficient to investigate the effect of mould material on the compact properties. The three materials used were latex as a very flexible material and urethane 50 and 70 which have two different hardnesses.

The results indicate no significant effect on density of tool material.

3.11   PRESSURE DENSITY RELATIONSHIPS

A total of 9 aluminum compacts, produced at pressures between 500 bar and 4000 bar, were used for pressure-density determinations.

Nine iron compacts were produced at pressures between 1000 bar and 4000 bar. No coherent iron compacts could be produced at pressures less than 1000 bar.

Three copper compacts were produced at pressures between 2000 and 4000 bar, and no coherent compacts were produced at pressures less than 2000 bar.

Eight lead compacts were produced at pressures between 350 and 4000 bar.

In view of the results of the previous section which showed no significant effect on density of tool diameter, it was decided to limit the density-pressure relationship experiments to compacts produced with a mould having an internal diameter of 30 mm (mould #1 in Table 6).

Nine aluminum samples were produced over a range of pressures of between 500 and 4000 bar. Two specimens were machined, as discussed in Section 3.7, from each sample. One 30 mm in length and one 10 mm both with a diameter of 20 mm. All the specimens used in density-pressure relationship were machined from the central region of the samples. The machined cylinders were accurately weighed and their dimensions determined using vernier micrometers. The densities of the cylinders were then calculated.

The difference in density between pairs of cylinders from the same compact was in all cases less than 1% of the theoretical density. Since this difference was experimentally insignificant, it was decided to limit subsequent tests to the shorter cylinders. Nine iron samples were produced. One specimen was machined from each sample. These specimens were then weighed and measured to determine their densities.

Similar procedures were followed for copper and lead with the exception that no coolant was necessary to obtain a good surface finish for the lead specimens.

3.12   RESULTS OF ISOSTATIC PRESSURE-DENSITY

3.12.1   Aluminum

The experimental pressure-density data for isostatically compacted aluminum powder are shown directly in Figure 13. The densities are expressed as relative densities related to an assumed theoretical density of 2.700 g/cm^3.

The first region observed from 0 to about 700 bar shows a rapid increase of density with pressure, while the rate of increase of density decreases above this pressure.

Expressing the experimental data in terms of the Shapiro equation (1) gives the relationship shown in Figure 14. It can be seen that the results exhibit the three characteristic regions observed by other investigators for a variety of materials. The first region from 0 to about 700 bar shows a rapid

increase of ln $(\frac{1}{1-D})$ with pressure; from 700 bar to about 2000 bar there is

an almost linear variation while above 2000 bar the slope decreases rapidly.

Very similar results were obtained by Hewitt [49] for the same type of

aluminum powder.

It is widely felt that these three regions correspond to different

mechanisms of compaction. Kunin and Yurchenko [14] define the first region

as the pressure at which the particles are brought closer together without under-

going significant deformation. Hewitt [8], however, concluded that extensive

plastic deformation can occur during the first region. The second region is

characterized by the particles undergoing brittle and plastic deformation and

the third by bulk compression. A similar classification has been made by

Heckel [13]. Donachie and Burr [58] suggest that the first region is one of

the transitional restacking, the second corresponds to local plastic flow and the

third to isostatic compression, both elastic and plastic. Greenspan [18] sug-

gested that the change in slope between the second and third stages is referred

to the strain hardening characteristics of the material.

It can be seen that there is still considerable confusion with respect

to the definition and classification of these stages of compaction and to the

role and extent of plastic deformation in powder compaction.

3.12.2   Iron

The pressure–density results are expressed directly in Figure 15.

The densities are expressed as relative densities of an assumed theoretical

density of 7.874 g/cm^3. It can be seen that the rate of increase of density,
with the increase of the compacting pressure, is very small. This may be
explained on the basis that iron powder is a relatively hard material, and
high pressure is required to cause the plastic flow associated with densification.

The experimental data expressed in terms of the Shapiro equation are
presented in Figure 16. The relation shows a linear behaviour, of the
In $(\frac{1}{1-D})$ versus pressure plot over the pressure range studied (up to about
4000 bar) except in the area below 1000 bar. Similar results were observed
by Heckel [16], for iron, nickel, copper and tungsten powder. The transi-
tion from the second to the third stage of compaction was not observed as a
result of the relatively low pressures employed.

3.12.3 Copper

It was difficult to obtain coherent copper compacts by isostatic
compaction at pressures lower than 2000 bar and since the range of study was
limited by the capability of the press to 4000 bar, the results obtained do not
provide observation of the three mentioned stages of compaction. Figure 15
shows the density of the compacts versus the compacting pressure. The densities
are expressed as relative densities related to an assumed theoretical density of
8.900 g/cm^3.

3.12.4 Lead

Figure 17 illustrates the pressure-density data for atomized lead
powder. The density values are expressed as relative densities related to an

assumed theoretical density of 11.34 g/cm^3.

The results expressed as ln $(\frac{1}{1-D})$ versus compacting pressure are shown in Figure 18. The transition from the first to the second stage of compaction is not obvious, while the transition from the second to the third stage can be noticed at pressure of about 700 bar.

3.13 METALOGRAPHIC EXAMINATION

Two techniques of metalographic examination have been applied to compacts produced in the isostatic press: scanning electron microscopy and optical microscope examination of etched and polished sections.

Electron microscopy as a method of investigation makes it possible to evaluate the shape and size of powder particles [50]. To obtain some observations concerning the consolidation phenomenon of the different types of powder investigated, fracture surfaces of different specimens compacted at different pressures were examined in a scanning electron microscope. The fracture surface of each specimen examined was cleaned ultrasonically before examination. The same procedures were applied for aluminum, iron, copper, and lead compacts.

Sections from aluminum and iron compacts were polished and etched for optical microscope examination. The following polishing procedure was used:

Initial grinding was carried out on 220 grit wet silicon carbide papers

followed by successively finer grinding on 320, 400, and 600 grit wet silicon carbide papers, the specimens being cleaned with water between operations. Final polishing was carried out on diamond wheels using 6μ and 1μ diamond paste successively, again cleaned with water between pastes.

The aluminum samples were etched by swabbing with Keller's reagent. The iron samples were etched by swabbing with a 2% nital solution.

3.14 RESULTS OF METALLOGRAPHIC EXAMINATIONS

3.14.1 Aluminum

Figure 19 shows a sequence of scanning electron micrographs of the fracture surface of the as-compacted powder pressed at different pressures. The surface is composed of individual powder particles. It is obvious that the powder particles have been deformed to produce mating surfaces, however, the original shape of the powder particles is still evident.

Polished and etched sections of aluminum compacts pressed at different pressures are shown in Figure 20. It can be seen that the size of the pores between the particles shrinks with increasing compacting pressure. The micrographs also show some of the small particles being forced into cavities formed by larger particles.

3.14.2 Iron

A sequence of scanning electron micrographs of the fracture surface of the as-compacted iron powder, are shown in Figure 21. It is clear

that the degree of plastic distortion in the surface regions of the particles is very small at low pressures, while it is more evident, at higher pressure, at points of contact between particle Figure 21(d). The smaller degree of distortion with iron can be referred to the relatively high hardness of the iron powder compared with aluminum.

Figure 22 shows the pore structure of iron compacts pressed at different pressures. Pores in between powder particles and intraparticle porosity are very clear. The degree to which the particles come closer and the pore size reduces as the compacting pressure increases can be easily observed.

3.14.3 Copper

Figure 23 illustrates the scanning electron micrographs of the fracture surface of the as-compacted copper powder at different pressures. Again it can be seen that as the compacting pressure increases, the amount of plastic distortion in the surface regions of the particles become more evident.

3.14.4 Lead

A sequence of micrographs of the fracture surface of lead compacts pressed at different pressures, are shown in Figure 24. The amount of plastic distortion in the particles is very clear even at relatively low compacting pressure, see Figure 24(a) 700 bar. This is a result of the very low elastic limit of lead which is of the order 1 bar [51].

It is noticeable that crystals with an octahedral shape can be seen

distributed among the irregular particles Figure 24(d). This is possibly due to

impurities in the loose powder. An x-ray analysis of these crystals did not

result in a definite classification.

4 DENSIFICATION HARDENING
IN ISOSTATIC COMPACTION

4.1 INTRODUCTION

One of the primary interest in powder metallurgy research is a study of the density distribution in green powder compacts. A number of experimental techniques have been used in these studies. They include sectioning and density determination by direct mass and volume measurements of each section, the observation of the distortion of heterogeneities in compacts when they are pressed, and the determination of pore volume by various microscopic techniques. One method, described by Kuczynski and Zaplatynskyi [28], involves the measurement of hardness at selected points in a sectioned compact. If a relationship exists and is known between hardness and compacting pressure, the density and pressure distribution in the compact may be obtained. Kuczynski and Zaplatynskyi obtained such a relationship by measuring the hardness and density of thin die pressed compacts. They made the assumption that for practical purposes, the hardness and density of such compacts would be uniform as a result of the small wall friction effect in thin compacts.

It was felt that the observed uniformity of density and hardness in isostatically compacted samples, (see Sections 3.8, 3.9 and 4.2.1), would allow better correlation between hardness-density and pressure than could be obtained by the method used by Kuczynski and Zaplatynskyi. The purpose of the following experiments was to initially explore this possibility.

53

Hardness measurements were attempted on the four powders described in Section 3.3. Owing to the relatively narrow range of pressures over which copper could be compacted in the available isostatic equipment, it would have been difficult to obtain hardness-density and pressure relations for the copper. Although lead compacted over a wide range of pressures and would have been an interesting material to study, severe difficulty was experienced in polishing the lead specimens to the fine surface finish required for the microhardness tests. In addition to these factors consideration of the key role played by iron in powder metallurgy today and the rapidly growing importance of aluminum led to the conclusion that the following experiments be carried out only for aluminum and iron.

4.2   MICROHARDNESS MEASUREMENTS

The term hardness of a material may be defined in several different ways. It principally relates to the resistance to deformation in such processes as indentation, abrasion, scratching and machining [52]. The last three have a limited application practice.

The microhardness measurements in this work were performed on a TUKON tester (model MO) providing Vickers hardness numbers often referred to as diamond pyramid hardness numbers. This test was devised about 1920 and employs a square-based diamond pyramid as the indenting tool. The angle between opposite faces of the pyramid is 136°.

There are two features of this test which are essentially different

and advantageous over the available alternative test, the Brinell method.

Firstly, there is geometric similarity between impressions under different

indenter loads, and hardness number is virtually independent of load. In

addition, the upper limit of hardness number is controlled by the diamond,

thus allowing examination of a wider range of materials than is possible

using the Brinell test which uses a steel ball indenter. The Vickers test

is very useful for surveying a specimen which has a variation in hardness

through the cross-section as a result of the small size of the indentation.

For both iron and aluminum hardness measurements, a load of 1.0

Kg was used, and the diamond pyramid hardness numbers were calculated from

the formula

$$D.P.H. = \frac{2 L \sin \frac{a}{2}}{d^2} \tag{7}$$

where

D.P.H. = diamond pyramid hardness number
d   = length of average diagonal in mm
a   = 136° apex angle
L   = load in Kg

It is interesting to note that the average diagonal of indentation for

the range of samples studied was about 10 to 15 times the average diameter

of the particles.

4.2.1 Aluminum

For similar reasons to those discussed in Section 3.11, it

was decided to use the large diameter compacts for hardness measurements.

The specimens used for microhardness measurements were the same specimens used for the pressure-density relationship. Machining of these samples is described in Section 3.8. The following polishing procedure was used.

Initial grinding was carried out on 220 grit wet silicon carbide papers followed by successively finer grinding on 320, 400 and 600 grit wet silicon carbide papers, the specimens being cleaned with water between grits. Final polishing was carried out on diamond wheels using 6μ and 1μ diamond paste successively, again cleaned with water between pastes.

Five indentations were produced on the polished surface of each specimen and the lengths of the two diagonals were measured enabling the average diagonal length to be calculated for each indentation. The mean value of the five values was used in the calculation of diamond pyramid hardness number for the specimen using equation (7)

It was observed, as stated in Section 4.1, that the hardness distribution was uniform within experimental accuracy along and across the isostatic compacts. The scatter in individual hardness values across the face of a compact was less than 10%, no obvious pattern being observed. The difference in average hardness values on the two faces of a sample was less than 1% indicating uniformity of hardness across and along the compacts.

4.2.2 Iron

Again the large diameter compacts were used for the hardness measurements. Specimens with dimensions of 10 mm length with 20 mm diameter were machined of green compacts as described in Section 3.7.

A similar polishing procedure to that described in the previous section was used to produce the hardness measurements for the sample, again using the mean values produced from five indentations.

4.3 RESULTS AND DISCUSSION

The experimental pressure-hardness data for aluminum and iron compacts are shown in Figures 25 and 26 respectively. It can be seen that in general as compacting pressure increases the hardness of the resulting compact increases. The aluminum results fall on a straight line up to a pressure of about 1400 bar at which time hardness begins to level off. The pressure at which this occurs is close to the pressure which marks the end of the second stage of compaction as described in Section 3.12. Over the range of pressure studied, the iron results can be considered to lie on a straight line to within experimental accuracy. The point at which hardness begins to level off was not reached for the iron powder so that a corresponding leveling off of hardness values could not be observed.

A possible explanation for the linearity of the hardness-pressure relationship for pressures in the second stage of compaction is the following:

during compaction of a metal powder, a non-linear load displacement characteristic results from the combined effects of the altered microstructure geometry and the strain hardening of the material as a result of plastic flow. Upon release of the pressure, however, unloading will occur elastically and therefore linearly. If pressure were reapplied, linear behaviour would persist until the pressure reached that originally applied, at which point yielding of the strain hardened particles would again occur.

Thus the pressure to which a compact was pressed corresponds to a yield stress for that compact. Since a linear relationship can be observed between yield stress and hardness for many metals, such a relation between compacting pressure and hardness could also be expected. This relationship would break down, however, during the third stage of compaction when little additional densification and strain hardening occurs owing to the very small pore size and the correspondingly small region in which significant plastic flow occurs as the pressure is increased.

Regression analyses have been carried out on the hardness-pressure data. A least square fit to a straight line has been performed for the iron data since these are all in the second stage of compaction. A straight line could have been fitted to the aluminum data below 1400 bar but in order to provide a smooth curve for the entire pressure range a least squares polynomial fit to the data was performed.

The equations so determined are:

For aluminum: $P = -853.8 + 231.5 \ H - 11.57 \ H^2 + .2428 \ H^3$ (8)

For iron: $P = 158.1 + 54.41 \ H$ (9)

H is in D.P.H. , P in bar

These curves are shown on the corresponding plots.

5 APPLICATION OF DENSIFICATION HARDENING

5.1 CLOSED DIE COMPACTION

5.1.1 Introduction

The objective of these experiments is to investigate qualitatively and quantitatively the distribution of density in a powder compact, as a function of pressure, and to investigate the distribution of the pressure exerted by the compact on both top and bottom working parts of the die set. Hardness was measured at selected points on the top and bottom of the compact. The hardness readings were translated into pressures and densities using the calibration curves obtained from Sections 4.3 and 3.12 respectively.

To allow a comparison between conventional and hydrostatic compaction, the relationship between die compact density and the applied pressure was investigated for both aluminum and iron powders, in a range of pressure up to about 16500 bar.

5.1.2 Die Compaction Press

The press utilized in this study of die compaction is a 500 ton capacity Vecor system built by Autodraulic Ltd. of Leeds, England. The unit comprises three main sections, two of which are of interest in this application.

1.   The main press frame consists of a single action hydraulic ram with an 18 inch diameter piston. When pressurized the ram raises the

movable central platten of the press towards the upper section of the press frame. Parallelism is maintained by four sliding bearings between the platten and the pillars of the press frame. On removal of the hydraulic pressure the weight of the mechanism is sufficient to return the platten to its neutral position.

2.   The hydraulic unit whose main component is a two stage pump driven by a 7.5 H.P. motor. The pump system has a maximum pressure capacity of 5000 psi (345 bar). The pressure is controlled by an open loop system consisting of a pressure control valve which is activated by a small electric motor via a variable ratio gear box, thereby introducing controllable rates of pressure application.

The third part of the press not needed in this work provides the facilities of controlled cycling and resistance heating of the system.

5.1.3   Closed Die System

The closed die compaction examinations were carried out using the arrangement shown in Figure 27. The system consists of the following items:

Compaction chamber consists of a carbide cylinder machined from tungsten carbide grade 44A which has a hardness of approximately 91 Rockwell A, and good resistance to wear. This type of carbide has an ultimate compressive strength of 51700 bar and a modulus of elasticity of 6.4 million bar [53]. These specifications make this type of carbide suitable for

compacting dies in addition to some other applications. The carbide die was provided with a steel binding ring.

The piston and the closure (parts 4 and 7 in Figure 27) were made from tungsten carbide grade 44A. The diametral clearance between the piston and the compaction chamber was on the order of $\pm$ .02 mm. This close clearance was held in order to achieve reasonable alignment of the system.

The composite disc was machined of carbide 44A and provided with a supporting steel ring. The guide sleeves were machined out of aluminum. Figure 28 shows the guide sleeves and pistons used.

5.1.4 Pressure Measuring Arrangement

The load was measured using a load cell model RA manufactured by Hottinger Baldwin Measurements Inc., Darmstadt, W. Germany, with a nominal maximum force specification of 200000 Kgf. It has a linearity deviation of no more than $\pm$ .01% and a sensitivity of 2 mV/V at full load. The measuring element of the load cell takes the form of a ring which receives the load axially. The transducer is designed so that side loads of up to about 20% of the axial load, which may occur as a result of inaccurate mounting, have only a small influence on accuracy.

The load was transmitted to the load cell through the bottom die. The load cell was connected with a DC powder supply, Hewlett Packard Model 6204 B capable of providing up to 40 volts DC.

To ensure constant pressing rate for all samples, the load history was recorded by connecting the output of the load cell to a strip chart recorder, Hewlett Packard Model 7100 B. A loading rate of about 8400 bar per min was used throughout.

5.1.5 Calibration of the Load Cell

The load cell was calibrated up to 90000 Kgf using McMaster-Mand hydraulic press with a maximum capacity of 200 tons, and up to 4500 Kgf using an Instron Universal Testing Instrument, floor-model (TT-C) with a full scale load of 4540 Kgf. The recommended supply voltage for the load cell was between 4 and 12 Volts. Calibration was carried out using 6 and 12 Volts. The load calibrations up to 90000 Kgf and up to 4500 Kgf are illustrated in Table 11 and Table 12 respectively. Also, the calibration curves for both 6 and 12 Volt settings are illustrated in Figure 29 for high loads and Figure 30 for the lower range of loads.

The load cell sensitivity evaluated from the calibration curves was 1.47 mV/V at full scale for both 6 and 12 calibration settings, while the technical data obtained with the load cell defined this sensitivity as 2.0 mV/V. The manufacturers were contacted and it was discovered that the technical data supplied with the load cell related to older models of the equipment and new specifications were subsequently provided which agreed with the experimental results.

5.1.6   Preparation of Samples

To facilitate controlled initial packing of the metal powder in the working volume of the die set, the loading process was carried out with the die set removed from the press. Parts one to nine (see Figure 27) were supported on a hydraulic lift outside the press and a pre-weighed amount of powder was poured into the compaction chamber; 17g in the case of Aluminum and 37g in the case of Iron. The upper guide sleeve was next located enabling the piston to be carefully inserted. The copper packing and carbide backing block were then placed in position. The complete assembly was subsequently replaced in the press, centrally positioned on the load cell.

To produce the compacts the pressure was raised to the desired value and held for a dwell time of 10 seconds before unloading. In many cases it was difficult to remove the compacted specimen from the die, because of the residual elastic stresses in the compact; in these cases the press was used to remove the samples from the equipment.

A total of 15 aluminum samples were produced over a pressure range of 270 to 16000 bar. 11 iron compacts were pressed in the range of 700 to 16000 bar. The samples were weighed and their dimensions obtained for density calculations. A selection of aluminum samples is presented in Figure 31; several iron samples are illustrated in Figure 32.

5.1.7 The Role of Shear Deformation in the Phenomenon of Densification of Metal Powders

To examine the consolidation phenomenon of aluminum powder a thin disc was produced by die compaction at a pressure of 5520 bar. The techniques used are described fully in the previous section. The disc was replaced in the die between two masses of loose powder equal in weight to the disc, and the complete specimen was compacted to a pressure of 12400 bar. The sample resulting from the test was in three pieces corresponding to the original disc and the second two powder masses which had been compacted into solid bodies, as shown in Figure 33.

It may be concluded from the above that since there is no bonding between the loose powder and the disc, in an area of direct compressive stress, that such a stress state is insufficient cause for bonding between particles, which requires the sliding and corresponding frictional welding effect. This can be seen in the bonding which occurred within the powder mass, and on several occasions between the aluminum samples and the die wall in the area where sliding friction can be expected to occur.

The above ideas are in general agreement with the conclusions of Hewitt [7] which state that consolidation is a result of a mechanical inter-locking and associated frictional welding created by surface shear deformation. Thus it is difficult to achieve consolidation between the precompacted aluminum disc and a loose powder of the same material. This fact is an important consideration for future investigation or design involving compacts with solid

inserts of both similar and dissimilar materials.

5.1.8   Microhardness Measurements

Three aluminum samples compacted at pressures of 1670 bar,
2090 bar and 3520 bar were examined. The faces of the samples on which
microhardness tests were to be performed were polished as described in
Section 3.13.   Tests were performed on both the top and bottom of each
sample using the Tukon hardness tester described in Section 4.2 and a load
of 1.0 Kg.   Sixteen indentations were made on each face of each sample.
The distance between adjacent indentations was 1.5 mm.

To examine the hardness distribution within the samples, the sample
compacted at 2090 bar was machined into half cylinders.

One of the semicircular specimens was mounted using a thermo-
plastic compound (acrylic lucite) so that microhardness tests could be made on
the sample cross-section.   It was then ground using a sequence of wet silicon
carbide papers (described in Section 3.13), and finally polished using diamond
wheels.

Microhardness tests were carried out using the Tukon tester described
previously, again with a load of 1 Kg.   Five rows of measurements, each of
sixteen indentations, were carried out on the sample.   The distance between
successive indentations in each row was about 1.5 mm, while the rows were
$\sim$ 2 mm apart.

For iron samples microhardness measurements were carried out on

both the top and bottom of three iron samples compacted at pressures of 4140

bar, 6830 bar and 13660 bar. Similar polishing procedures to those described

in Section 4.2 were carried out and microhardness measurements were per-

formed. Again sixteen indentations were made on each side of the sample.

Using a load of 1.0 Kg, D.P.H. numbers were obtained as described in

Section 4.2.

5.1.9   Results and Discussion

5.1.9.1   Pressure-Density Relationship

Pressure-density data for die compacted aluminum

and iron powders are shown in Figure 34. It can be seen that, for both

materials, an increase of pressure leads to increased density of compacts. A

slight increase of pressure at the beginning of compaction gave a substantial

increase of density. When high pressure is attained, a further increase of

pressure results only in a slight increase of density.

Expressing the results for both powders in terms of equation (1)

due to Shapiro and Kolthoff gives the relationship shown in Figure 35. It

can be seen that the pressure-density relationships for both powders exhibit

the three characteristic regions observed by other investigators for a variety

of materials. For aluminum powder the first region from 0 to about 1700 bar

shows a rapid increase of $\ln\left(\frac{1}{1-D}\right)$ with pressure. From 1700 to about

7600 bar there is an almost linear variation while above 7600 bar the slope

decreases.

The corresponding regions for iron are 0 to 3100 bar, 3100 to 10000 bar and above 10000 bar.

These three regions correspond to different mechanisms of compaction as discussed in Section 3.12 which referred to isostatic compaction. The pressures and densities corresponding to each region in die compaction may not be the same but it is felt that similar mechanisms are involved in both types of compaction.

5.1.9.2 Pressure and Density Distributions on Top and Bottom of Closed Die Compacts

The hardness measurements on the top and bottom of the aluminum compacts pressed at average pressures of 1670 bar, 2090 bar and 3520 bar are shown in Figure 36. Using the curve derived in Section 4.2.1 for the hardness-pressure relation for aluminum, pressures are calculated from these hardnesses and these are shown in Figure 37.

Integration of the pressure on top and bottom of the compact should give the total load applied to these faces. A numerical integration of the pressures has been carried out using the trapezoidal rule. The results are shown in Table 13 where they are compared with the actual loads. It can be seen that the ratio of calculated load on the top of the sample to the actual load on the sample decreases as the compacting pressure increases. This may be referred to decrease in the amount of lateral movement of the top particle layer with the increase in the compacting pressure. This reduction

in movement will reduce the shearing forces on the top surface and consequently lower its hardness.

The calculated pressure values have been converted to densities following the curve given in Figure 13. The resulting density distributions are shown in Figure 38.

From the plots it can be seen that hardness and consequently pressure and density near the edge of the compacts is higher than at the middle of the compacts for the top surface (close to the movable piston), while it is less at the edge than at the middle for the bottom surface of compact (close to the immovable plunger). Comparing the results obtained from compacts pressed at different pressures it can be seen that, as the compacting pressure increases the nonuniformity of the distributions of hardness and consequently pressure and density, become more evident.

The difference between the load on the top and bottom pistons of the die compaction apparatus provides a measure of the friction between the cylindrical wall of the compaction chamber and the compact. The ratio of calculated load on the bottom of the sample to that on the top is given in Table 13. A possible reason for the relative inconsistency of the results is the effect of residue from previous runs which clings to the die walls and would alter their friction characteristics.

5.1.9.3 Density Contours Across Die Compacts

Hardness contours in cross-section of cylindrical aluminum compact are shown in Figure 39. These have been converted to pressures according to the results of Section 4.3 and these pressures converted to densities following Section 3.12. The resulting density contours are shown in Figure 40.

It can be seen that along the axis of symmetry of the specimen the density is less at the top than at the bottom. Also it can be seen that the dense parts of the compact are at the outer circumference at the top surface (near the movable piston), and in the vicinity of the central part of the bottom surface. The lowest density region is at the bottom at the outer circumference. Similar results were obtained by Kamm, Steinberg and Wulff [27], and Roman, Perelman, and Doroshkevich [39].

The character of stress distribution within the die wall was analyzed by Fedorchenko, Kovynev, and Polukhin [32]. It was concluded that compaction pressure transmission between the upper and the lower punch is effected through particle chains which form "skeletons" within the mass being pressed. It is probable that interparticle friction plays an important, perhaps dominant, role in the formation and stabilization of such a chain.

The same investigators in earlier work [54] observed that in a container densely packed with model particles made of an optically active mass, compaction pressure is transmitted from the upper to the lower punch

over particle chains located between the upper corners of the compact cross-section and the central part of the lower punch. The orientation of these chains as suggested by Fedorchenko, Kovynev, and Polukhin are shown schematically in Figure 41.

Taking into account all the factors mentioned above, it can be visualized that the formation of particle chains and skeletons results in a non-uniform compact density. The formation of a denser zone in the upper corners of the compact cross-section is due to the action of external friction forces, which impede the free downward displacement of the powder particles. In the lower part of the compact, powder densification results from the downward displacement of particles along any chains which may have formed. When all particle displacements within the powder mass along these chains are essentially completed, deformation of the compact as a whole begins. However, the pattern established during the deformation of loose powder persists in the pressed compact, resulting in a nonuniform density distribution over the compact cross-section.

Train [55] proposed a simple explanation for the formation of the dense axial core in the compact adjacent to the stationary plunger, on the basis of high intensity force wedges developing adjacent to the punch which increase with applied pressure. Reference to Figure 42 illustrates vertical and horizontal force components set up in the top corners of the compact. The longitudinal component is resisted by the punch in one direction Z

and the lower particulate matter in an opposite direction Y. The radial

components X and W are those resisted by the die wall and the internal core

of particulate matter respectively. Thus the internal components W and Y

develop a resultant reaction V along a diagonal as indicated, whose focal

point is at H.

The position of the focal point H may be considered as a function

of the height to diameter ratio of the compact which can affect the values

of the longitudinal and radial force components Y and W and the resultant

reaction V; also factors affecting the interparticle friction may have some

effect.

The influence of wall friction points out the importance of the

coefficient of wall friction and the great importance of wall finish. A

ground and carefully polished die interior wall can be expected to give much

more uniform compacts than a die wall that has been finish-ground only.

Using adequate lubrication is expected to result in achieving more uniformity

of density distribution in metal powder compacts.

An attempt was made to perform the same analysis for iron as that

given above for aluminum but some difficulties were experienced. It was

found to be very difficult to polish the iron samples compacted at low pressures.

As a result, hardness tests were carried out on three samples compacted at

the relatively high average pressures of 4140, 6830, and 13660 bar. Since

these pressures are well outside the range of the results from isostatic com-

paction it was felt that less consistency would exist in the results than for those of aluminum. Hardness values for the top and bottom faces of the samples are shown in Figure 43. These hardness values have been converted to pressures, Figure 44, assuming that the linear hardness-pressure relation observed in Section 4.2.2 holds up to the pressures experienced in the die compaction. This is the simplest assumption which could be made and the results show it to have been reasonable.

Integrated pressures and actual loads for the three iron samples are shown in Table 14. The ratio of integrated load to actual load averages 1.260 with a maximum deviation of 7%; this value may be considered as a correction factor for the results. The fact that the results for isostatic compaction can be extrapolated so far with reasonable accuracy is an important advantage of this technique.

An estimate of the wall friction for the iron compacts has been made following the method of Section 5.1.9.2 for aluminum. Table 14 illustrates the results. The wall friction would appear to be generally smaller for the iron powder than for aluminum.

The calculated pressure values have been converted to densities following the curve given in Figure 15. The resulting density distributions are shown in Figure 45.

5.2 OPEN DIE COMPACTION

5.2.1 Introduction

To study the laws governing the pressing behaviour of powders and to discover any unusual pressing characteristics of powders, it is necessary to determine the effect of individual parameters on the compaction process and their mutual relationships. In particular, measurements must be made of the load applied to the punch and the pressure distribution exerted by the material being compacted. It is reasonable to assume that the distribution of compact hardness at the interface between the powder and the working parts of the die set will be similar in character to the distribution of pressure and density.

The objective of these experiments is to study the pressure distribution of a thin disc compacted between two parallel surfaces of the dies in the single-ended open volume pressing of aluminum and iron powders.

5.2.2 Open Die Equipment

5.2.2.1 General Arrangement

The system built for open die compaction was designed for easy use and to ensure repeatability of the compaction condition. The construction and an external view of the system are presented in Figures 46 and 47 respectively.

A detailed description of the components is included in the following subsections.

5.2.2.2   Compaction Dies

The upper die or piston is illustrated in Figure 48, and was ground from Canadian General Electric grade 44A Tungsten carbide. The die was supported by a shrink fitted ring of high strength machinery steel, Atlas Ultimo-4. The ring provides an initial radial compressive stress to increase its axial load carrying ability. A mild steel safety ring is subsequently force fitted onto this assembly to contain any fragments in the event of a failure of the relatively brittle component parts. To complete the manufacture of the die the two working forces were ground parallel.

The lower die and spacer were machined from Ultimo 4 steel, and as above hardened to 50 Rc. The use of a spacer disc allowed minimization of the thickness of the lower die itself, and increased hardenability of the _smaller cross-section.

5.2.2.3   Compaction Moulds

Since rubber is a very flexible material and can deform easily under small loads, it was decided to use moulded rubber to hold the loose powder in position before compaction. Initially, flexane 60, mixed with a curing agent was poured into an aluminum mould, Figure 49, and a rubber tube was obtained. The dimensions of the rubber tube were 45 mm internal diameter, 6.2 mm wall thickness and 90 mm height. The tube was sliced into small rings, each of 17.5 mm height. These rings were torn during the first application of load. It was concluded that this type of rubber could

not sustain the high strains associated with the application of load in this case.

Flexane 80 was tested instead of flexane 60 and the same procedures were applied as described above.   No problems were experienced with this material.

5.2.2.4   Guide Sleeve

The guide sleeve shown in Figure 46 was machined from aluminum.   Its purpose was to locate the spacer and the bottom die, on top of the load cell and to guide the top die while sliding during load application.   The guide sleeve was placed on top of the load cell and clamped using three screws separated by an angle of 120°.

5.2.3   Preparation of Samples

The rubber ring, part 3 Figure 46, was placed on top of the bottom die.   Due to space limitation both parts were moved out of the press and the compaction space was filled with about 17 g of aluminum powder for aluminum compacts or 30 g of iron powder in case of iron compacts.   The die with the powder was placed on top of the spacer on the press.   The top die was placed on top of the powder using the guide sleeve.   Samples of each powder were produced at pressures between 2000 bar and 9600 bar.

5.2.4   Pressure Measurement

The load was measured using the load cell described in 5.1.4. The load cell was placed on top of the lower platten of the press and fixed

in position using an aluminum fixture. The aluminum fixture was clamped by one end into the lower platten by means of three screws, at 120°, while the other end of the fixture was clamped into the load cell by means of three similar screws.

The load was transmitted to the load cell through the steel disc and the same recording device described in Section 5.1.4 was used. The output voltage of the load cell was translated into load units using the calibration curves shown in Figures 29 and 30. The loading rate recorded was about 8300 bar per min for all samples.

5.2.5   Die Set Failure

The die set was broken on the tenth application of load. The die set consisted of two circular discs machined from Ultimo 4 steel (Atlas Steel Company), hardened to 50 Rc. The top disc was fractured by three radial cracks and a similar pattern of cracks was observed in the top face of the spacer.

The most obvious cause of failure was a rapid increase of the load applied by the press due to a temporary mechanical problem. The fracture load recorded by the load cell was 185500 Kgf.

A finite element solution has been obtained to examine the stresses in the die due to the application of the fracture load. The mesh used is shown in Figure 50. The applied load was derived from the pressure contours obtained in Section 5.2.7.

The element exhibiting the largest Von Mises equivalent stress is shown shaded. The value of this equivalent stress is 14000 bar which may be compared with the manufacture's yield stress specification of approximately 14700 bar [55]. As the value of the yield stress is quite sensitive to small changes in the heat treatment of the material, the possibility of fracture under this load can be appreciated.

A second die set was machined from the same material and experiments were continued with the applied load never exceeding 135000 Kgf. No further difficulties were encountered.

5.2.6   Microhardness Measurements

Sixteen indentations were made on both the top and bottom surfaces of each compacted disc. The indentations were separated by a distance of 2.5 mm. The discs obtained had very weak edges which prevented any polishing of the surfaces, and made hardness test impractical close to the immediate edge of the compact. However the as pressed surfaces were of sufficient quality to permit microhardness measurements to be achieved with reasonable accuracy. These tests were carried out using a Tukon testing machine with a load on the indenter of 1.0 Kg., (see Section 4.2).

5.2.7   Results of Open Die Compaction

5.2.7.1   Aluminum

Samples obtained from the open die system of compaction pressed at different loads are illustrated in Figure 51. It can be seen that a small quantity of material has been extruded towards the edge of the compact.

Cracks are evident which start at the periphery and extend towards the centre of compacts pressed under higher loads (Numbers 2,3 & 4 in Figure 51). Green compacts have relatively low tensile strength and these cracks apparently resulted from tensile stresses generated in the circumferential direction during the compaction process.

Hardness measurements for three compacts of aluminum, produced at averaged pressures of 807, 2650 and 4050 bar are shown in Figure 52. It is evident that as the effective compacting pressure is increased the average hardness on both top and bottom surfaces increases. The hardness pattern is similar for the different samples. However, it is noticeable that with increased compacting pressure the hardness at the edges of the compact increases, while showing a tendancy to decrease at the middle.

It is reasonable to assume that the distribution of compact hardness at the interface between the powder and the working parts of the die set will be similar in character to the distribution of compacting pressure in this area. Pressures interpreted from the hardness readings following the results of Section

4.3 are illustrated in Figure 53.

Integration of these pressures over the face of the compacts gives loads shown in Table 15. The ratio of integrated to actual load for the top and bottom of each sample is also given. These ratios are much less consistent in value than the corresponding ratios for closed die compaction presented in Section 5.1.9.2.

A possible explanation for this difference is the following. In isostatic compaction, the macroscopic stress state is one of isostatic compression. In closed die compaction there are external shear stresses as a result of the non deformable walls but the predominant component of the stress state is again one of isostatic compression. Thus the better correlation between closed die and isostatic compaction hardness-pressure results which are shown in Section 5.1.9 may be expected. The situation, however, is different for open die compaction. Near the center of the compact it would be expected that again near isostatic compression would exist. At larger radii, however, the macroscopic stress state departs considerably from this ideal. Near the outer edge, the material is near-uniaxial compression.

A simple theory has been presented by Wakatsuki, Ichinose and Aoki [37] to attempt to describe the stress distribution in the gasket of a Bridgman Anvil ultra-high pressure device. The loading of this gasket is very similar to the loading of the compact in the present experiments so that it would be expected that the two cases would be analogous. Wakatsuki et al

postulate that the circular gasket may be divided into two zones as shown in Figure 54 where r_1 is the radius of the boundary of the zones. For $r < r_1$ the material is being compressed elastically i.e. no flow is taking place. For $r > r_1$ the material is flowing outwards. Friction with the anvils in this area supports the material closer to the center. The pressure distribution in the gasket can then be considered to be as shown in Figure 54. It can be shown that as the load increases the radius r_1 decreases.

Assuming this model to hold for the open die compaction of powder, it would be expected that the ratio of integrated load to actual load for the region $r < r_1$ would be near 1 as a result of the similarity of the conditions here to those found in isostatic compaction. In the region $r > r_1$, the material experiences considerable external shearing and corresponding additional strain hardening as a result of its flow. It would thus be expected to reach a given hardness at a lower pressure than would be required in osostatic compaction. The ratio of integrated to actual load for this region would thus be greater than 1. As the load is increased r_1 decreases. Thus the effect on inegrated load of the flow region will be greater and the ratio of loads for the entire compact would increase. This is the behaviour observed in these experiments. Thus it is to be expected that the pressure obtained will not be an accurate representation of the actual pressures especially at high loads. The general trends of the pressure curves, however, can probably provide useful information.

It can be seen that the maximum value of pressure occurs in the

central region of the compact pressed at 807 bar. The other two samples compacted at higher pressures, showed a lower pressure values at the middle region than at some non-zero distance from the center, Figure 53. Near the edges of the samples, pressures tended to zero.

It is noticable that the pressure distribution on the bottom of the compacts exhibits approximately the same pattern as the distribution on the top side.

The low pressure region at the middle of the compacts might be referred to deformation in the working parts of the dies. Since the top composite-die was made for tungsten carbide[*], no significant deformation was expected. The bottom die was made of ultimo-4 steel with a relatively lower Young's modulus and yield stress and such deformation might have occurred. An elastic finite element solution has been obtained to examine the displacements in the die due to the application of the loads. The mesh used is shown in Figure 50. The displacements obtained are shown in Figure 55. The middle of the die surface moved downwards about 1.3 times the movements of the edges. This may result in lower pressure and consequently density at the middle than at a distance from it.

---

[*] See Section 5.2.2.2

5.2.7.2   Iron

Figure 56 shows four iron compacts pressed at averaged pressures of 4100, 5450, 7000, and 8450 bar (from left to right). It was noticed that the iron compacts had edges with almost no green strength and no cracks or extrusion of the compacts was observed. This may be explained on the basis of the difference in mechanical properties between the two metals. However, cracks might be expected for iron compacts pressed at higher pressures.

The hardness measurements for three iron samples pressed at averaged pressures of 7450, 8900 and 10300 bar are shown in Figure 57. The results obtained are similar in pattern to those obtained for aluminum compacts.

The converted hardness readings into pressures are shown in Figure 58. The complex pattern of the pressure distribution at the middle regions of the compacts could be explained as discussed for aluminum.

The ratios of integrated to actual loads for the iron compacts are given in Table 16. The values appear very consistent as opposed to those for aluminum but it must be noticed that the range of loads used for the iron was much more limited than that used for aluminum. This was due to the relatively narrow range of loads below the workable limit of the load cell in which usable iron compacts could be obtained. If higher pressure samples could have been produced it would be expected that similar behaviour to that observed for aluminum would occur.

6 DISCUSSION AND CONCLUSIONS

6.1 GENERAL DISCUSSION

While slight variations in density along the length of isostatic compacts have been reported in the literature [41], the results of this investigation are in agreement with the more usual conclusion that within the bounds set by experimental error the compacts are uniform in density. A second series of experiments indicated that the density was also uniform across the diameter of the cylindrical compacts.

The present experimental work also included a study of cylindrical moulds made in a series of diameters from three different elastomers. It was found that neither the geometry nor the material had any measurable effect on the density of the final compacts.

These conclusions would be expected if one considers the uniformity of the powder to be compacted and the stress state to which it is subjected, in the case of moulds whose rigidity may be neglected in comparison with that of the final compact.

In comparison of the compaction pressure versus density data between the four powders studied it is evident that increased effectiveness of compaction in terms of a relative theoretical density produced under the same pressure. is in the same sequence as the hardness of the materials, namely lead, aluminum, copper and iron. In general terms it may be concluded that harder materials, with higher yield stresses, produce compacts with larger

values of ultimate porosity.

From the characteristic compressibility curves of iron and aluminum powders, Figure 34, it is evident that isostatically pressed specimens are more dense than those prepared by die compaction at the same pressure. The results indicate that to produce compacts of equivalent density, the die compaction operation requires an increase in pressure of about 40% over that required in isostatic compaction. Differing ratios have been obtained by other investigators with difference of up to 200% of the isostatic pressure being reported [30]. It is to be expected that this ratio would be highly dependent upon pressures involved, the particular powder, and the form of the single acting die, since the main contributing factor is friction in the die compaction process. The friction between the die walls and the powder mass restricts the reorientation and rearrangement of particles during the initial stages of compaction leading to an increase in the porosity of the final compact. At higher final pressures this phenomenon has a reduced importance and it is reported that at pressures greater than 20 kilobars, the two compaction processes become similar in effect [8].

Metallographic examination has shown that the powders studied undergo plastic deformation from very early stage in the compaction process. While this is in agreement with some recent work [57], it is in contradiction with authors who classify the first stage of compaction as the pressure region in which only rearrangement of particles takes place.

A comparison of results for the range of powders studied shows in general that the extent of plastic distortion of the particle surfaces increase with applied pressure. This is particularly evident with lead powders and may be related to the low elastic limit of the material.

The experimental results obtained were compared with the Shapiro equation which was consistent with the results over a limited range of pressures for the iron and aluminum compacts. No linear dependence could be observed between pressure and $\ln\left(\frac{1}{1-D}\right)$ for the copper or lead powders. The Shapiro equation over-estimates the density at high pressures. Some attribute this effect to work hardening of the powder particles. Hewitt [24], however, has shown that the conventional limits of work hardening would be insufficient to produce the discrepancies observed.

Comparing the plots of $\ln\left(\frac{1}{1-D}\right)$ against pressure for atomized aluminum powder (Figure 14, Figure 34), it can be seen that compacts produced by isostatic or die compaction exhibit the three characteristic regions observed by many investigators. However the transitions between stages in die compaction occurred at higher pressures compared with those for isostatic pressing. Data obtained for the consolidation of iron by isostatic compaction does not allow observation of the third stage of compaction due to the relatively low isostatic pressure available. However these three regions were observed for iron in the case of die compaction.

It has been shown by trying to compact loose powder with an

inserted solid pre-compacted disc of the same material, that consolidation is a result of mechanical interlocking and associated frictional welding. Similar conclusions were reached by Hewitt et al [25]. The externally applied shear forces due to die wall friction which do not occur in isostatic compaction may thus explain the ability to obtain coherent compacts at lower pressures by die compaction than by isostatic compaction. This is true in spite of the higher density obtained at a given pressure by isostatic compaction.

The aluminum pressure-hardness data Figure 25 shows a linearity up to about 1400 bar at which time hardness begins to level off. It is interesting to note that the pressure at which this occurs is close to the pressure which marks the end of the second stage of compaction. It is also noticable that over the range of pressure studied, the iron results can be fitted by a straight line to within experimental accuracy and no leveling off of hardness values are observed. Similar results were obtained between pressure and density for the same material (Section 3.12.2).

It can be seen that the pressure-hardness data follow a similar pattern to the pressure-density results. A study of the former should provide additional insight into powder compaction phenomena which currently are being studied only on the basis of the latter. The area of interpretation of pressure-hardness data would appear to provide much scope for future research.

The method examined in the present work to determine qualitatively and quantitatively, the pressure and density distributions in green powder compacts would appear to warrant further consideration. Hardness measurements may be carried out with far greater ease than density or pressure measurements and would appear to provide similar accuracy to the lead grid method [27] in the anlysis of these quantities.

Hardness-pressure-density data obtained from isostatically compacted specimens appears to be well suited for the anlaysis of closed die compaction but less applicable to open die compaction as a result of the significant difference in the stress state of samples produced by this process when compared with isostatic or closed die samples. It may however, be true that the hardness of a compact is of greater technological importance than its density, possibly providing better correlation with other properties of the compact such as green strength. This is an area for future research.

The pressure and density distributions determined for some die pressed samples by this method follow similar patterns to those determined by other investigators employing various techniques, and can probably be explained on the basis of the formation of chains and skeletons as discussed in Reference 54.

The formation of an increased density zone in the upper corners of the compact cross-section is due to the action of external friction forces which retard the downward displacement of the powder particles in this region. In

the lower part of the compact, powder densification results from the downward

displacement of particles along any chains which may have formed. When all

particle displacements along these chains are essentially completed, deformation

of the compact as a whole begins. The explanation proposed by Train [55]

to account for the formation of a dense axial core in the compact adjacent

to the stationary plunger seems quite reasonable and goes slightly beyond

5.1.9.3 in detail.

Since the pattern established during the formation of loose powder

persists in the pressed compact, resulting in a nonuniform density distribution

over the compact cross-section; it could be possible to obtain die compacts

with uniform density by isostatically precompacting the loose powder to obtain

a coherent compact, before final die compaction. This would allow a com-

bination of the advantages of the uniform density obtained by isostatic com-

paction and the close dimensional control available with die compaction.

6.2   CONCLUSIONS

A device for isostatic pressure measurement and recording has been designed, built and calibrated. The method utilizes the expansion of the pressure vessel under load. The ealstic expansion of the pressure vessel has been determined.

Open and closed die compaction systems utilizing a single action hydraulic press were developed.

The $\ln \left(\frac{1}{1-D}\right)$ versus pressure curves for atomized aluminum powder and reduced iron powder were found to exhibit the three characteristic regions observed by other investigators for a variety of materials. The atomized lead powder does not exhibit these characteristic regions.

The results indicate the higher efficiency of the isostatic compaction method as compared to the die method.

It has been shown that although plastic deformation occurs during consolidation of powder compacts, it does not cause it: consolidation is a result of mechanical interlocking and interparticle shearing.

The phenomenon of densification hardening was investigated. Pressure–hardness relationships have been obtained experimentally for atomized aluminum and reduced iron powders, compacted by the isostatic method. The results exhibit linearity over a pressure range corresponding to the second stage of compaction.

These results were applied to tests conducted on open and closed

die compacts, enabling pressure and density distributions to be satisfactorily determined by hardness measurements.

It has been shown that density and hardness are essentially uniform within compacts produced by the isostatic method, while the die compacts showed remarkable variation of hardness and density within the samples.

ILLUSTRATIONS
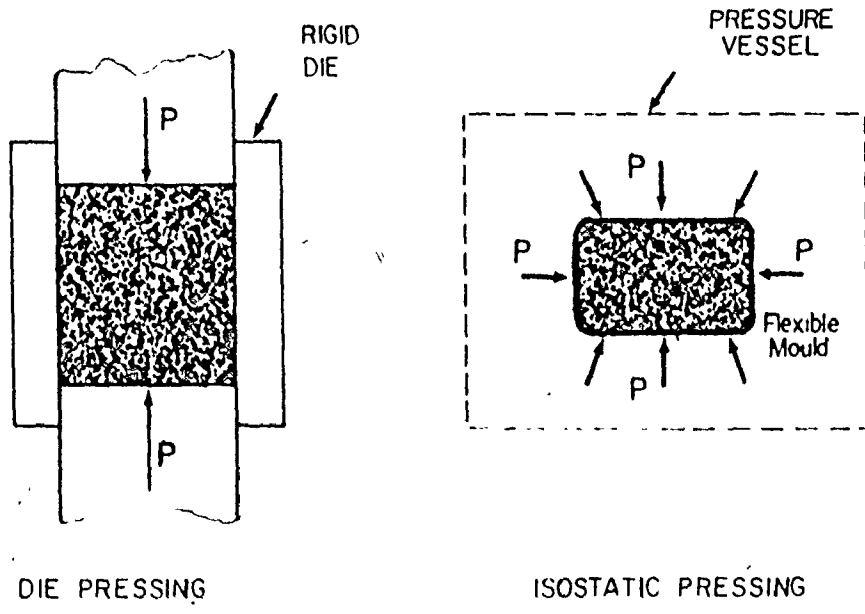
FIGURE 1   SCHEMATIC COMPARISON OF DIE AND ISOSTATIC PRESSING
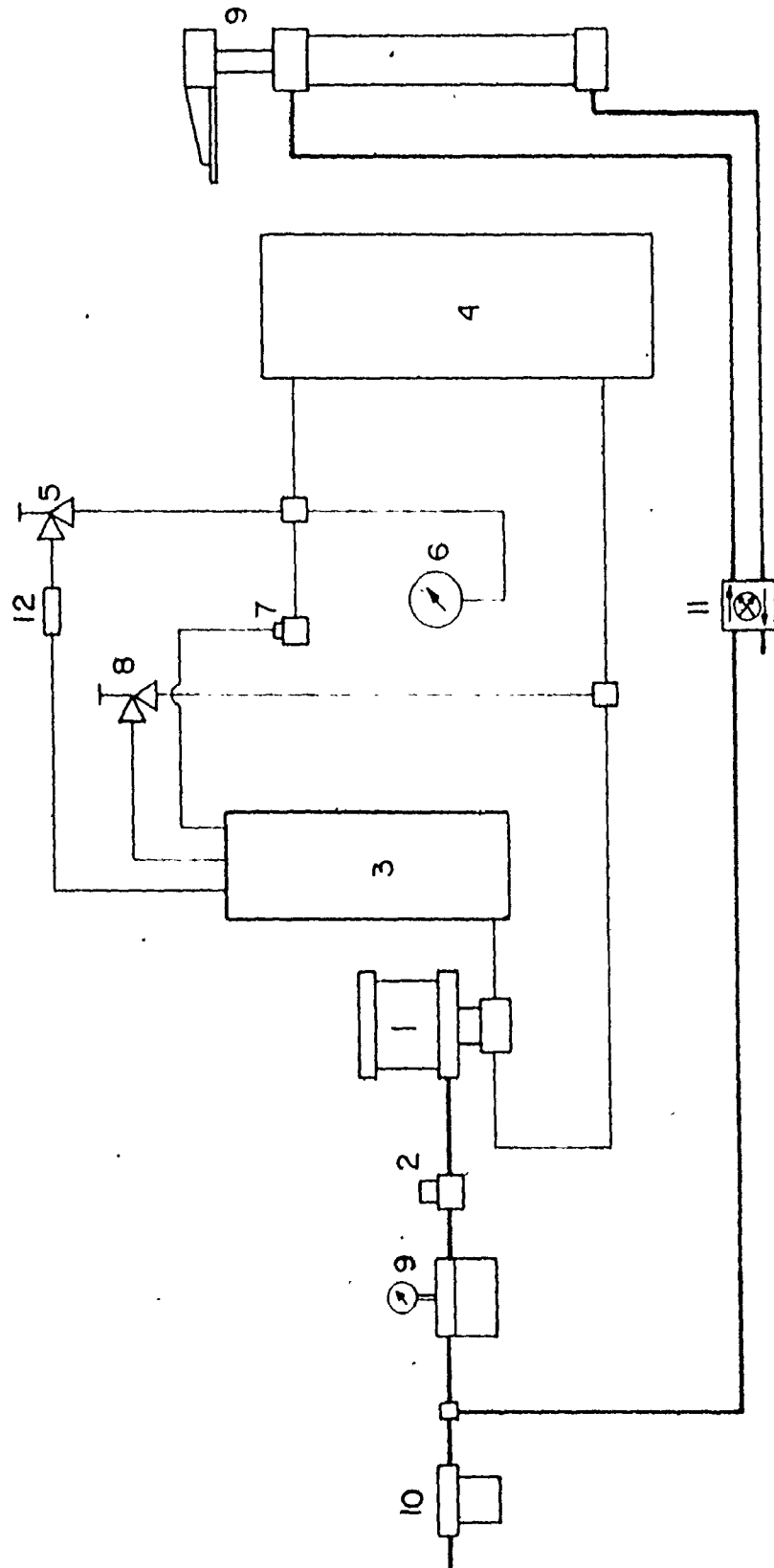
FIGURE 2   SCHEMATIC PIPING SYSTEM OF AN ISOSTATIC PRESS

KEY TO FIGURE 2

1.   Haskel Pump

2.   Skinner Valve

3.   Fluid Reservoir

4.   Pressure Vessel

5.   Shut-off Valve

6.   Pressure Gauge

7.   Safety Head Assembly

8.   Pressure Release Valve

9.   Air Cylinder

10.   Filter

11.   4-Way Control Valve

12.   Window

FIGURE 3   TRANSDUCER MOUNTING AND CABLE CARRIER

(a)

(b)
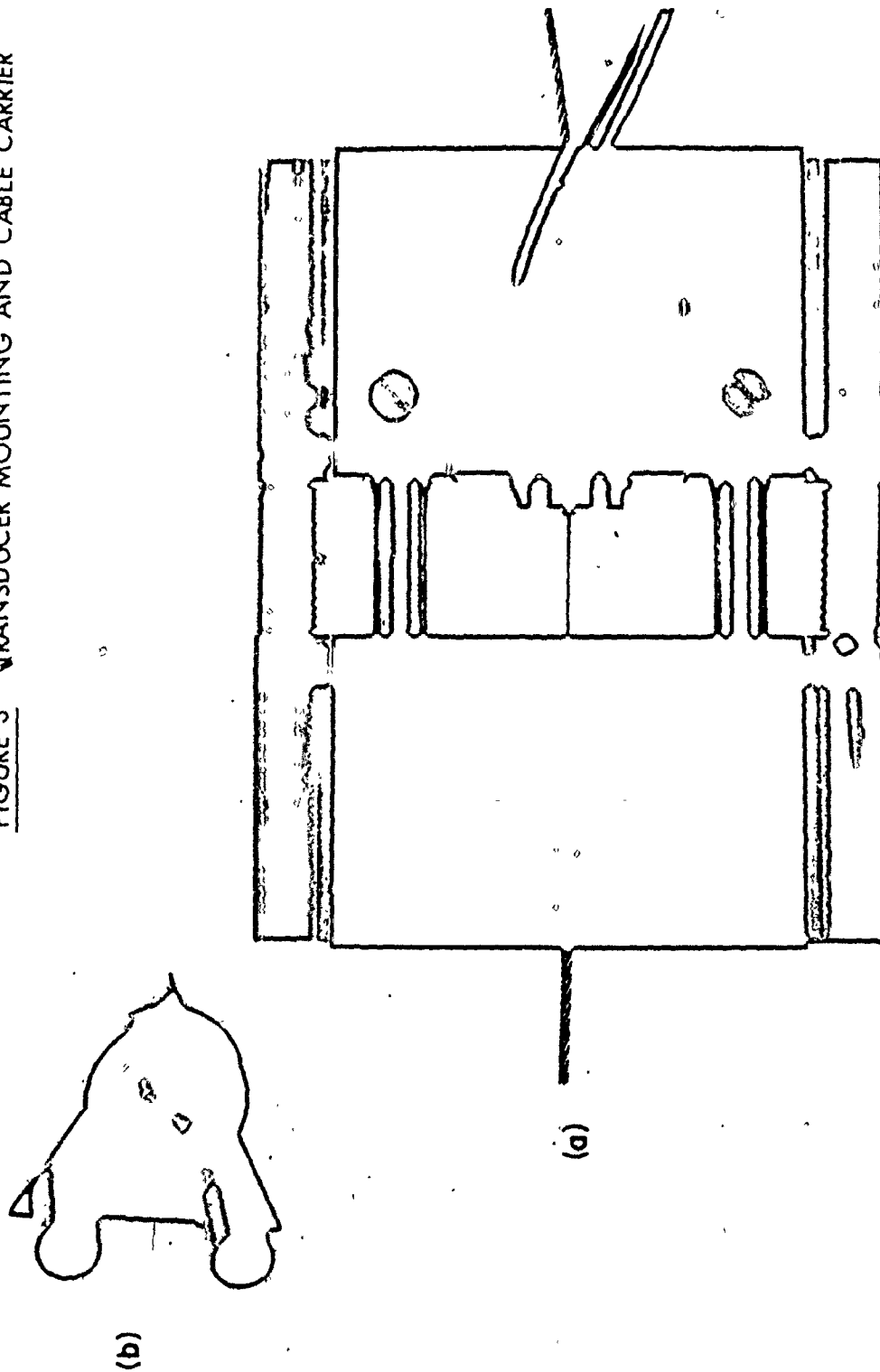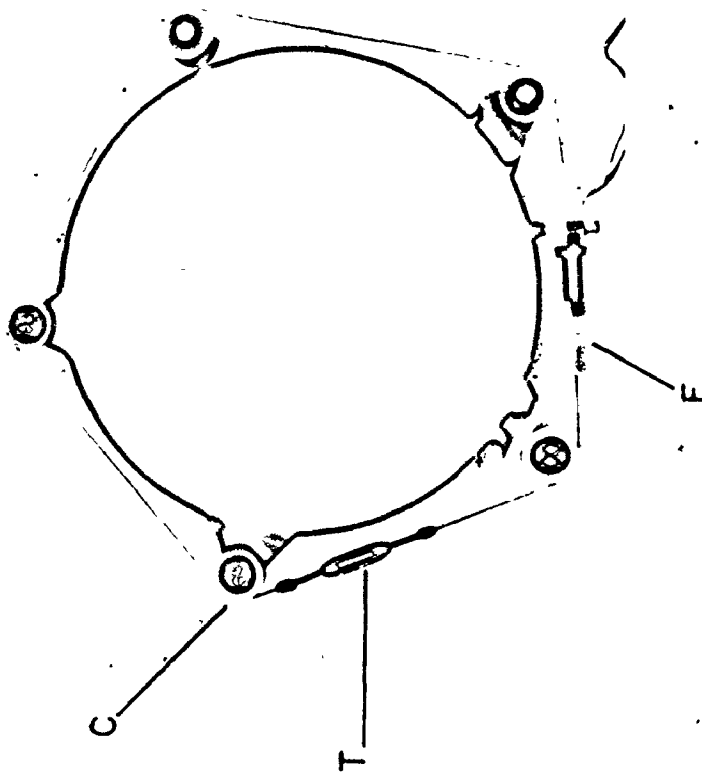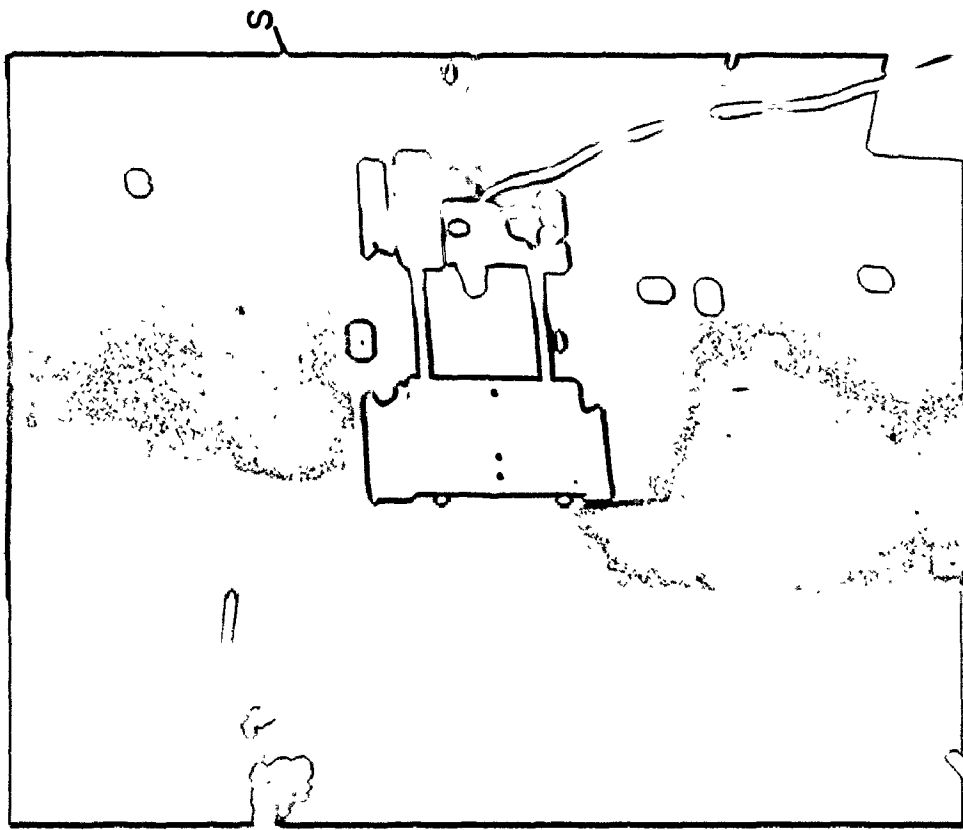
FIGURE. 4   EXTERNAL VIEW OF TI   ASURING SYSTEM
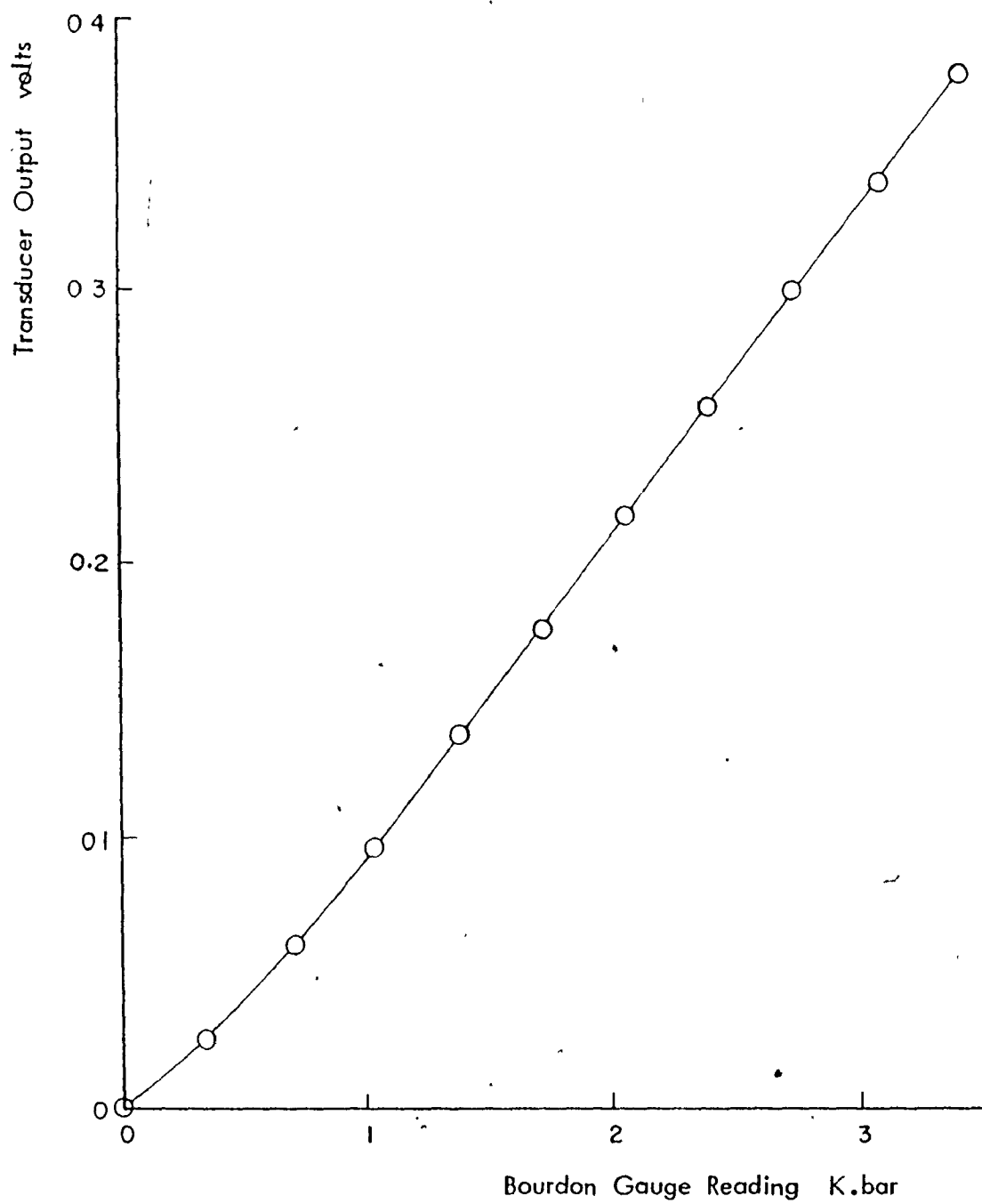
FIGURE 5   CALIBRATION OF PRESSURE MEASURING SYSTEM
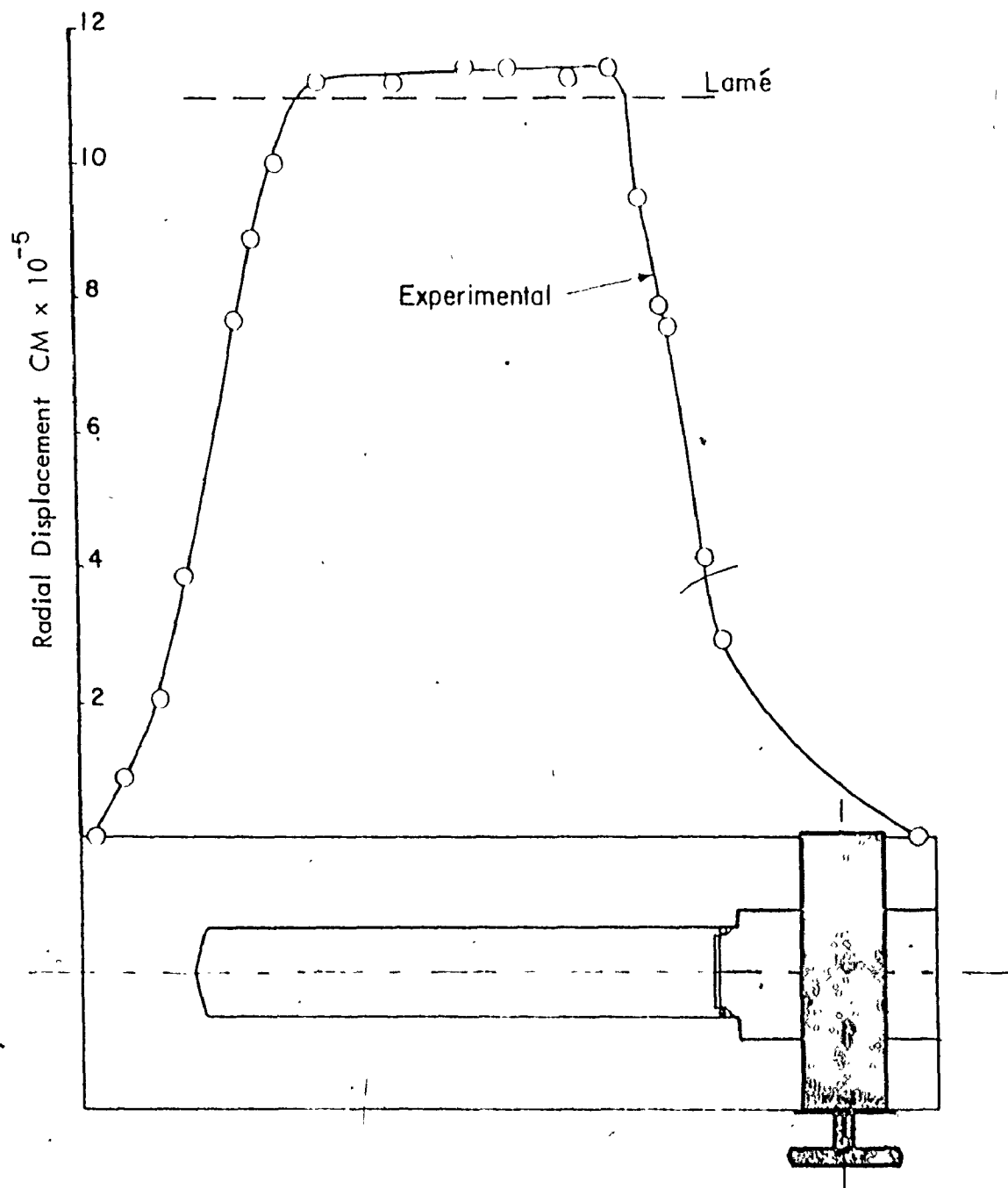
FIGURE 6   RADIAL DISPLACEMENT OF THE PRESSURE VESSEL
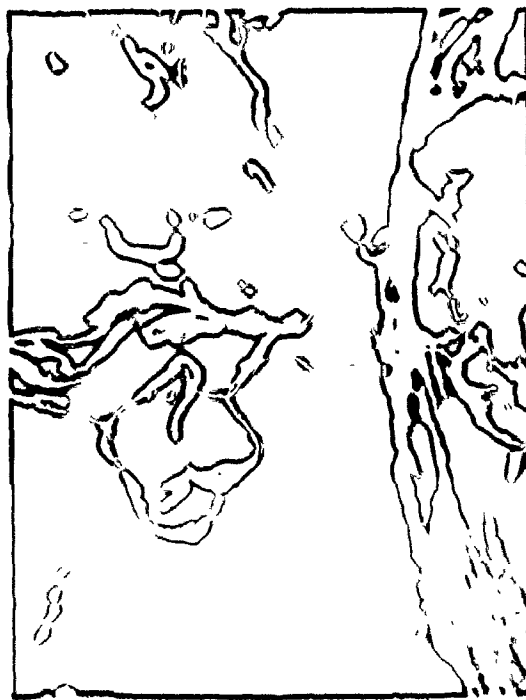
190X   950X

FIGURE 7   SCANNING ELECTRON MICROGRAPHS OF ALUMINUM POWDER

190X   950X

FIGURE 8   SCANNING ELECTRON MICROGRAPHS OF IRON POWDER
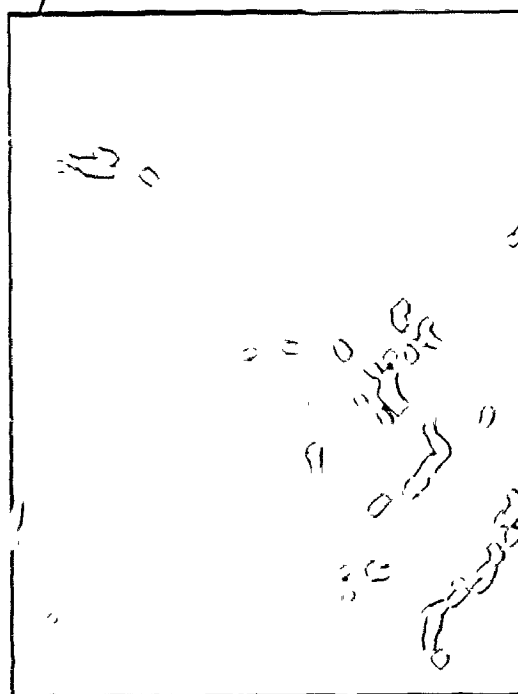
950X   1900X

FIGURE 9   SCANNING ELECTRON MICROGRAPHS OF COPPER POWDER
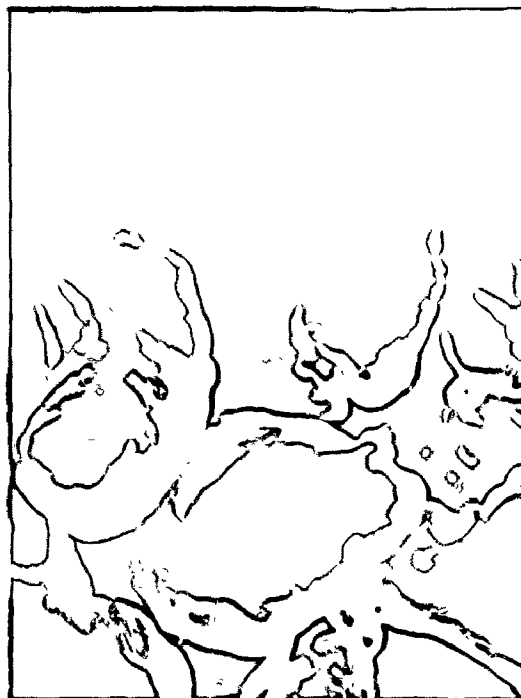
950X   1900X

FIGURE 10   SCANNING ELECTRON MICROGRAPHS OF LEAD POWDER
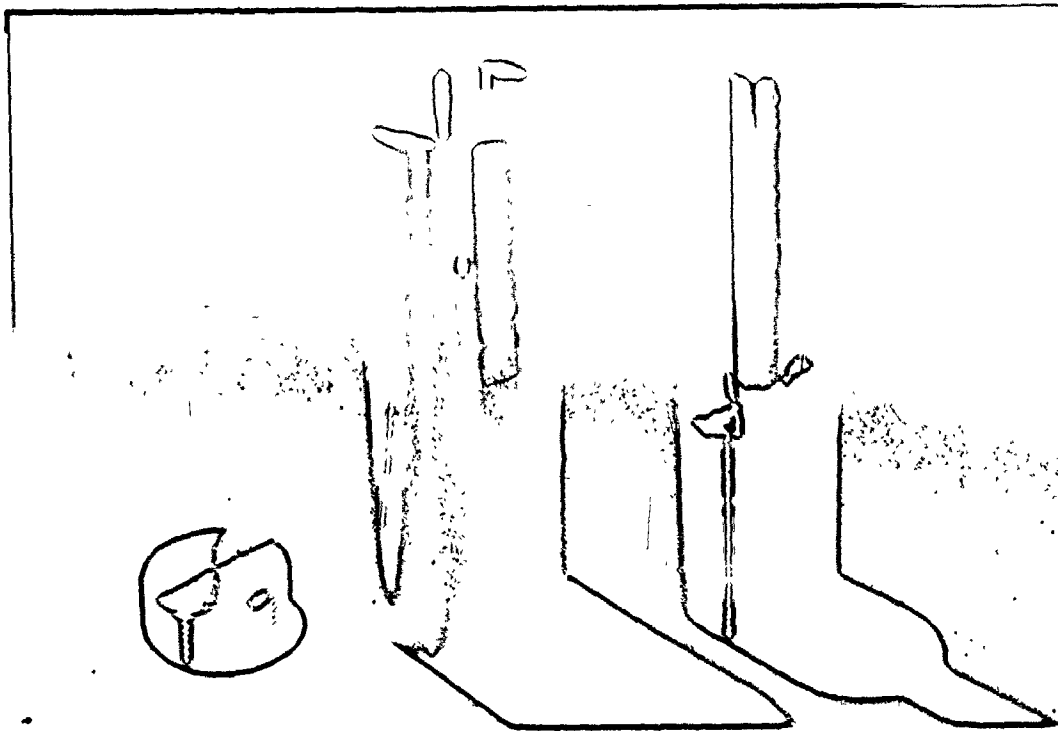
FIGURE 11   EXTERNAL VIEW OF ALUMINUM MOULD
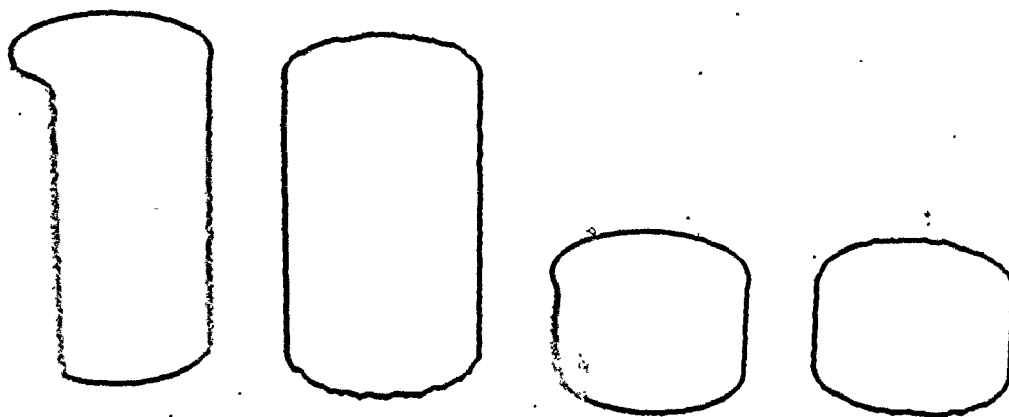
FIGURE 12   EFFECT OF USING COOLANT IN MACHINING
ALUMINUM SAMPLES
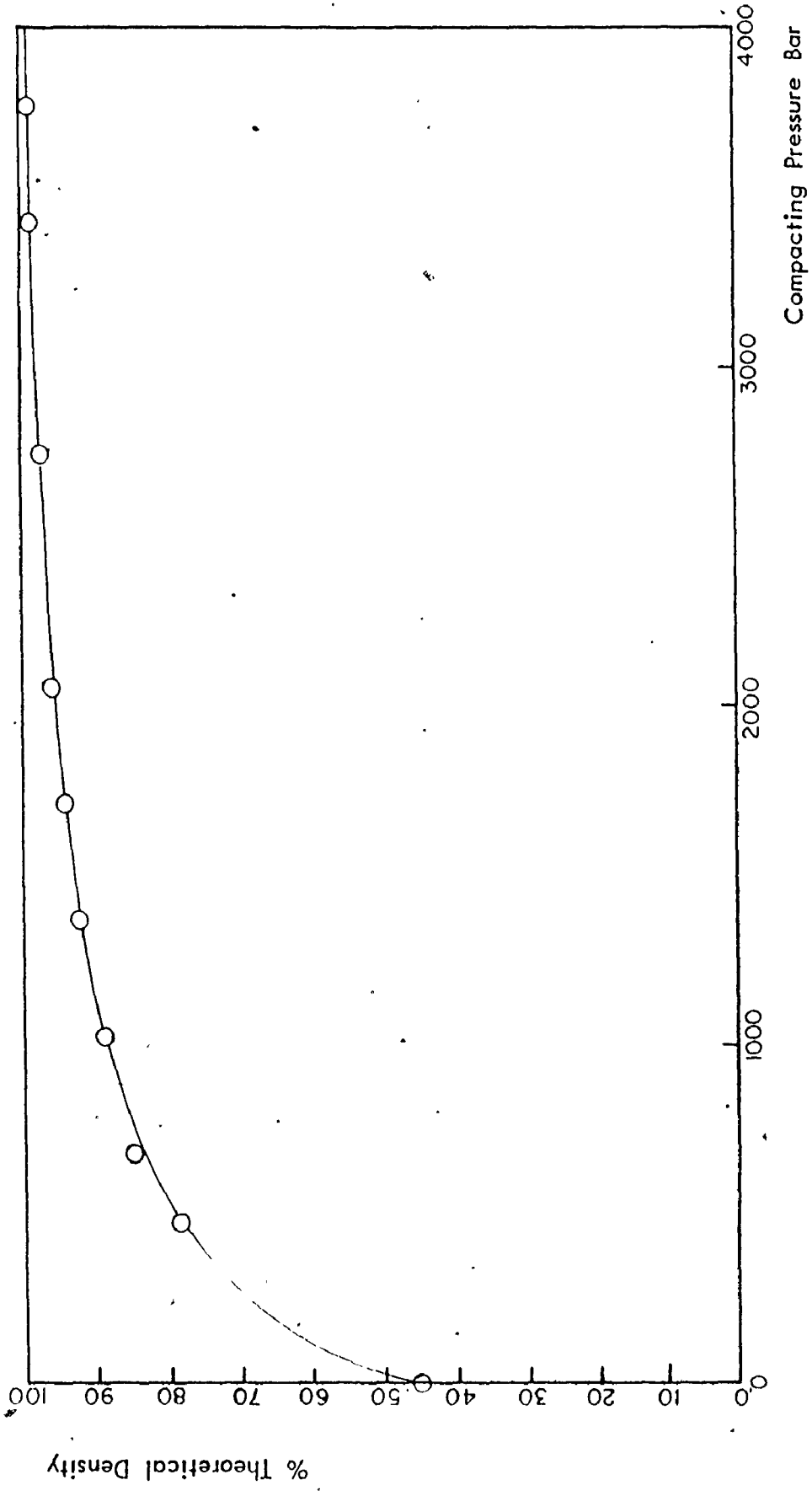
FIGURE 13   EXPERIMENTAL PRESSURE-DENSITY DATA EXPRESSED DIRECTLY
FOR ISOSTATICALLY COMPACTED ALUMINUM COMPACTS
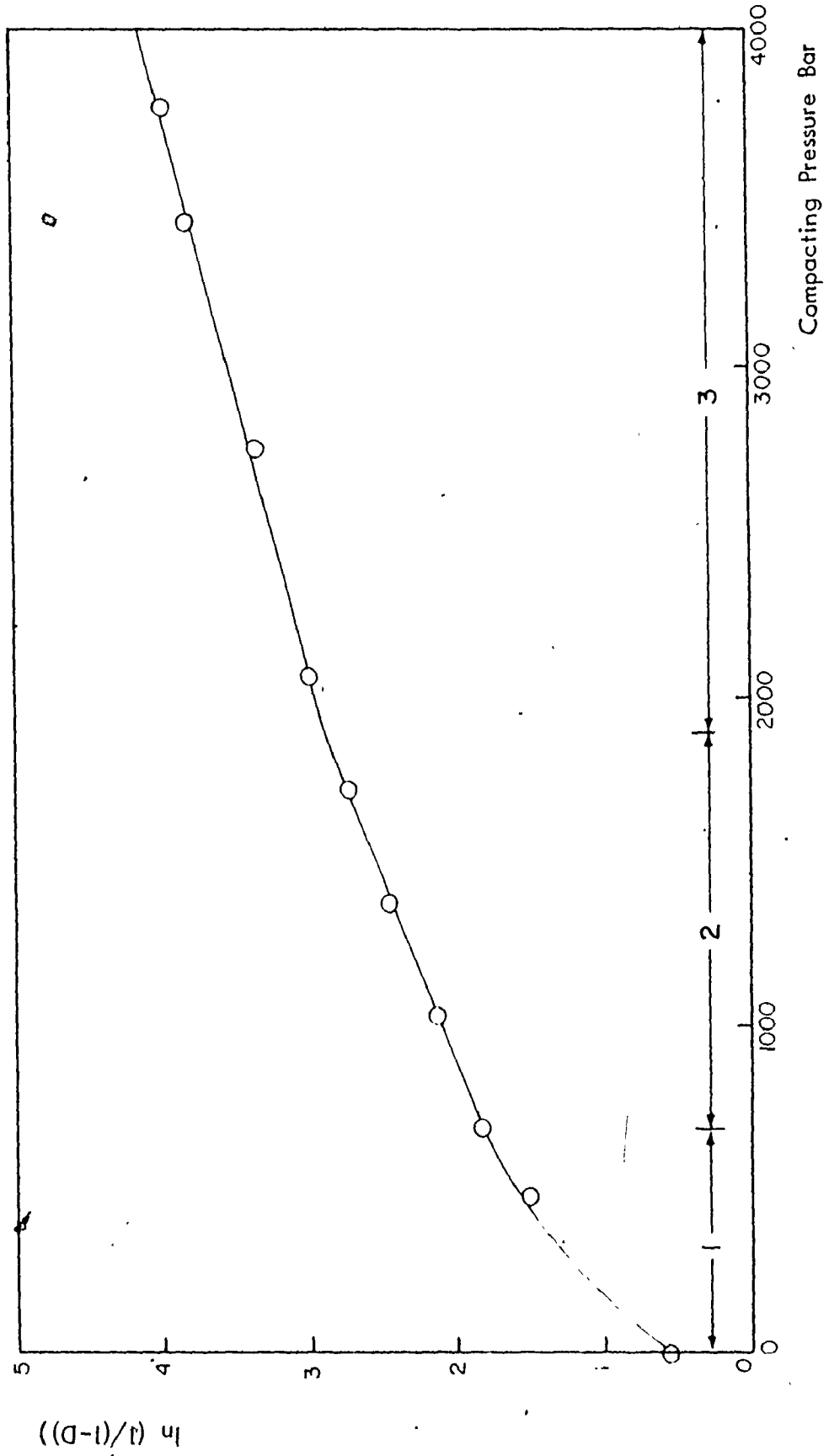
FIGURE 14 Ln (1/(1-D)) VERSUS PRESSURE FOR ISOSTATICALLY
COMPACTED ALUMINUM POWDER
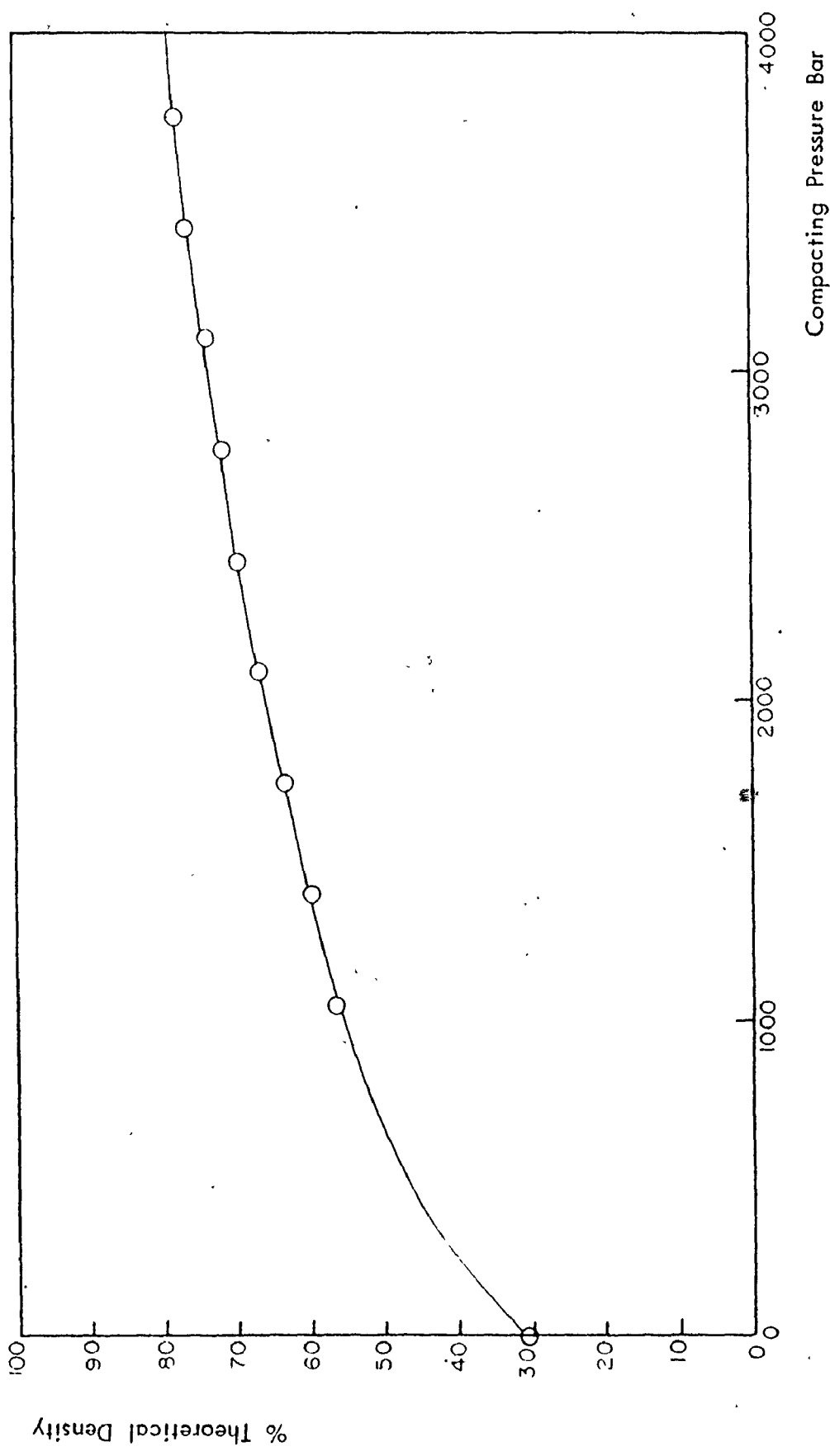
FIGURE 15   EXPERIMENTAL PRESSURE–DENSITY DATA EXPRESSED DIRECTLY
FOR ISOSTATICALLY COMPACTED IRON POWDER
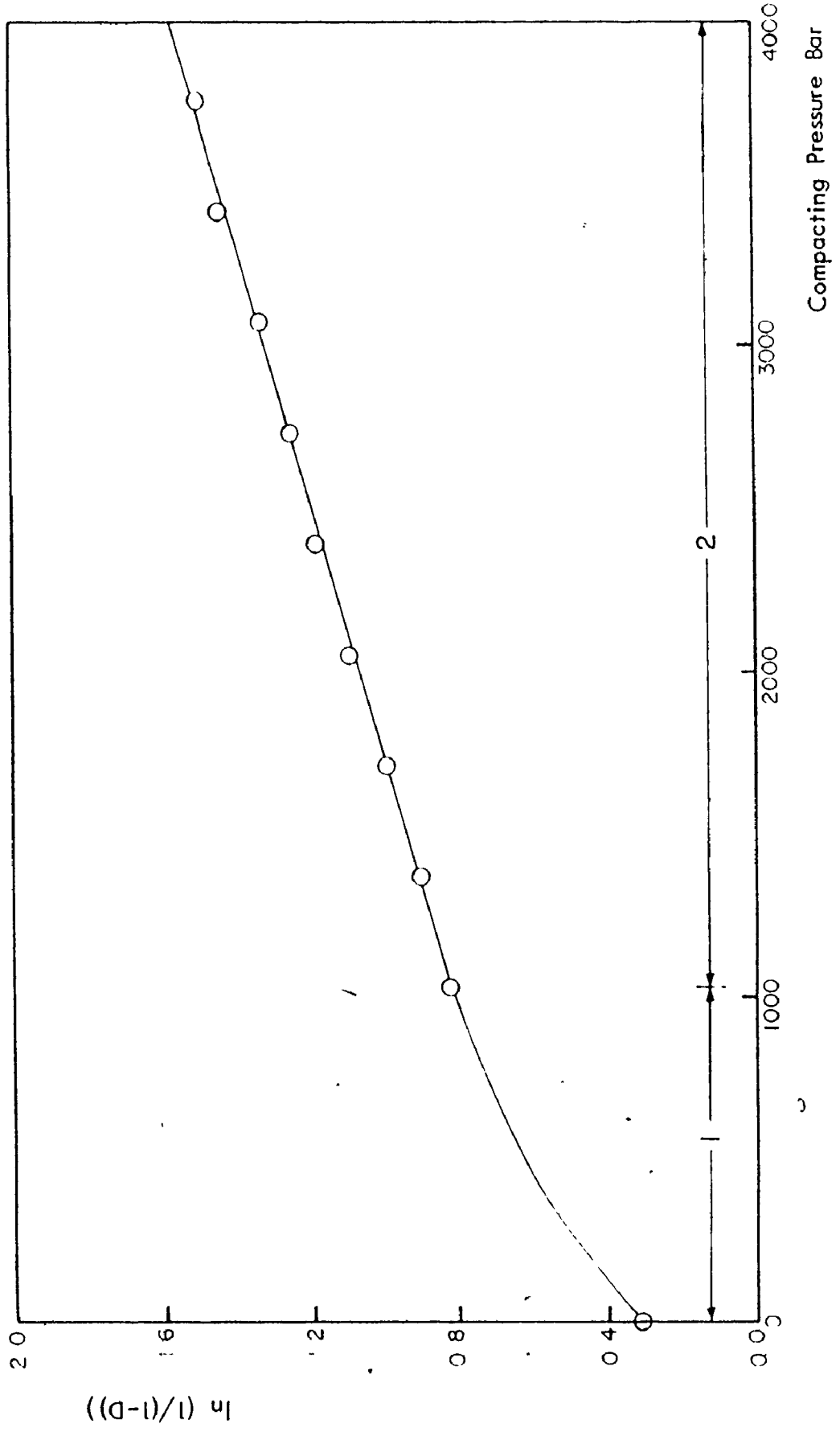
FIGURE 16   Ln (1/(1-D)) VERSUS PRESSURE FOR ISOSTATICALLY
COMPACTED IRON POWDER
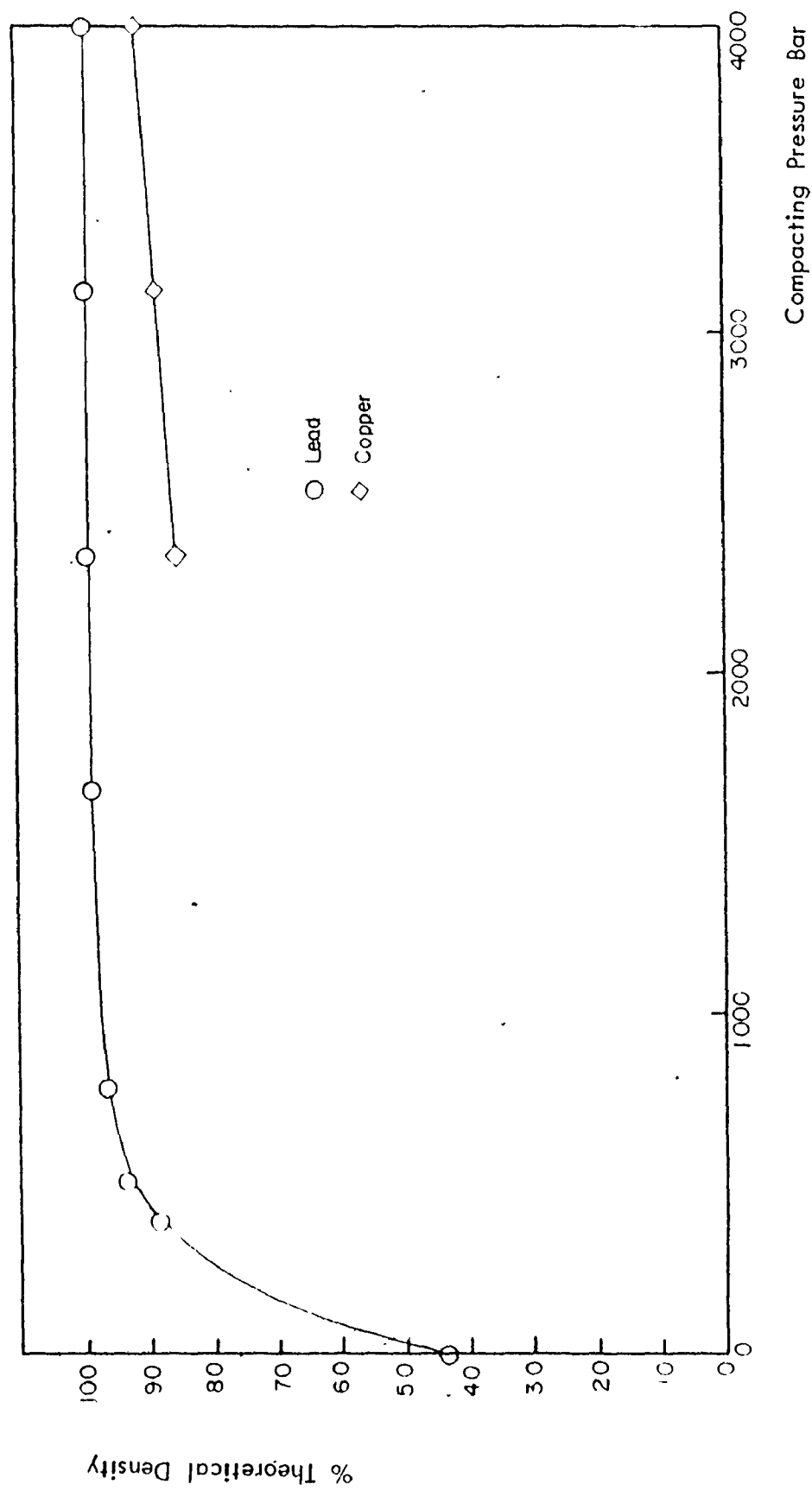
FIGURE 17   EXPERIMENTAL PRESSURE-DENSITY DATA EXPRESSED DIRECTLY
FOR ISOSTATICALLY COMPACTED LEAD AND COPPER POWDER
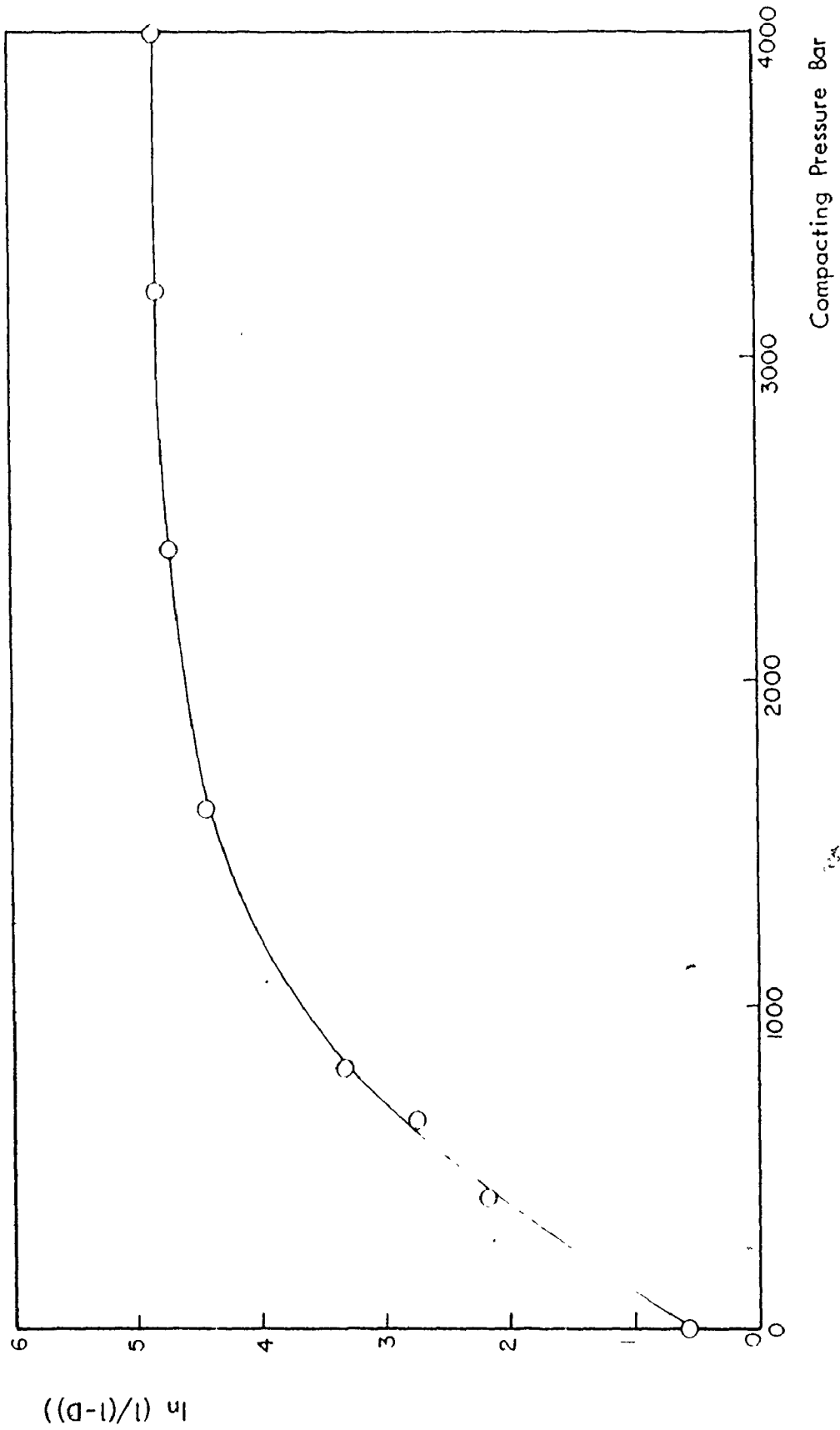
FIGURE 18   Ln (1/(1-D)) VERSUS PRESSURE FOR ISOSTATICALLY
COMPACTED LEAD POWDER

690 bar   250X

690 bar   1200X

1380 bar   250X

1380 bar   1200X
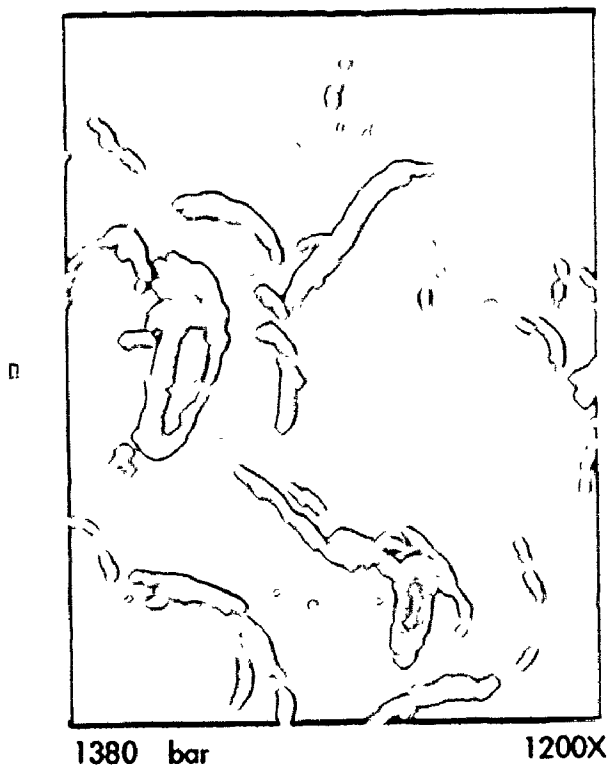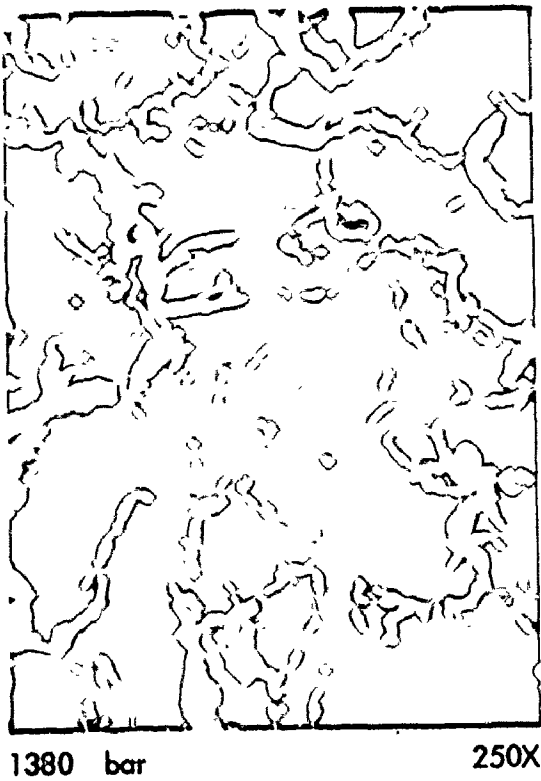
FIGURE 19   SCANNING ELECTRON MICROGRAPHS FOR ALUMINUM
COMPACTS
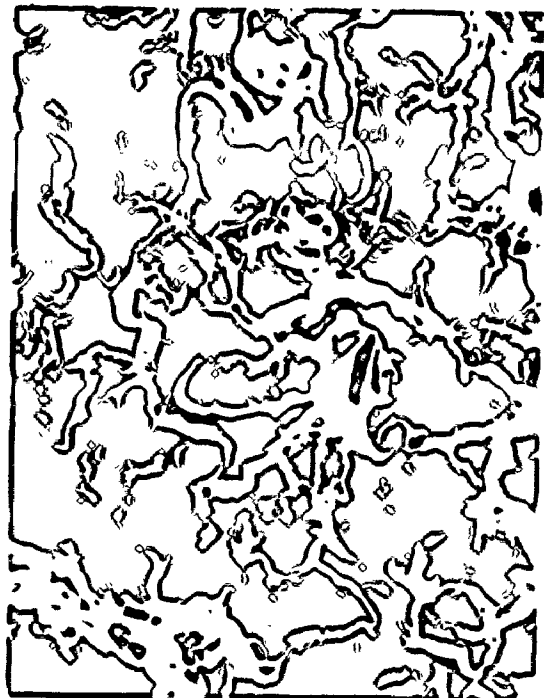
2760   bar   250X
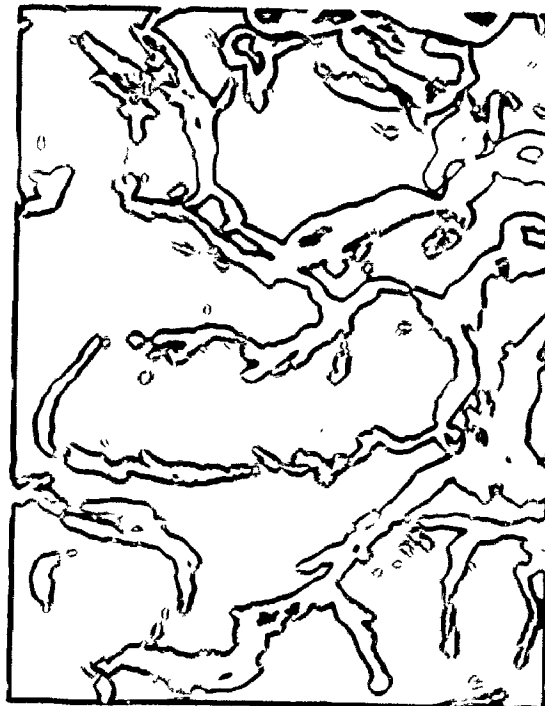
2760   bar   650X

3790   bar   250X

3790   bar   650X

FIGURE 19 (Cont.)   SCANNING ELECTRON MICROGRAPHS FOR
ALUMINUM COMPACTS
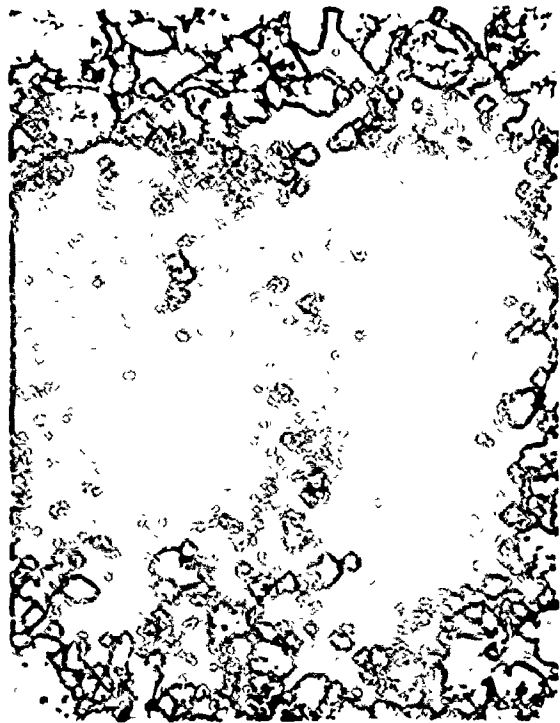
690 bar   103X
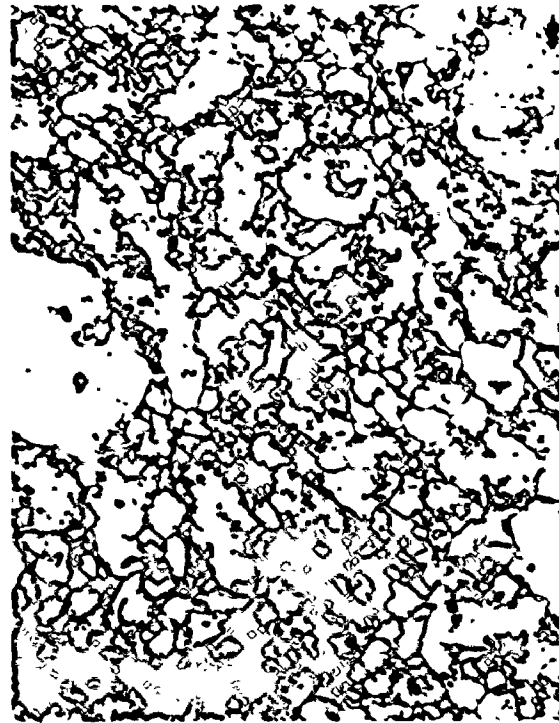
1380 bar   103X

2070 bar   103X

3450 bar   103X

FIGURE 20   POLISHED AND ETCHED SURFACE OF ALUMINUM COMPACTS
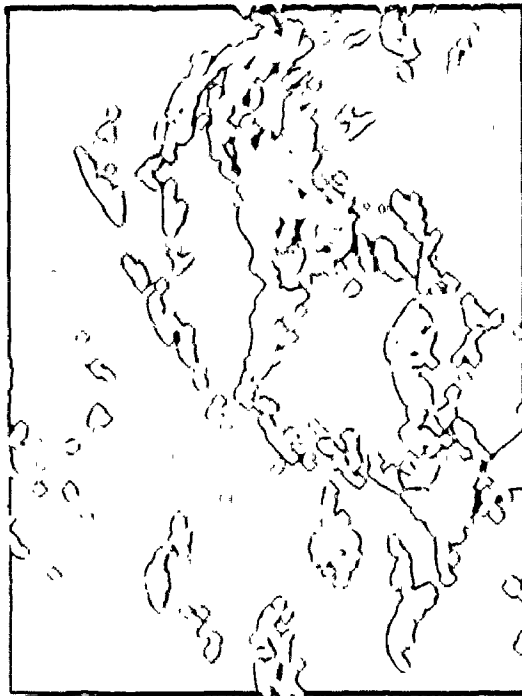
2070 bar   250X

2070 bar   1200X
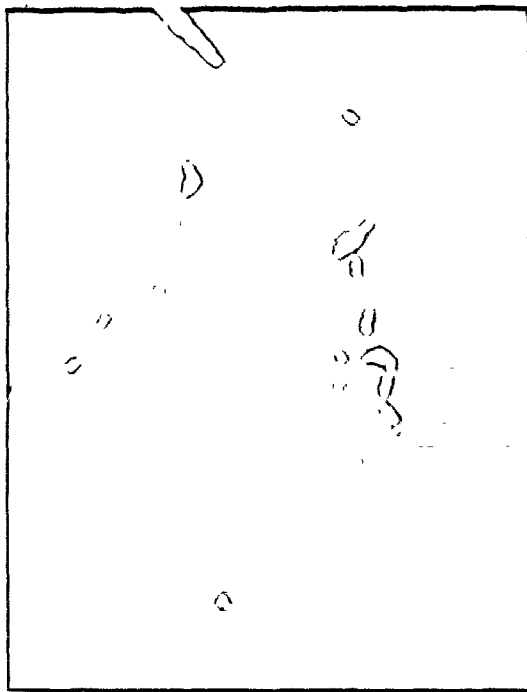
2760 bar   250X
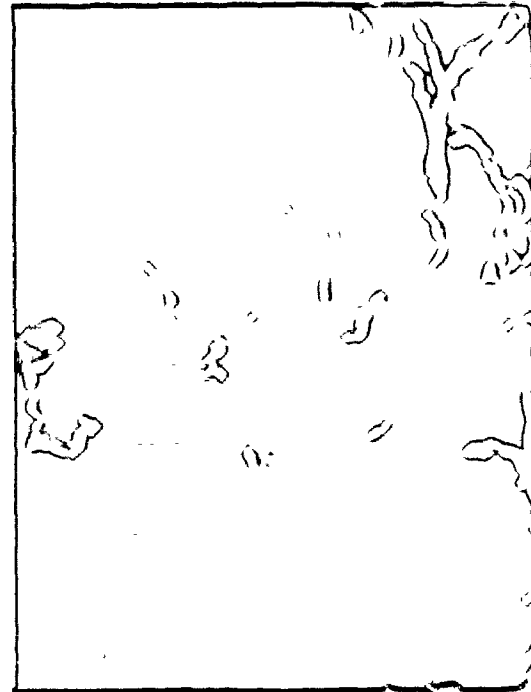
2760 bar   1200X

FIGURE 21   SCANNING ELECTRON MICROGRAPHS FOR IRON COMPACTS
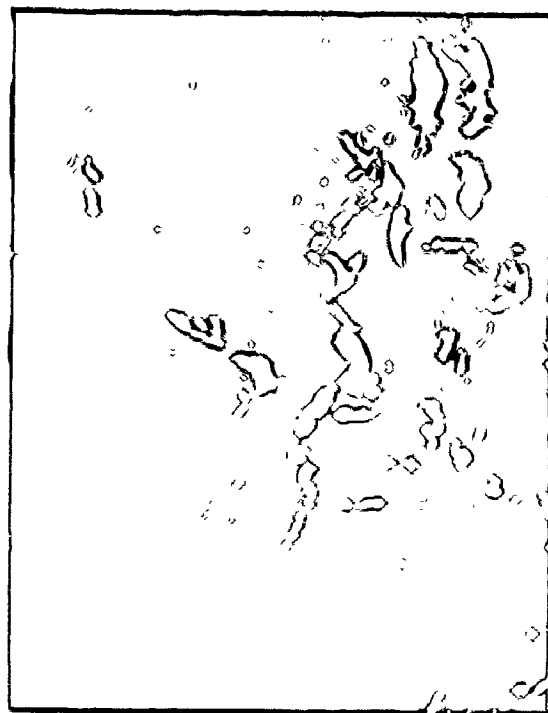
3450　bar　　　　　　　　　　250X
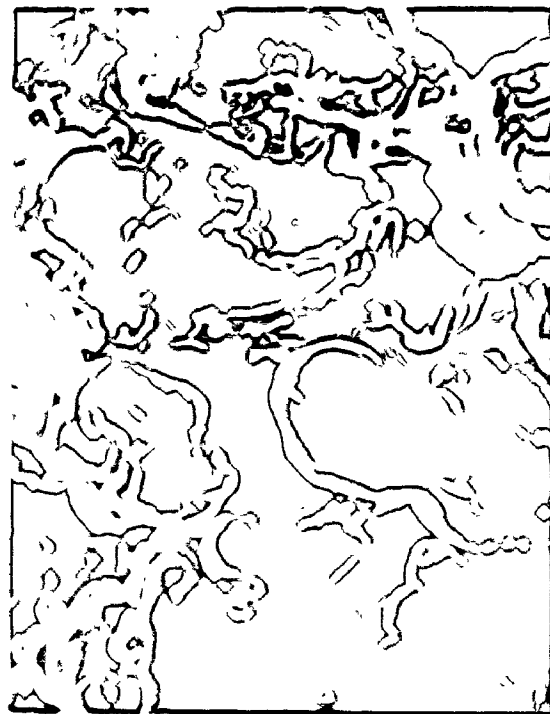
3450　bar　　　　　　　　　　1200X
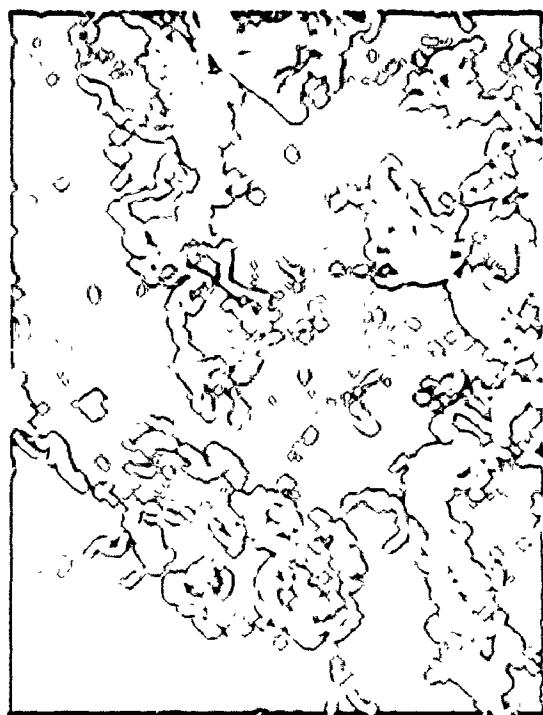
3790　bar　　　　　　　　　　250X
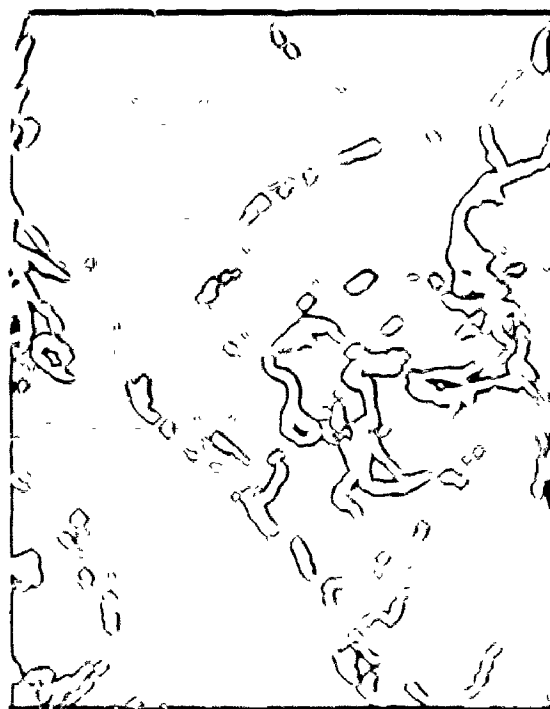
3790　bar　　　　　　　　　　1200X

FIGURE 21 (Cont.)　　SCANNING ELECTRON MICROGRAPHS FOR IRON COMPACTS
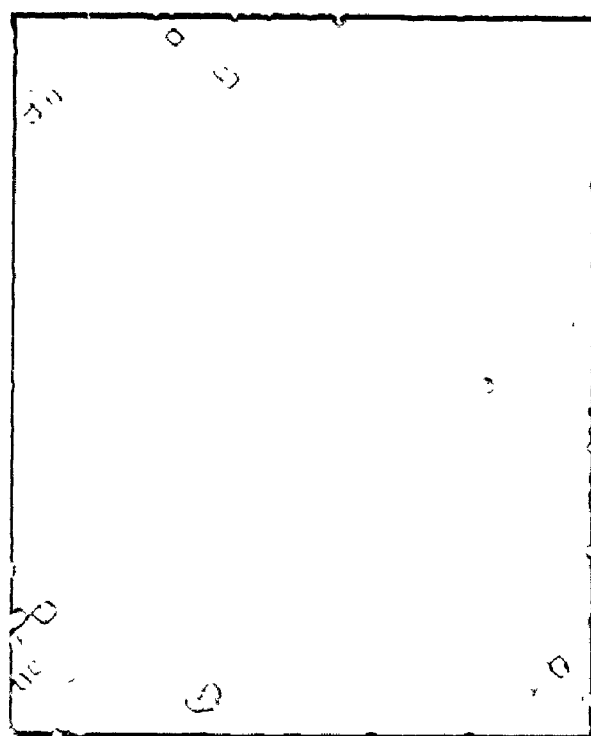
2040 bar   180X
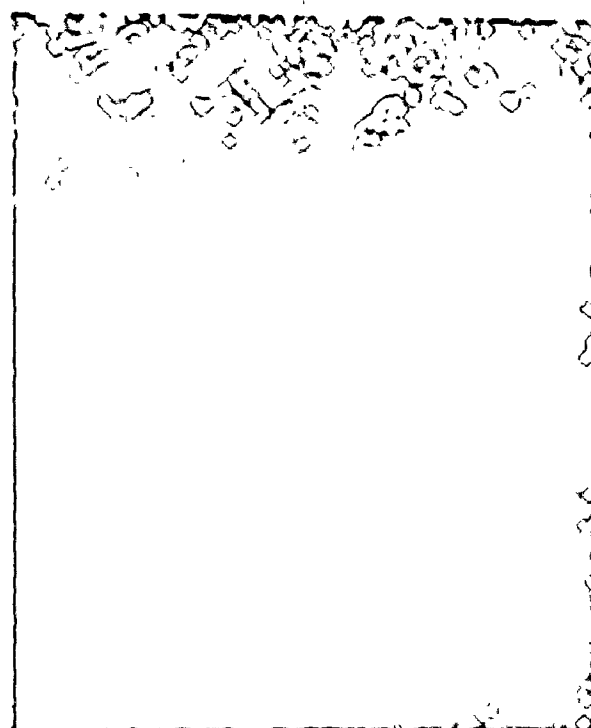
1700 bar   180X

2760 bar   180X
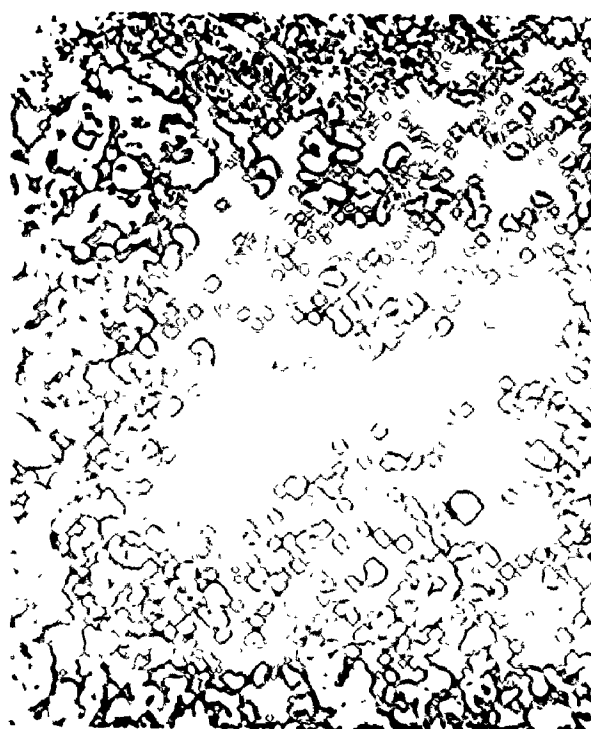
3450 bar   180X

FIGURE 22   ·POLISHED AND ETCHED SURFACE OF IRON COMPACTS

2070 bar   650X

2070 bar   1300X

3450 bar   650X

3450 bar   1300X

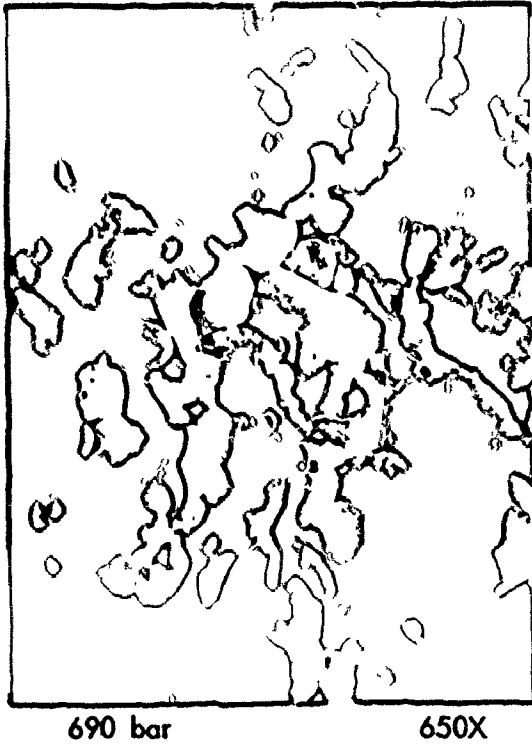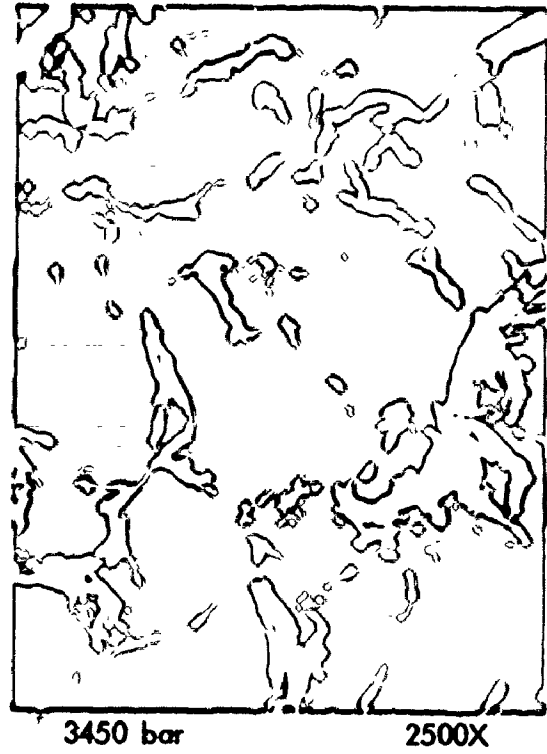FIGURE 23   SCANNING ELECTRON MICROGRAPHS OF COPPER COMPACTS

690 bar   650X   690 bar   2500X

A

1380 bar   650X   1380 bar   2500X

B
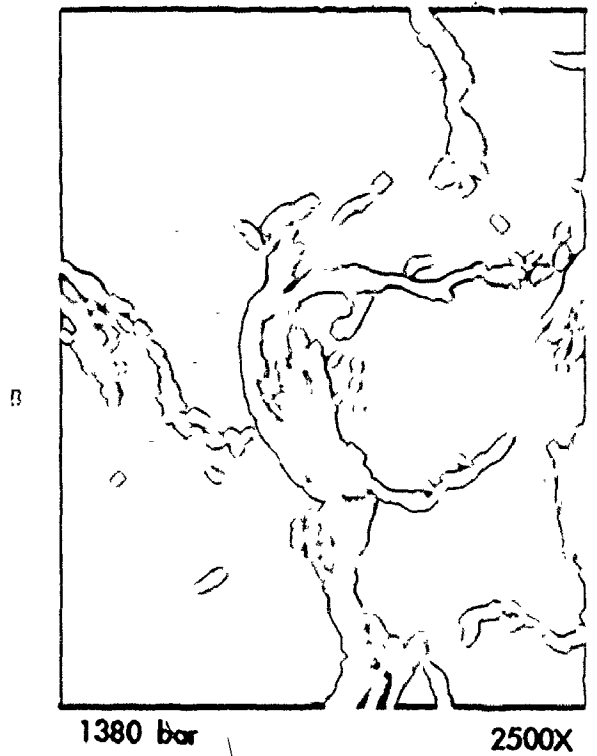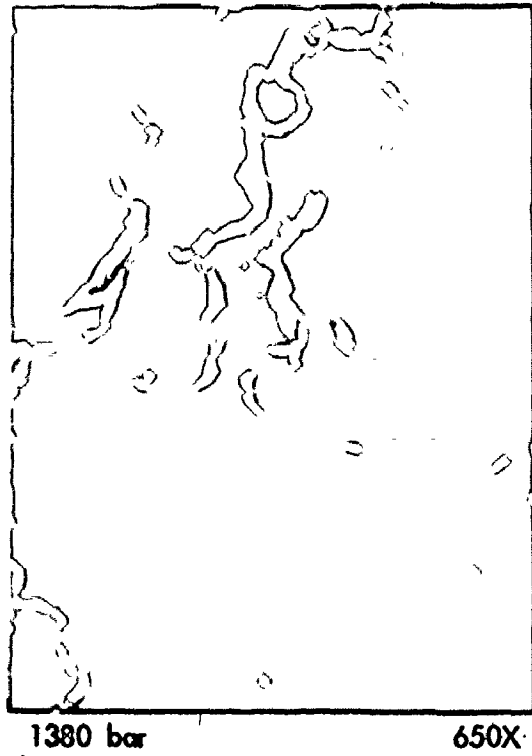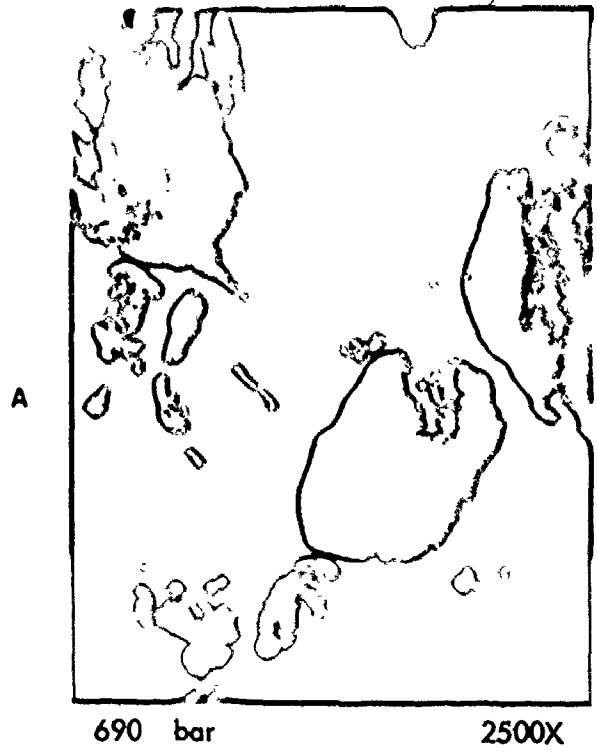
FIGURE 24   SCANNING ELECTRON MICROGRAPHS OF LEAD COMPACTS

2070 bar   650X

2070 bar   2500X

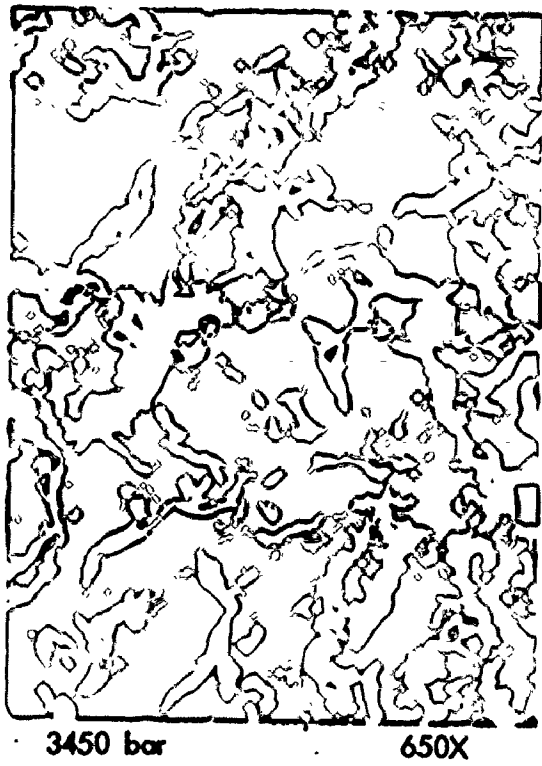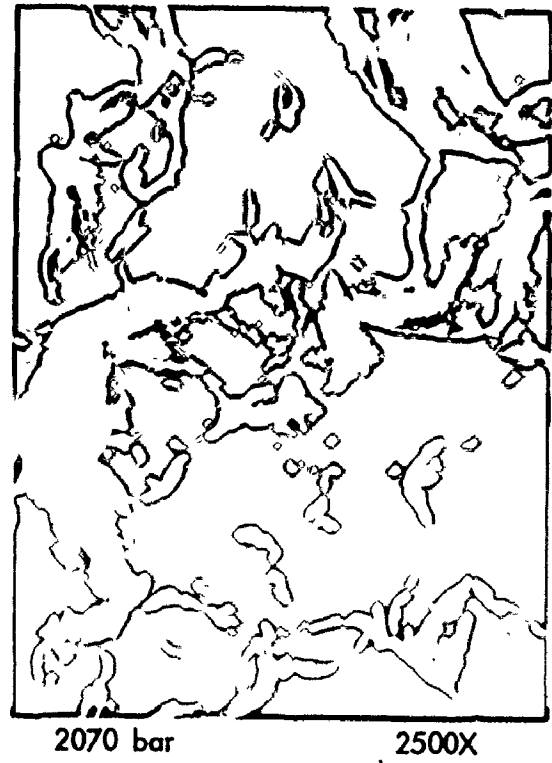3450 bar   650X

3450 bar   2500X

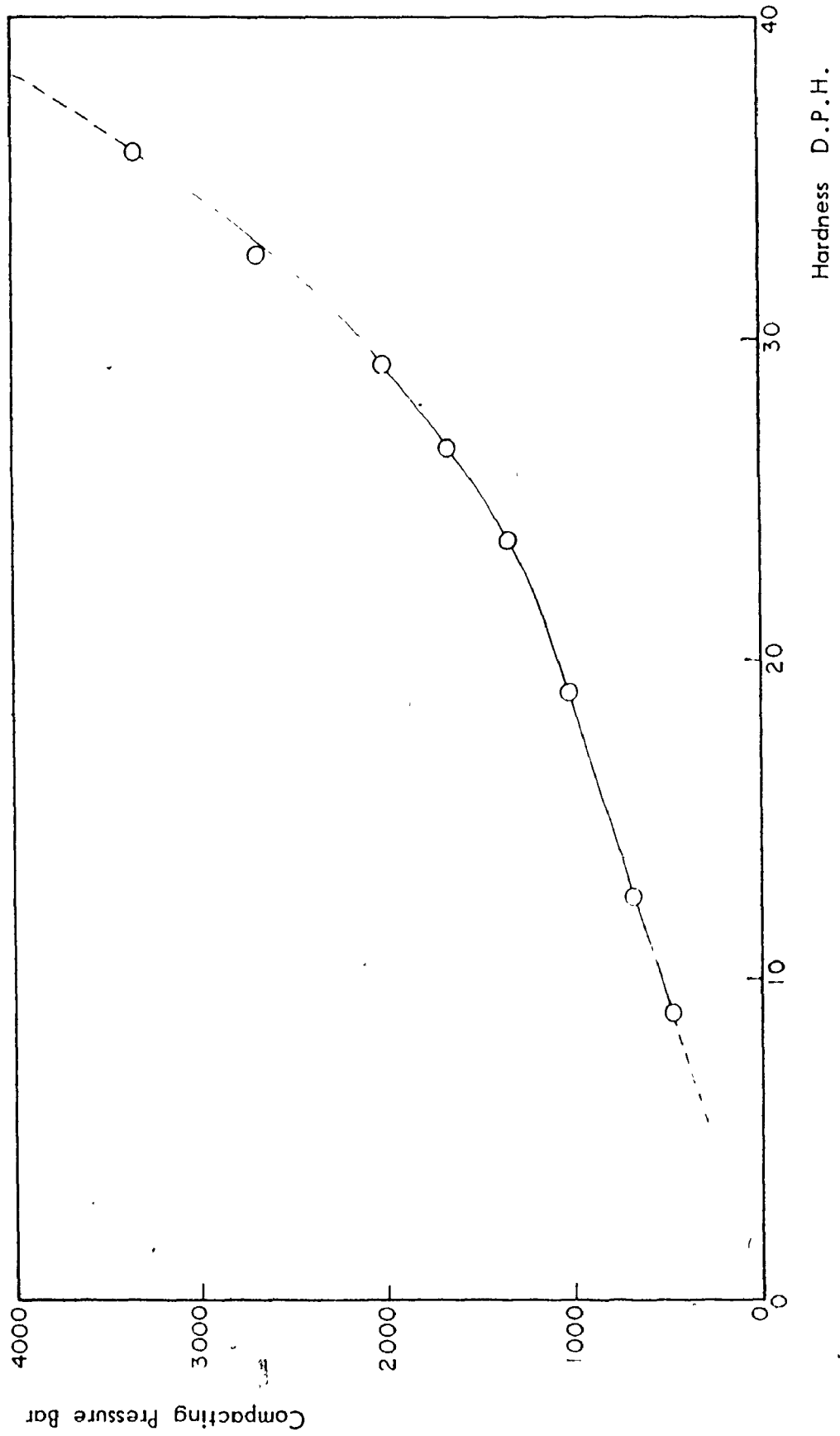FIGURE 24 (Cont.)   SCANNING ELECTRON MICROGRAPHS OF LEAD COMPACTS

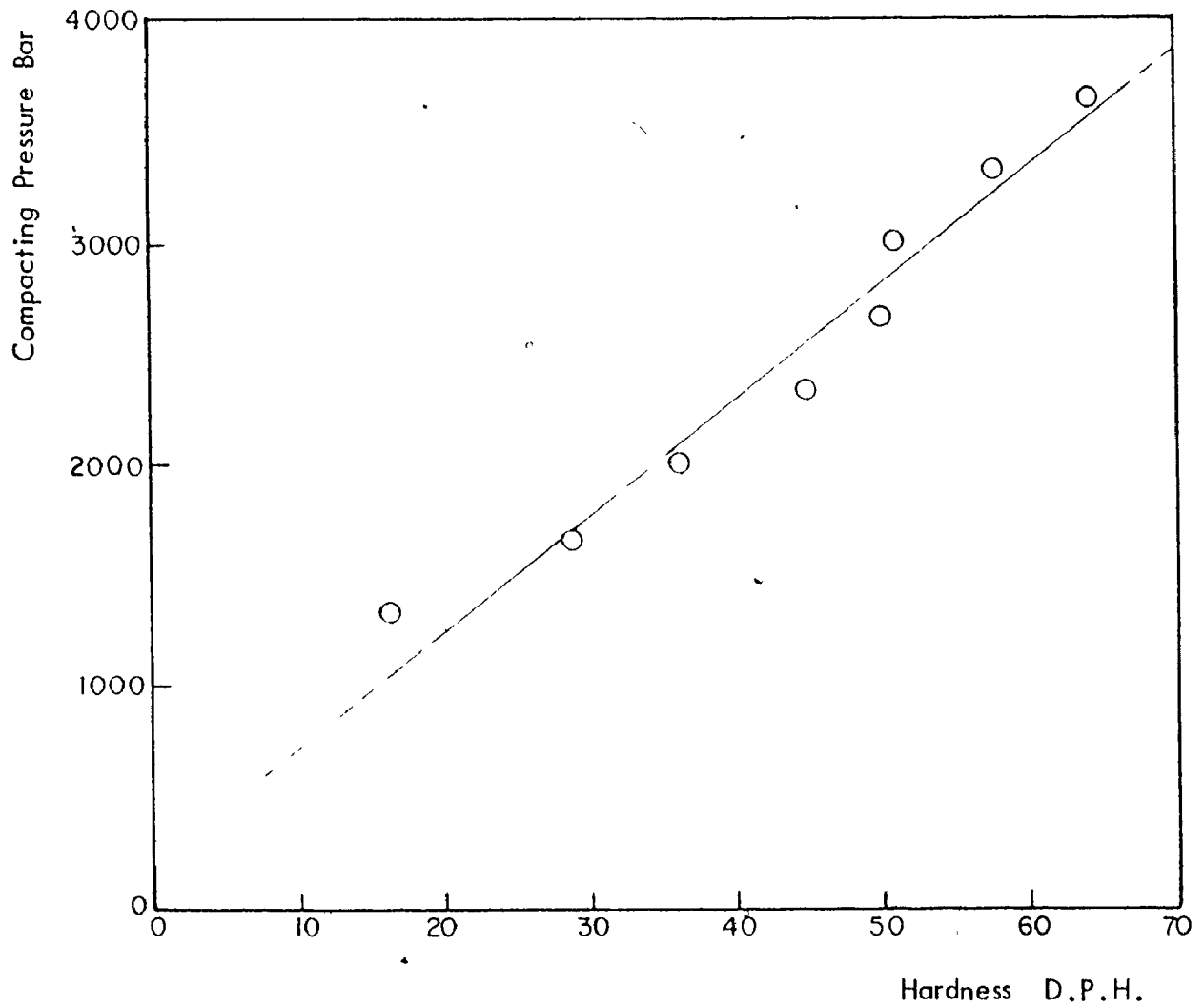FIGURE 25   PRESSURE-HARDNESS DATA FOR ALUMINUM COMPACTS
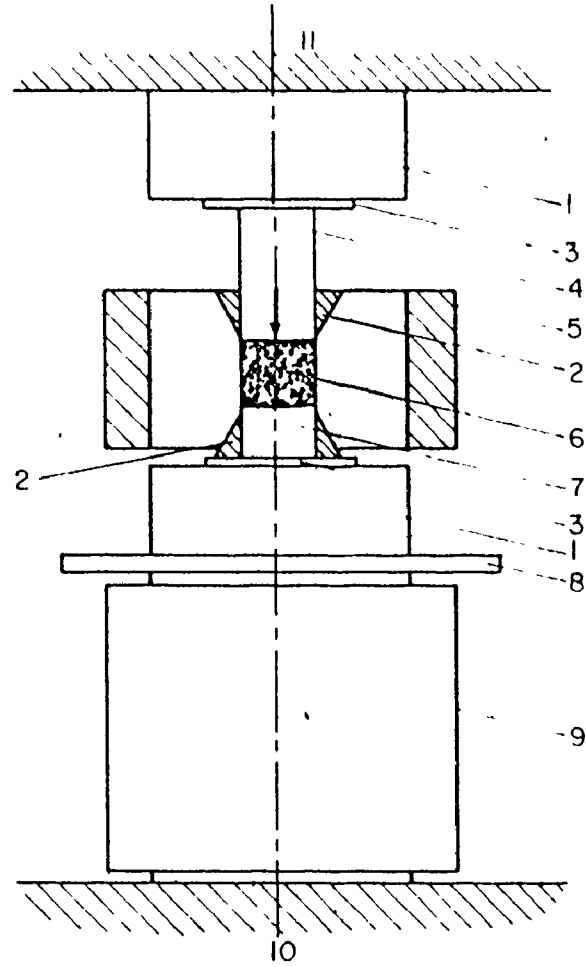
FIGURE 26   PRESSURE-HARDNESS DATA FOR IRON COMPACTS

FIGURE 27   SCHEMATIC CLOSED DIE SYSTEM

KEY TO FIGURE 27

1.   Composite disc.

2.   Guide sleeves.

3.   Copper shims.

4.   Tungsten carbide piston.

5.   Tungsten carbide die set with shrink fit steel support ring.

6.   Compaction chamber.

7.   Tungsten carbide closure.

8.   Support plate for removal of die assembly.

9.   Load cell.

10.   Movable platten of Vecor press.

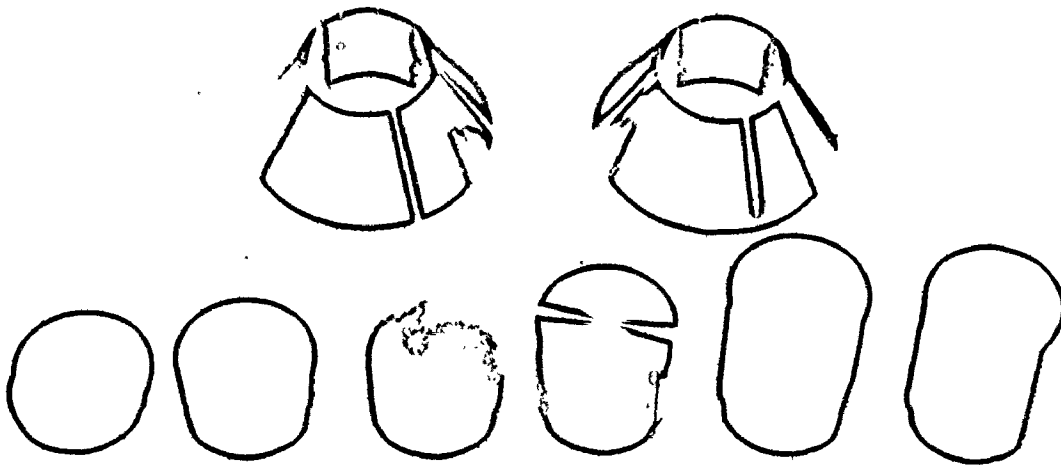11.   Fixed platten of Vecor press.

FIGURE 28   EXTERNAL VIEW OF GUIDE SLEEVES AND PISTONS
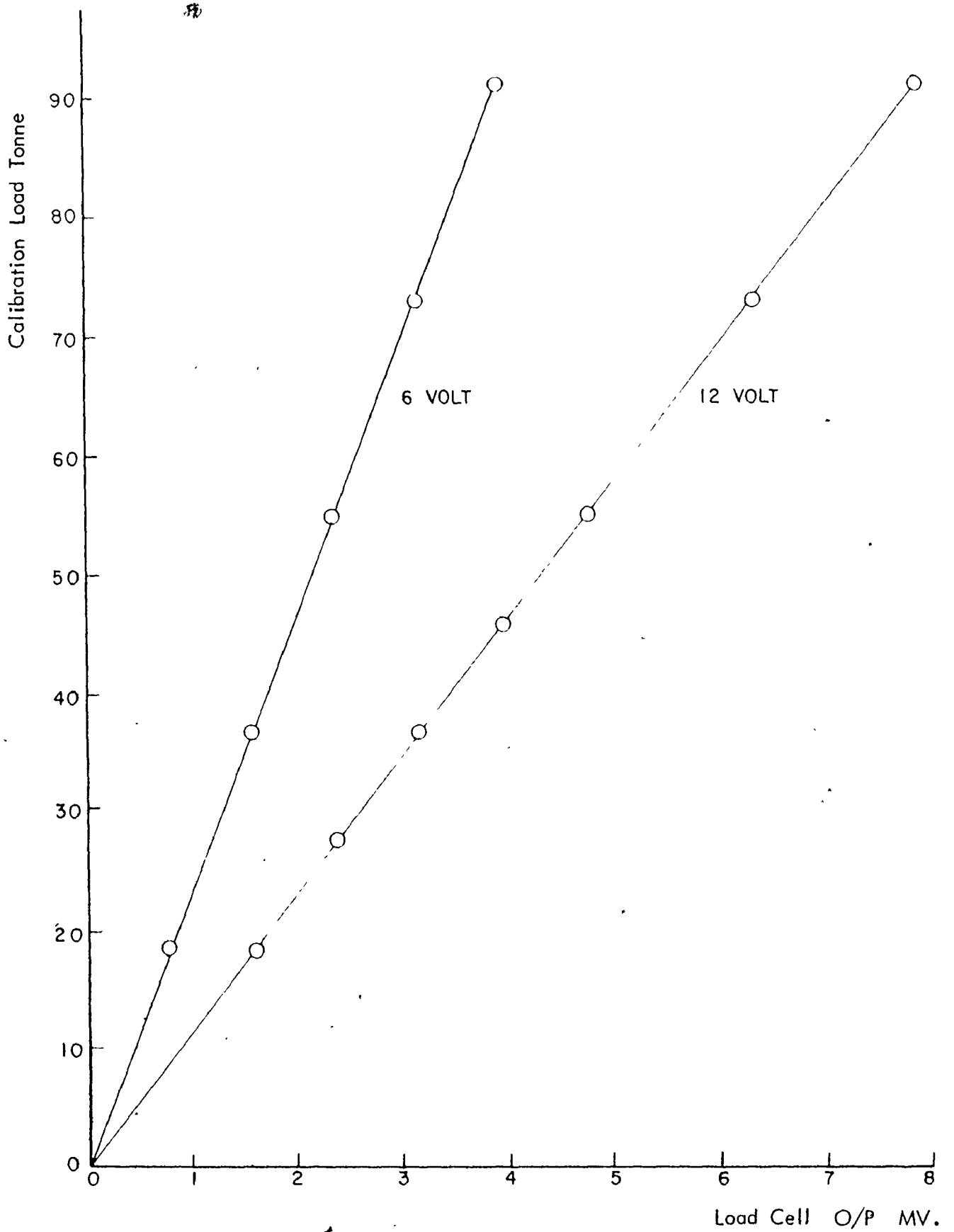
FIGURE 29   LOAD CELL CALIBRATION   (HIGH LOADS)
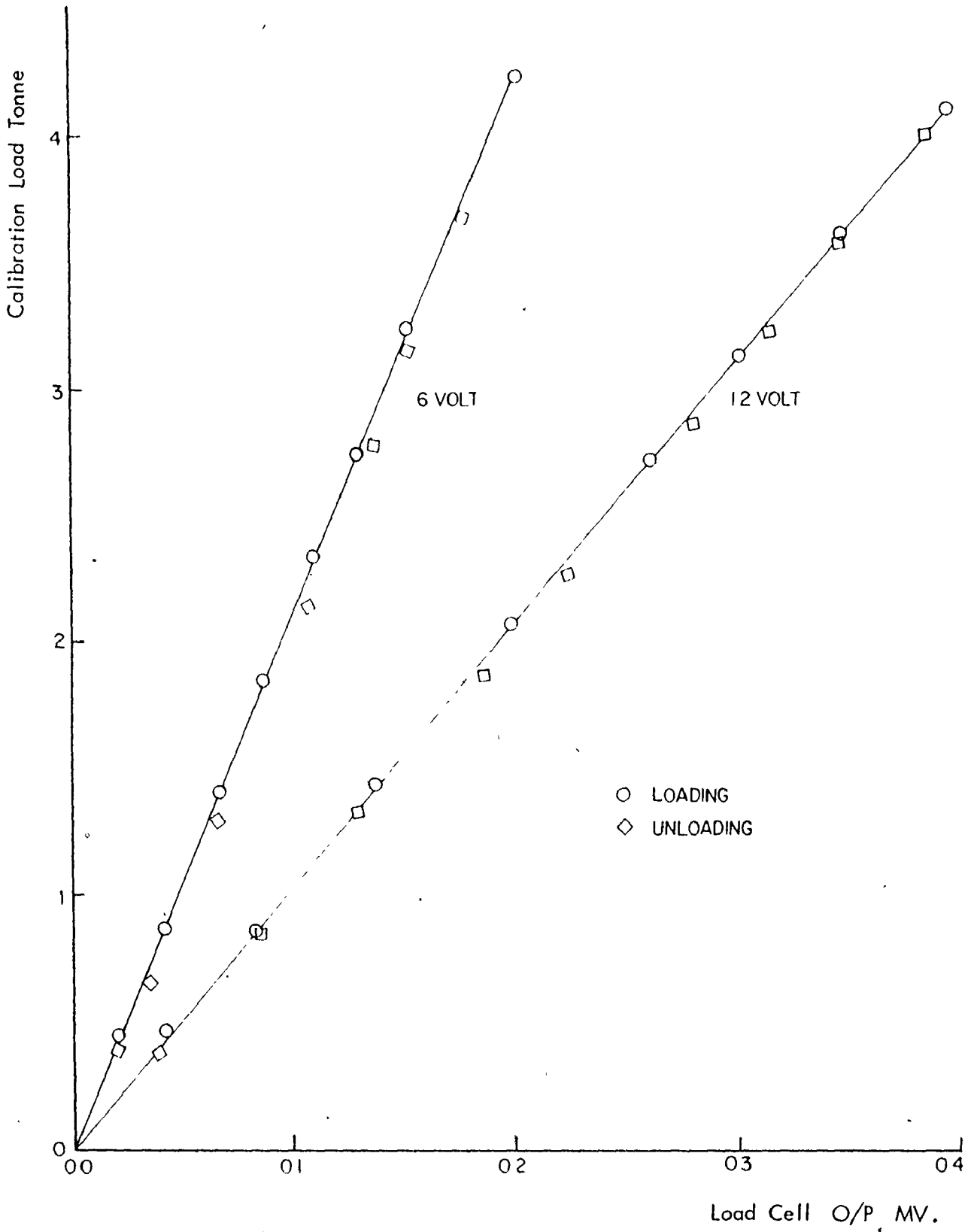
FIGURE 30   LOAD CELL CALIBRATION (LOW LOADS)
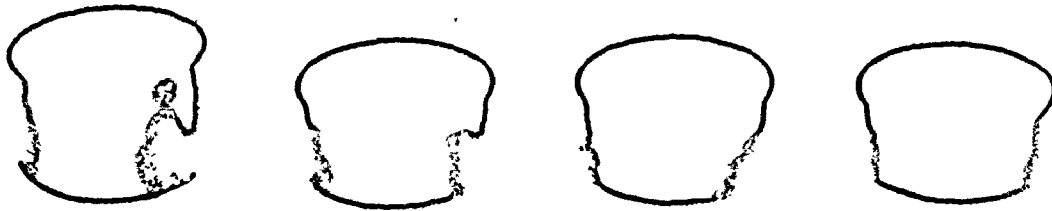
FIGURE 31   DIE COMPACTED ALUMINUM SAMPLES
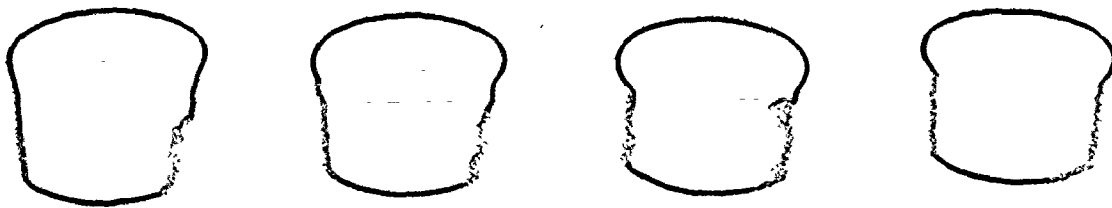
FIGURE 32   DIE COMPACTED IRON SAMPLES
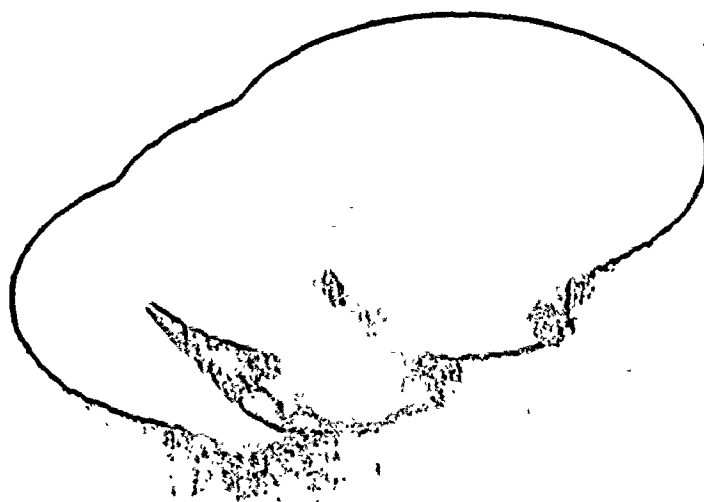
FIGURE 33   EFFECT OF INSERTING PRE-COMPACT WITHIN THE
POWDER VOLUME
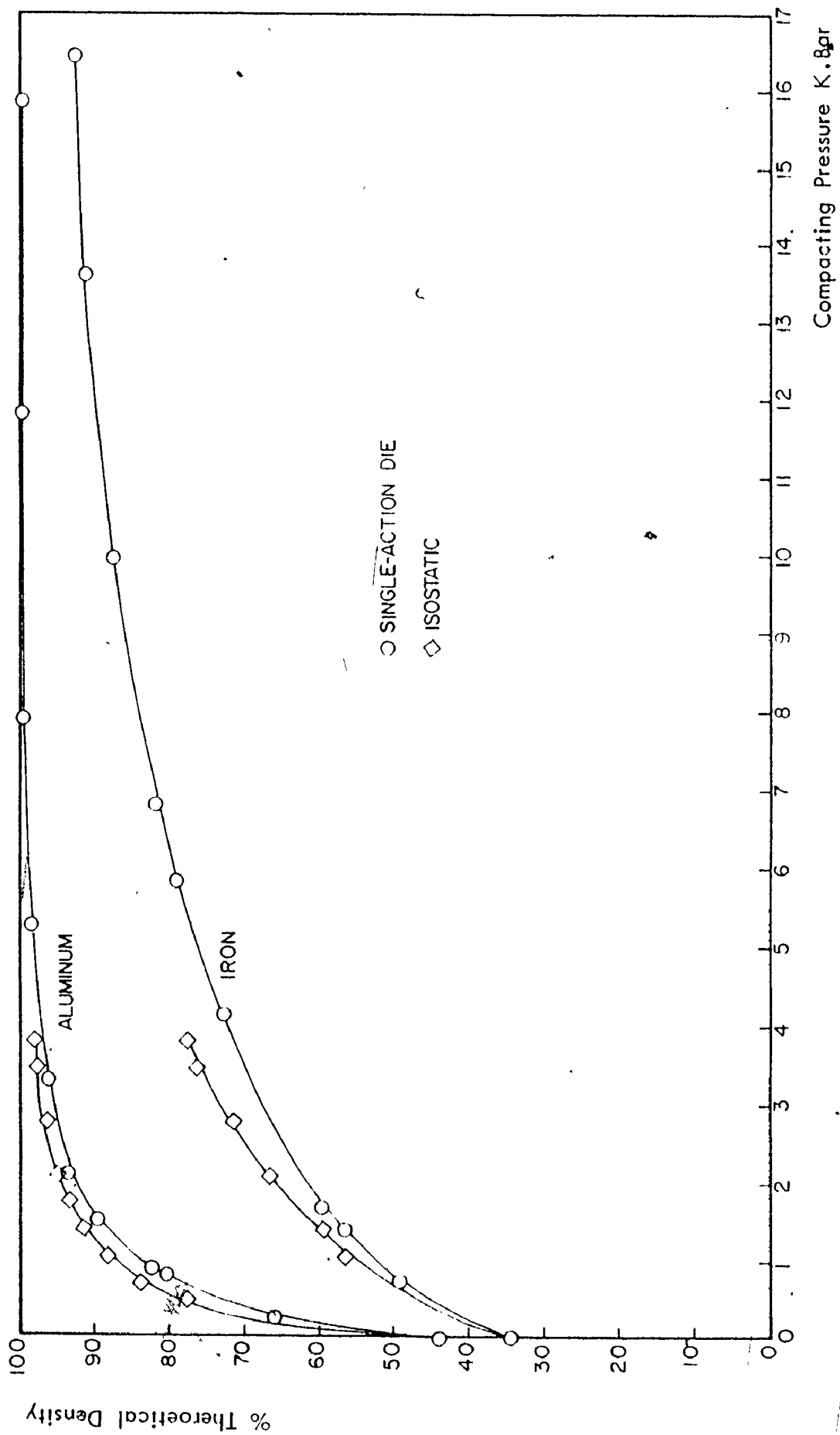
FIGURE 34   PRESSURE–DENSITY DATA EXPRESSED DIRECTLY FOR DIE
COMPACTED ALUMINUM AND IRON POWDERS
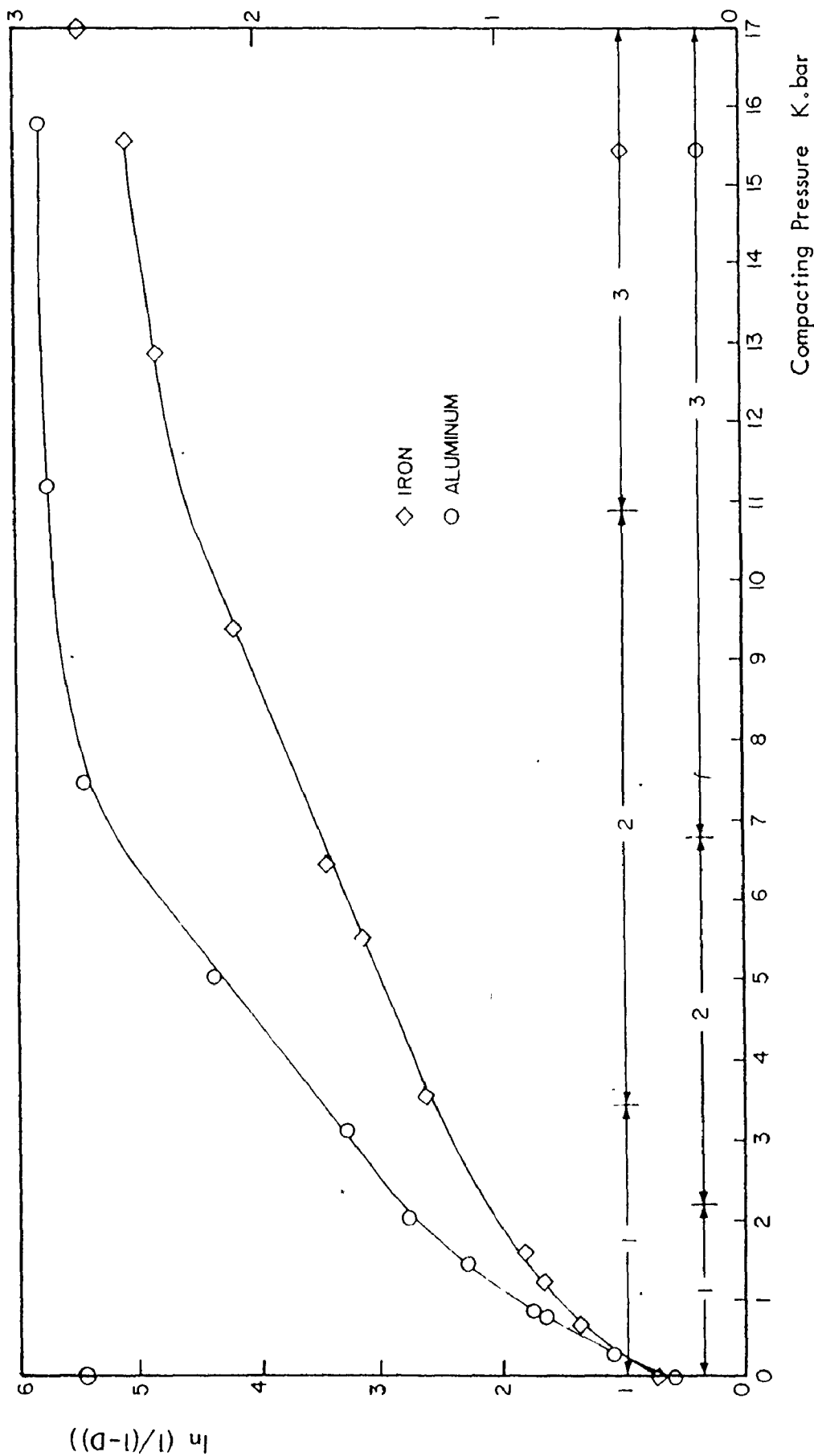
FIGURE 35   Ln (1/(1-D)) VERSUS PRESSURE FOR DIE COMPACTED
ALUMINUM AND IRON POWDERS

Hardness D.P.H.

Radial Distance mm
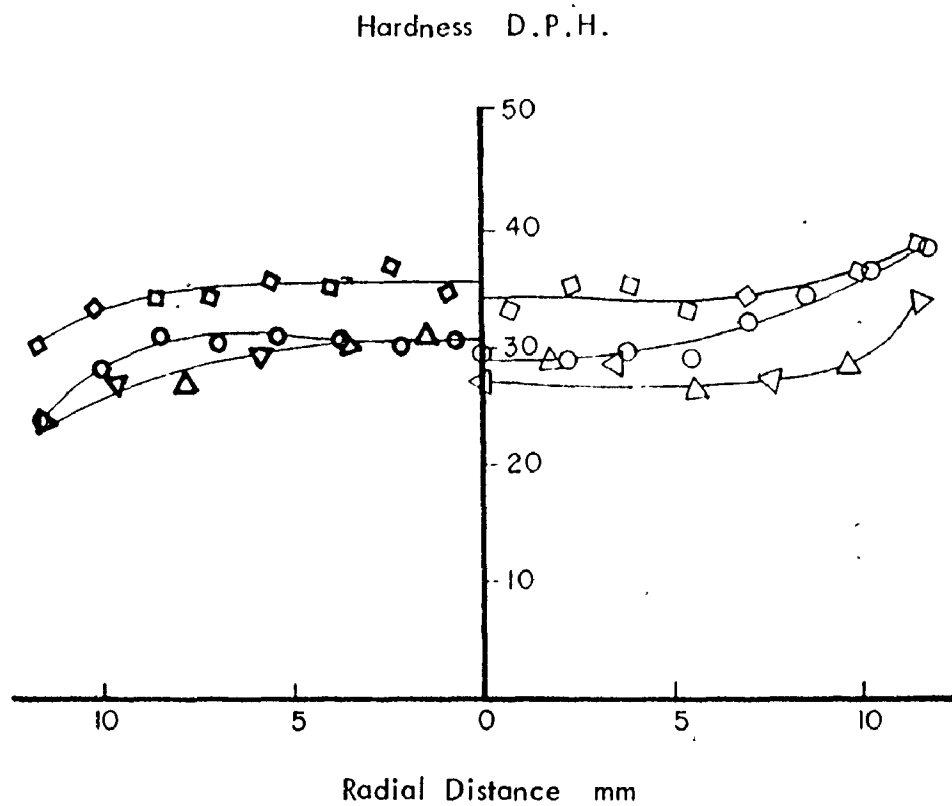
FIGURE 36   HARDNESS DISTRIBUTION ON TOP AND BOTTOM OF
CLOSED DIE ALUMINUM COMPACTS ·

BOTTOM   TOP

◆   ◇   3520 Bar
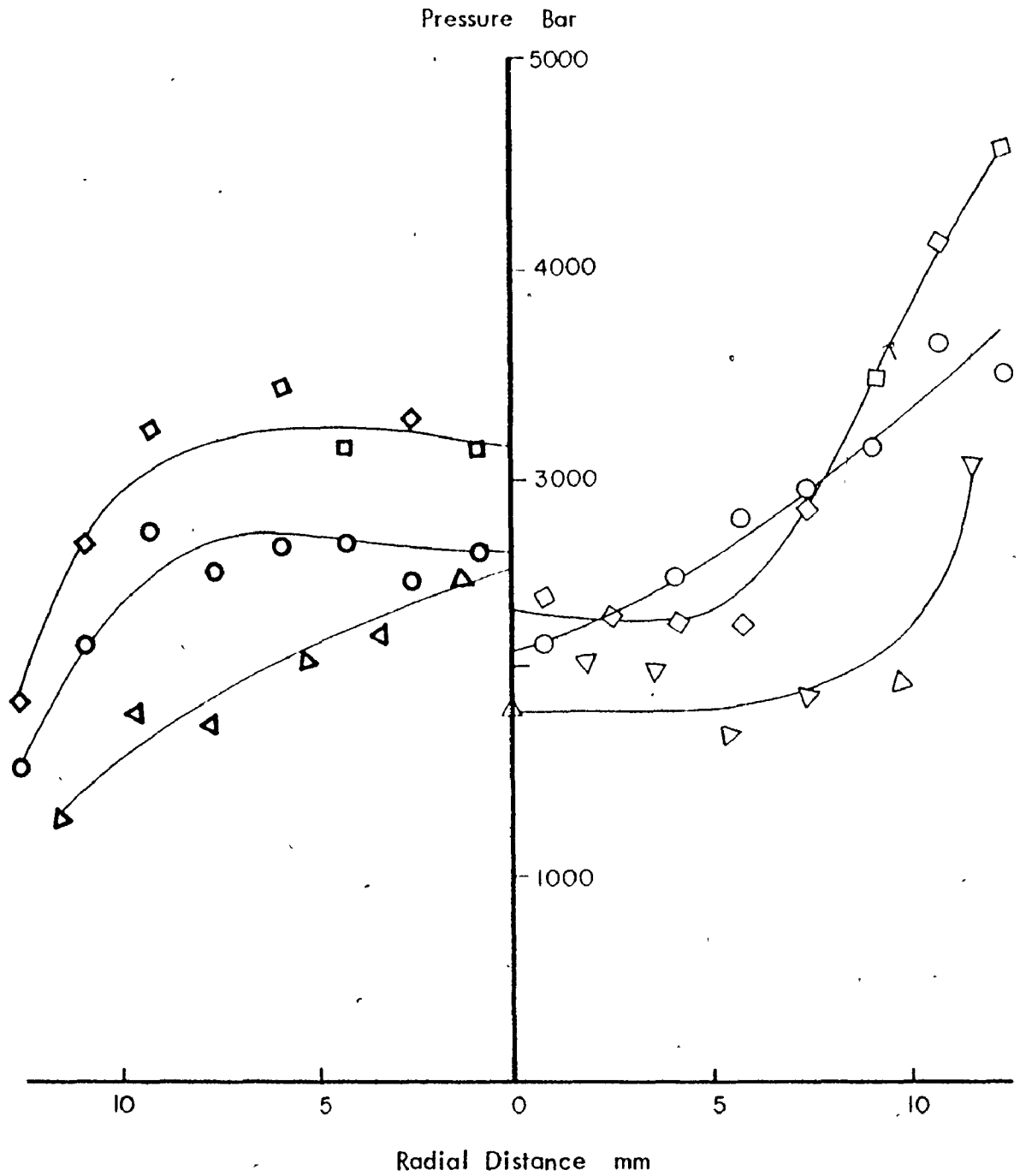
●   ○   2090 Bar

▼   ▽   1670 Bar

FIGURE 37   PRESSURE DISTRIBUTION ON TOP AND BOTTOM OF
CLOSED DIE ALUMINUM COMPACTS

% Theoretical Density

Radial Distance mm.
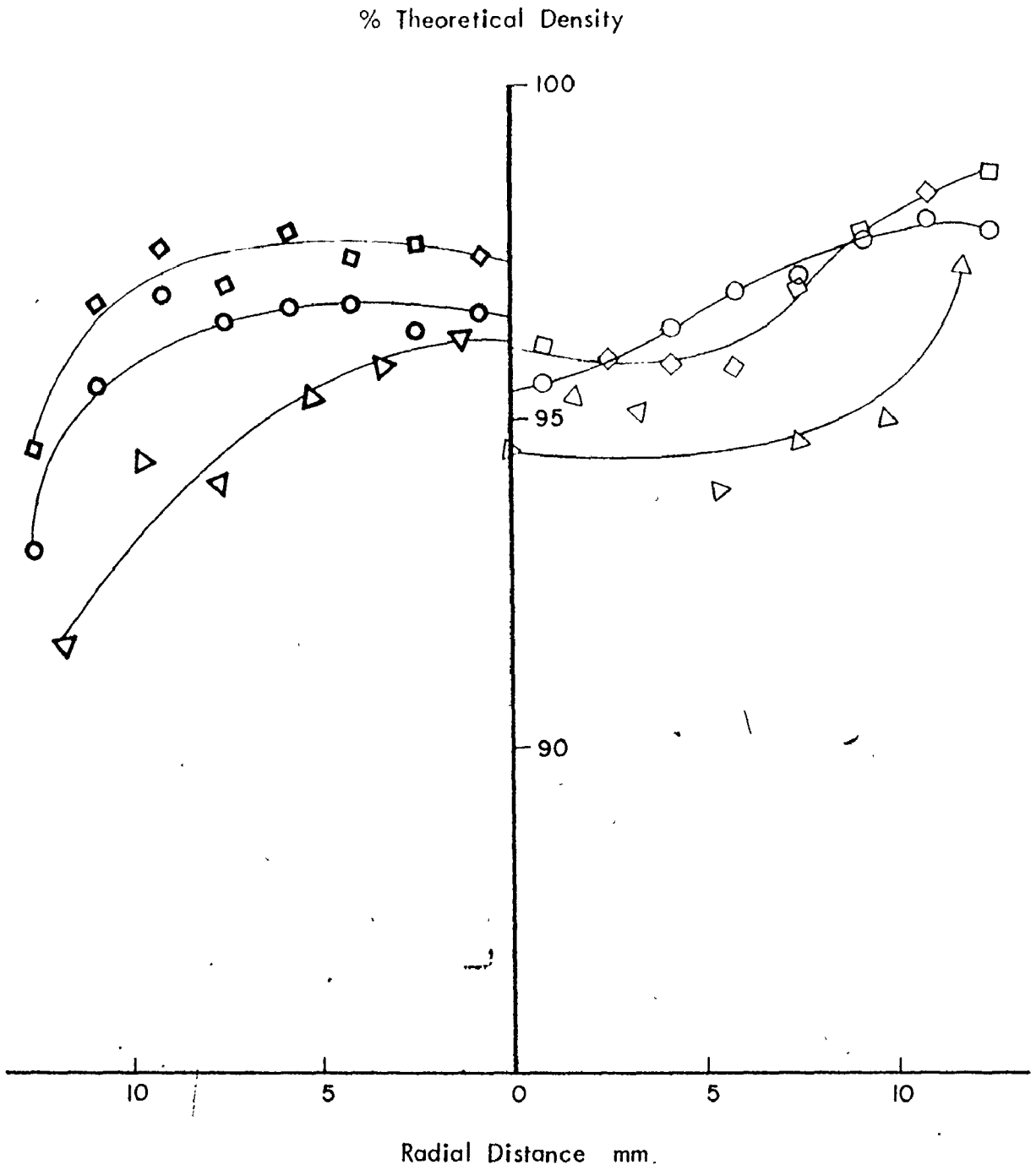
FIGURE 38   DENSITY DISTRIBUTION ON TOP AND BOTTOM OF
CLOSED DIE ALUMINUM COMPACTS

BOTTOM	TOP	
◆	◇	3520 Bar
⬤	○	2090 Bar
▲	△	1670 Bar
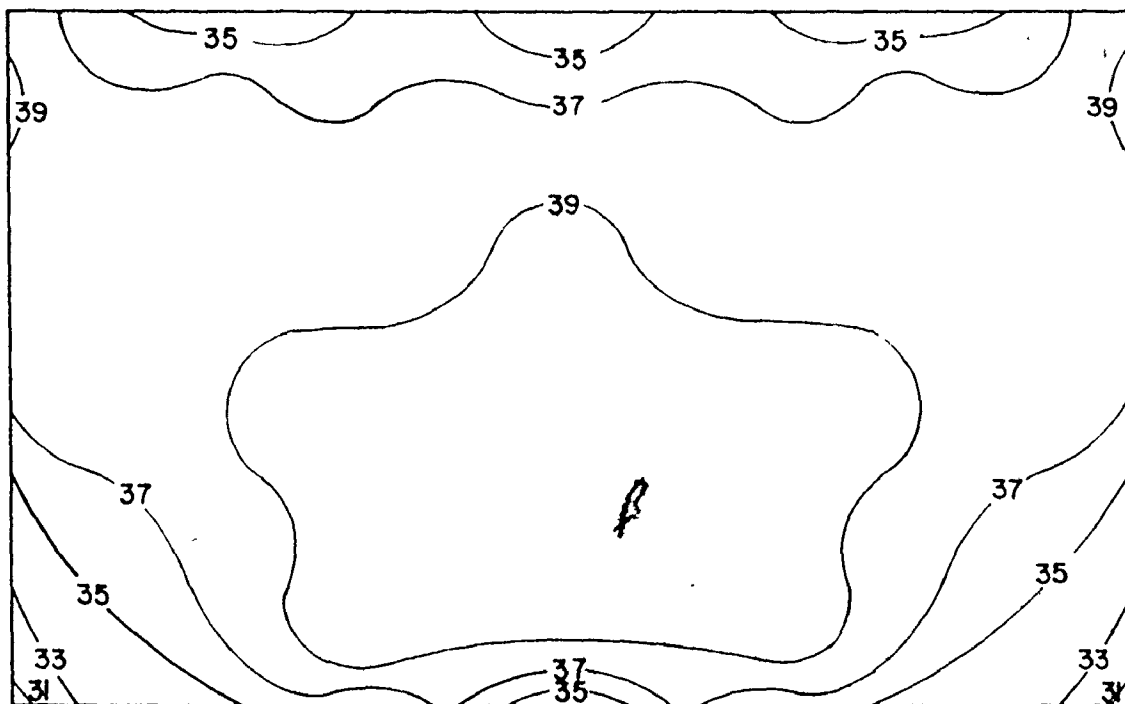
FIGURE 39   HARDNESS CONTOURS ACROSS ALUMINUM DIE COMPACT
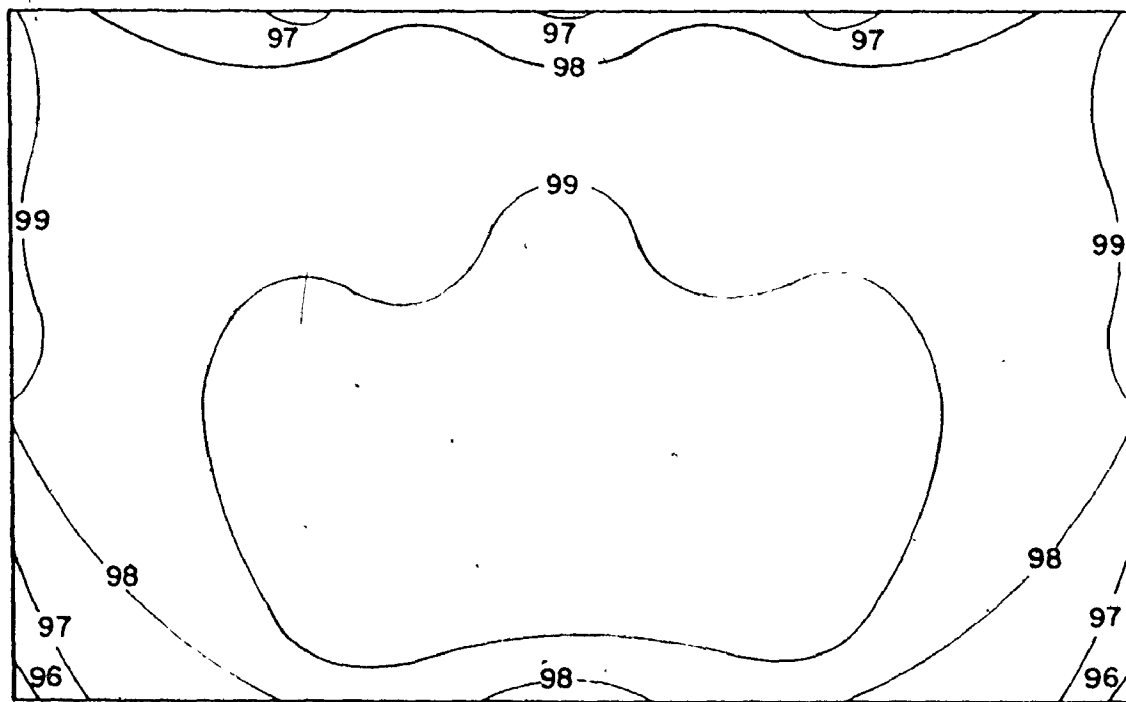
FIGURE 40   DENSITY CONTOURS ACROSS ALUMINUM DIE COMPACT
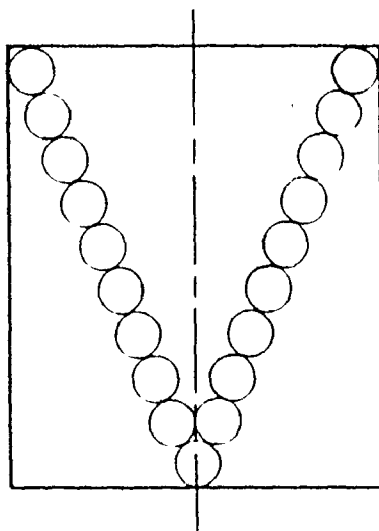
FIGURE 41   CHAIN FORMATION WITHIN THE COMPACT
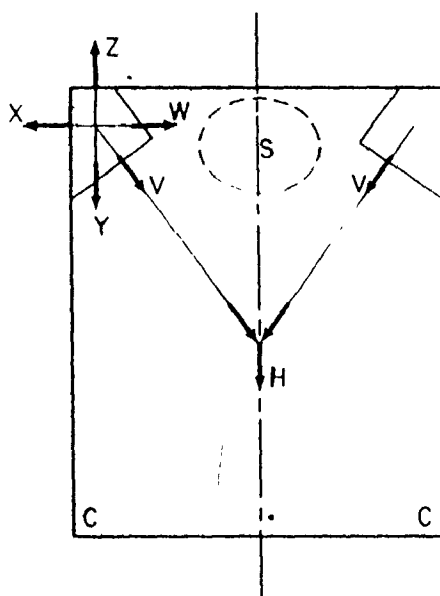
FIGURE 42   DEVELOPMENT OF PRESSURE PATTERN WITHIN THE COMPACT

Hardness D.P.H.

Radial Distance mm
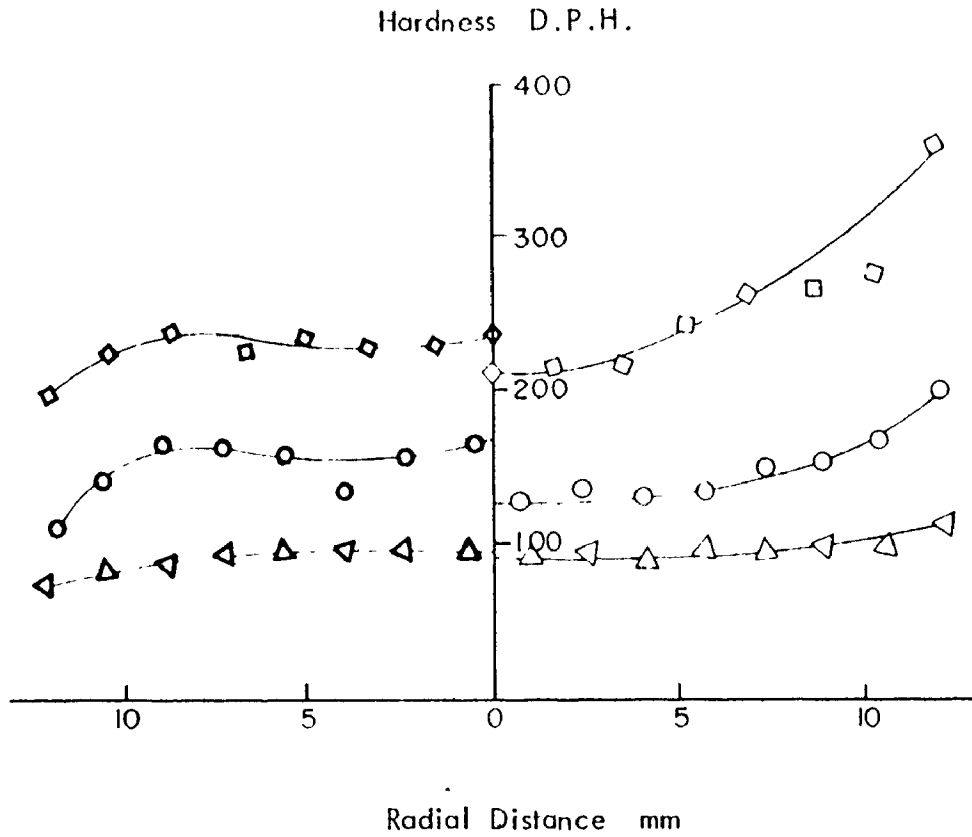
FIGURE 43   HARDNESS DISTRIBUTION ON TOP AND BOTTOM OF
CLOSED DIE COMPACTED IRON

BOTTOM TOP

◆   ◇   13600 Bar
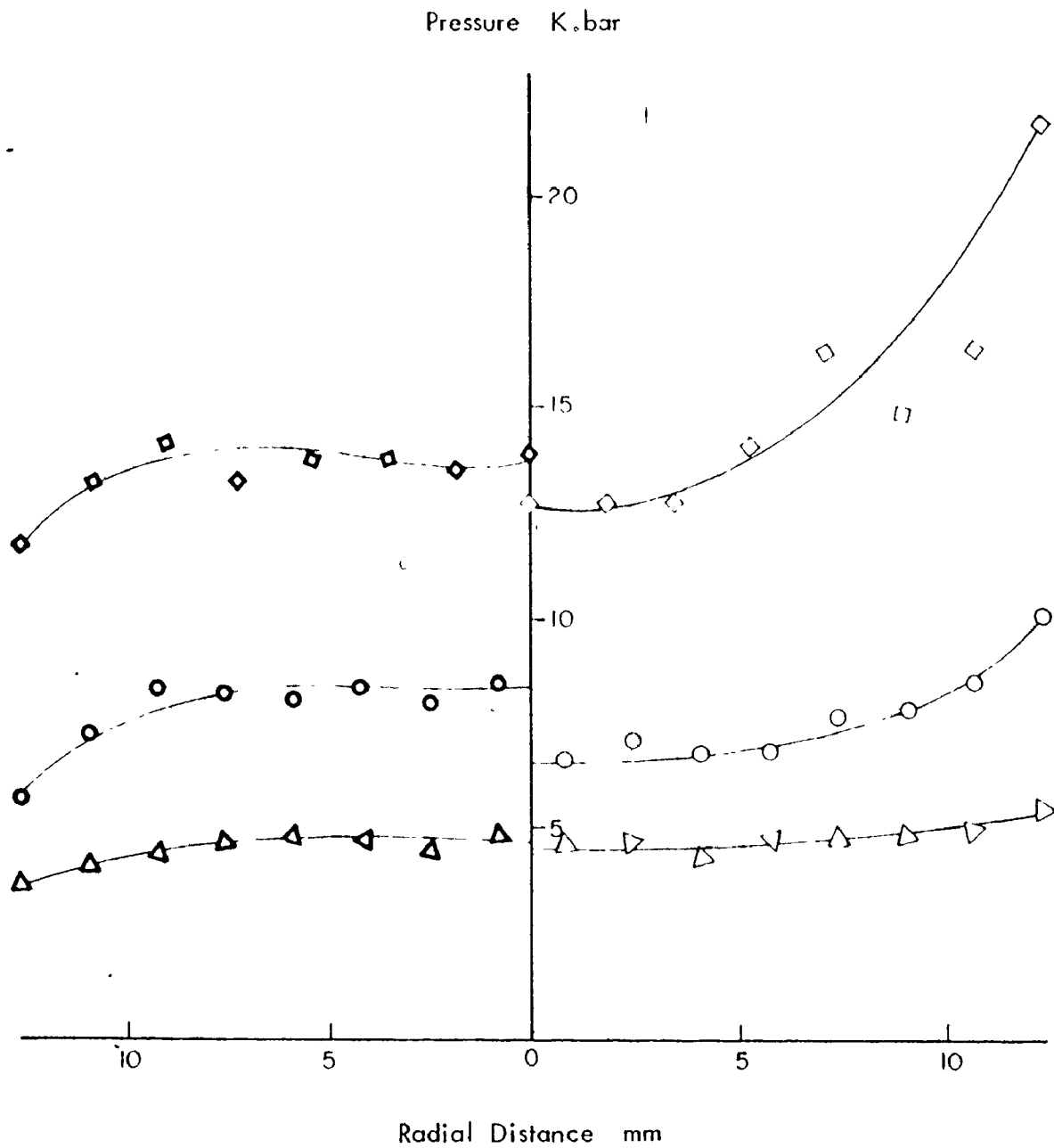
●   ○   6800 Bar

▲   ∧   4100 Bar

FIGURE 44   PRESSURE DISTRIBUTION ON TOP AND BOTTOM OF
CLOSED DIE COMPACTED IRON

BOTTOM	TOP	
◆	◇	13600 Bar
●	○	6800 Bar
▲	△	4100 Bar

% Theoretical Density

Radial Distance mm
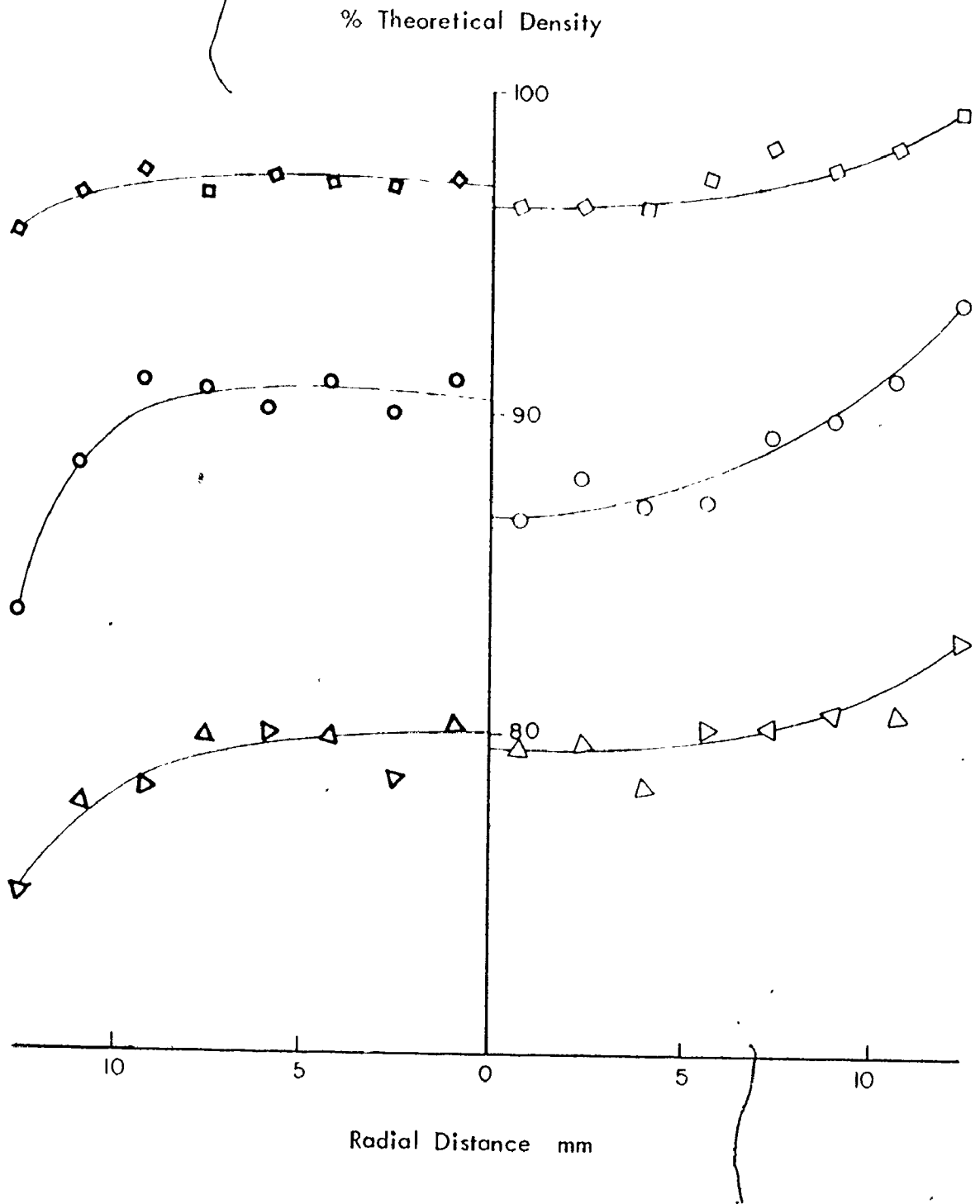
FIGURE 45   DENSITY DISTRIBUTION ON TOP AND BOTTOM OF
CLOSED DIE COMPACTED IRON

BOTTOM	TOP		
◆	◇	13600	Bar
●	○	6800	Bar
▲	△	4100	Bar
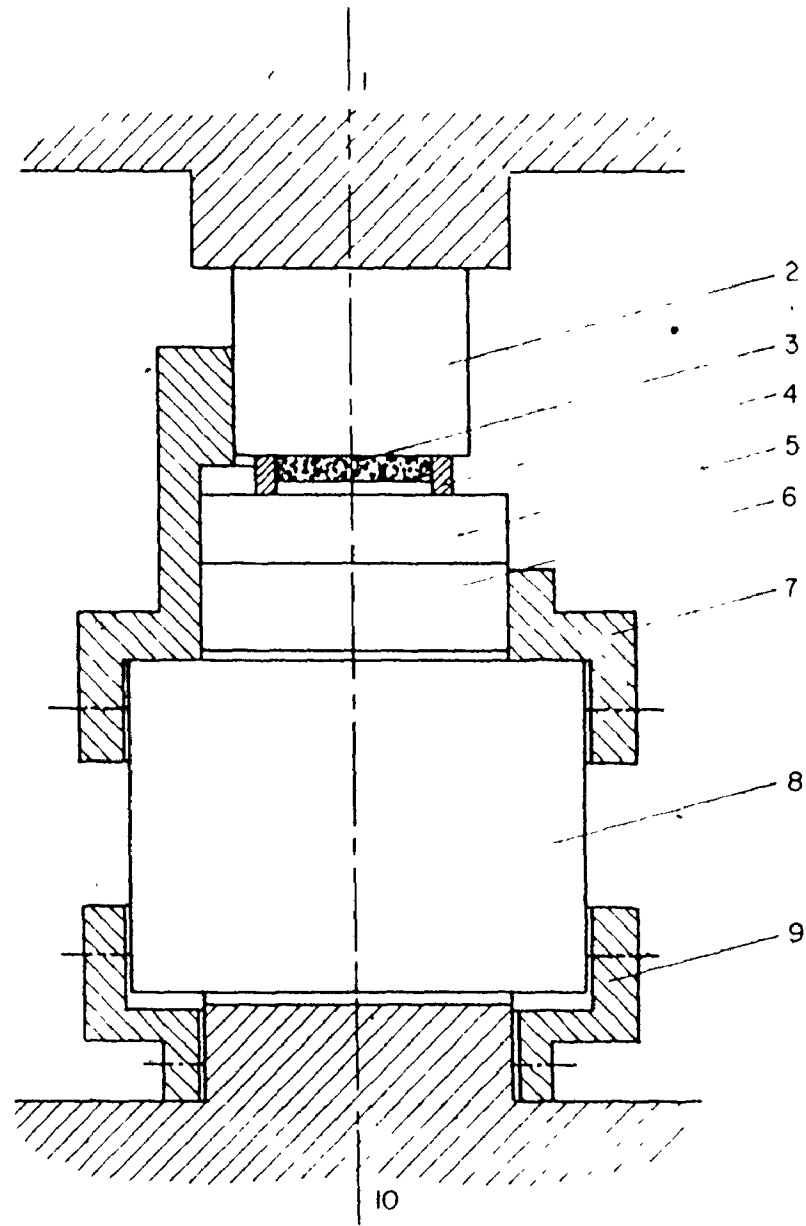
FIGURE 46   CONSTRUCTION OF OPEN DIE SYSTEM

KEY TO FIGURE 46

1. Upper platten of press

2. Upper die

3. Compaction space

4. Rubber ring

5. Bottom die

6. Spacer

7. Guide sleeve

8. Load cell

9. Fixture

10. Lower platten of press
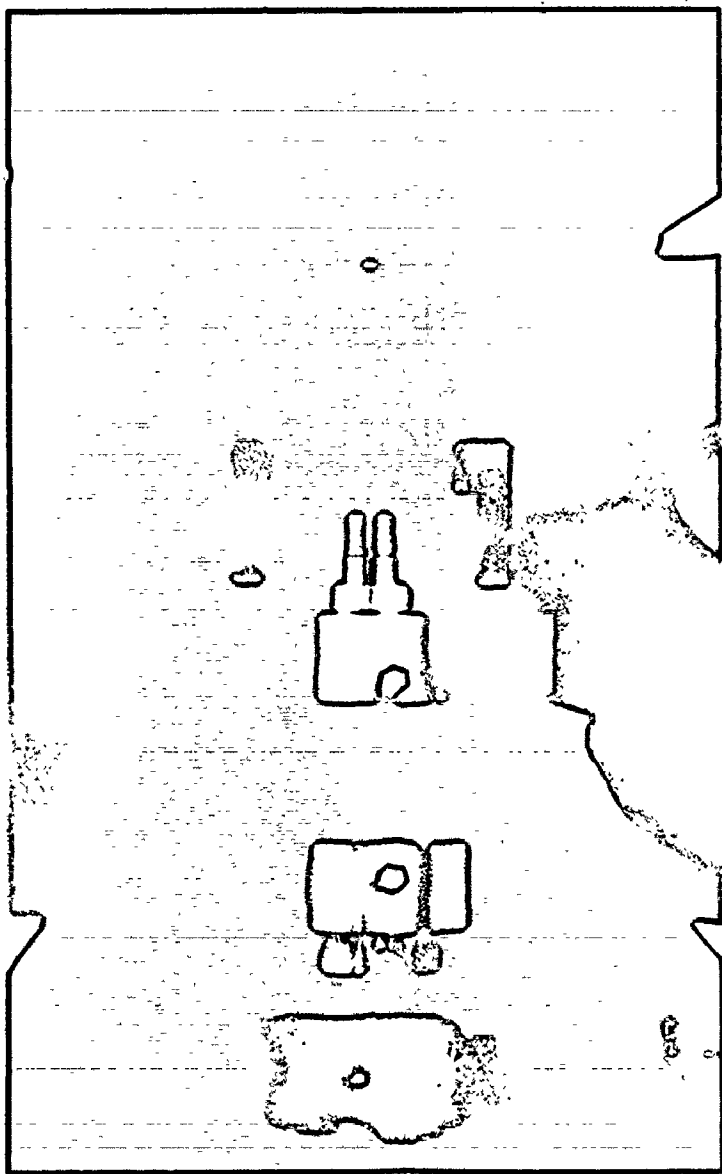
FIGURE 47   EXTERNAL VIEW OF OPEN DIE SYSTEM

SUPPORTING
STEEL RING
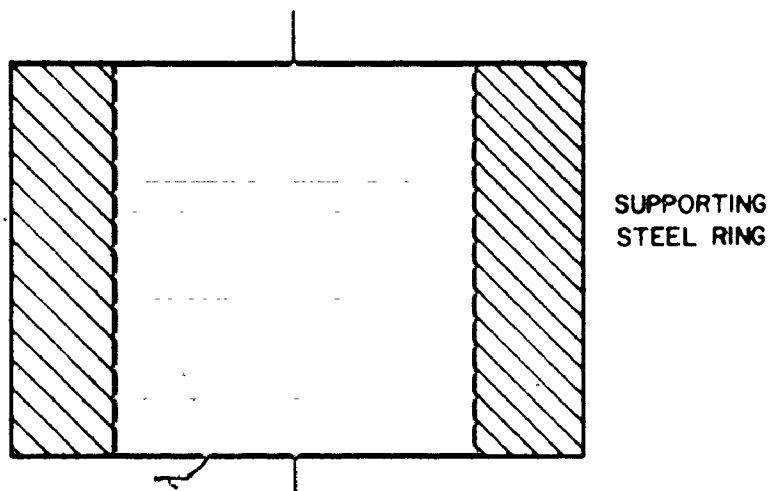
FIGURE 48   UPPER DIE FOR OPEN DIE SYSTEM
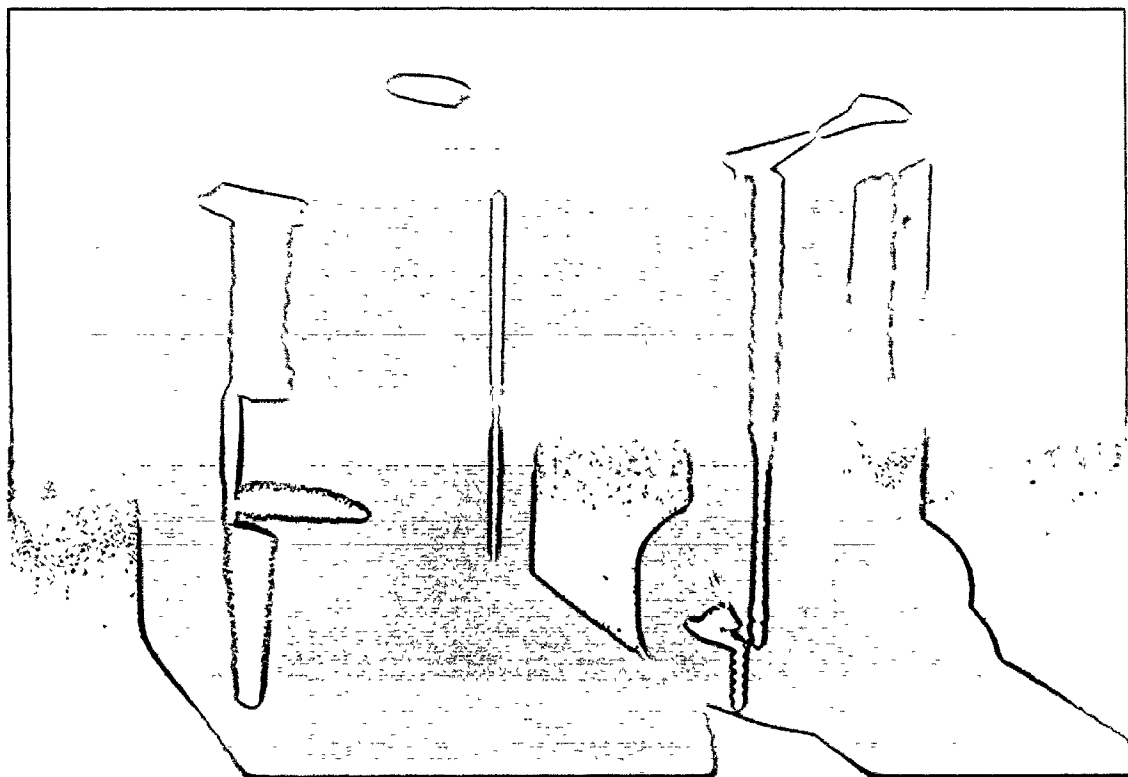
FIGURE 49   EXTERNAL VIEW OF MOULD FOR RUBBER RING
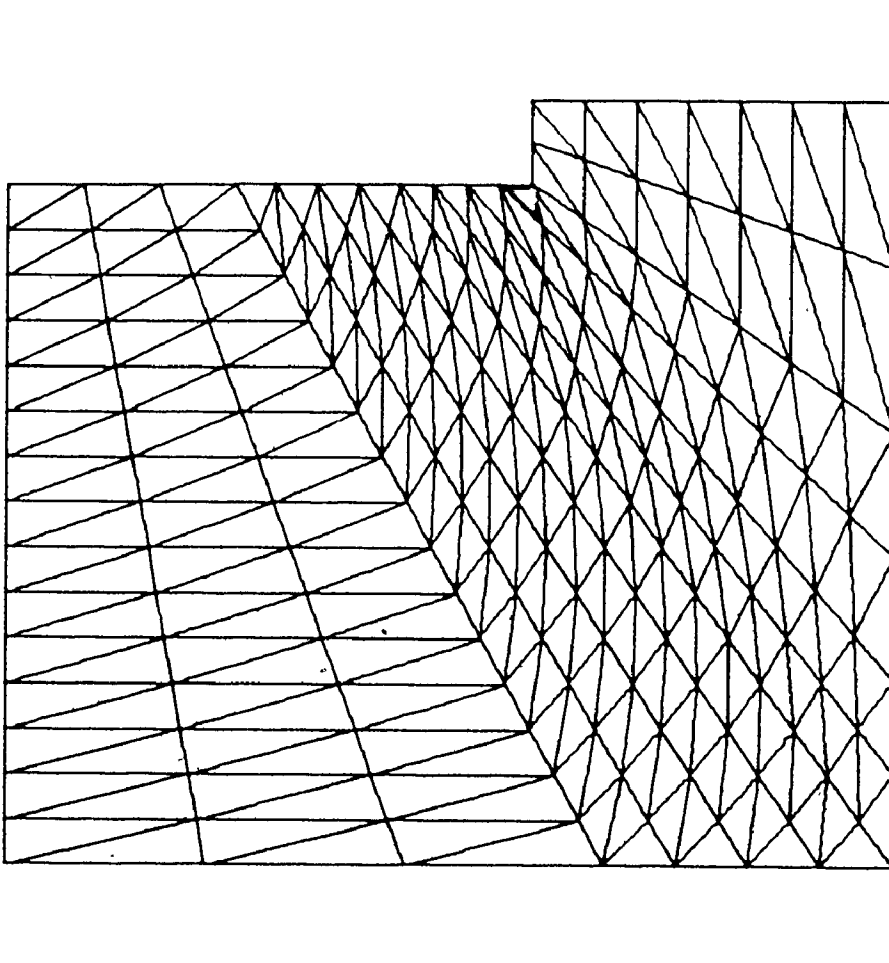
FIGURE 50   MESH FOR FINITE ELEMENT ANALYSIS
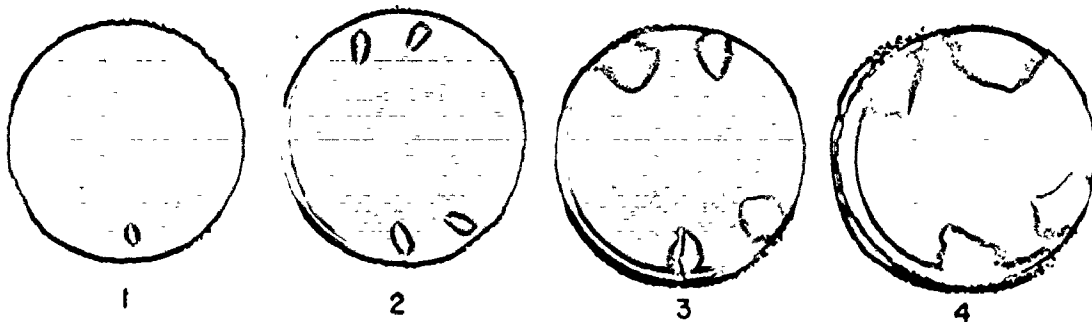
FIGURE 51   OPEN DIE ALUMINUM COMPACTS

Hardness   D.P.H.

TOP

Radial Distance   mm

◆ 4050 Bar
○ 2650 Bar
◇ 807 Bar

Hardness   D.P.H.

BOTTOM

Radial Distance   mm
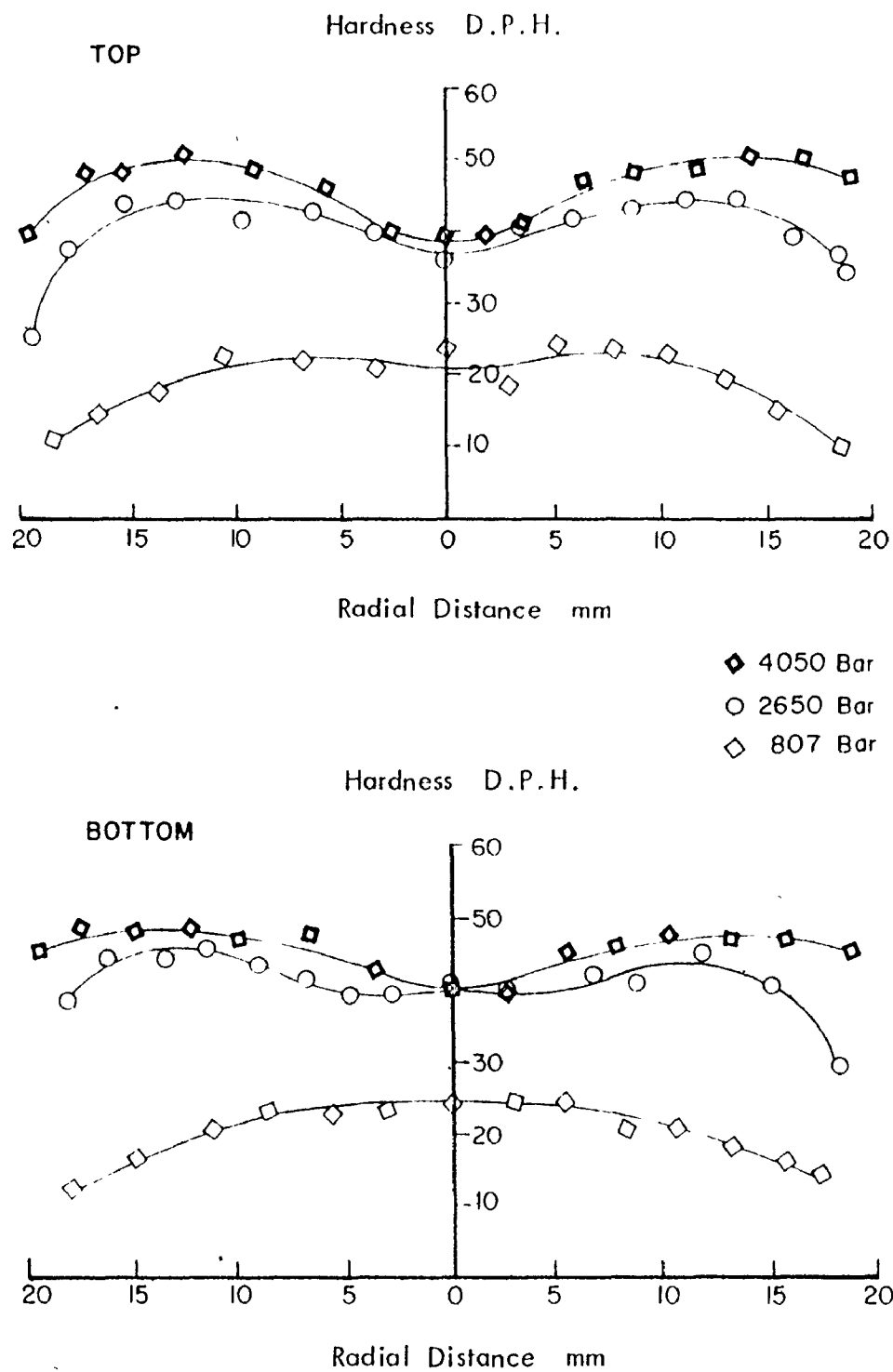
FIGURE 52   HARDNESS DISTRIBUTION ON TOP AND BOTTOM OF OPEN DIE ALUMINUM COMPACTS
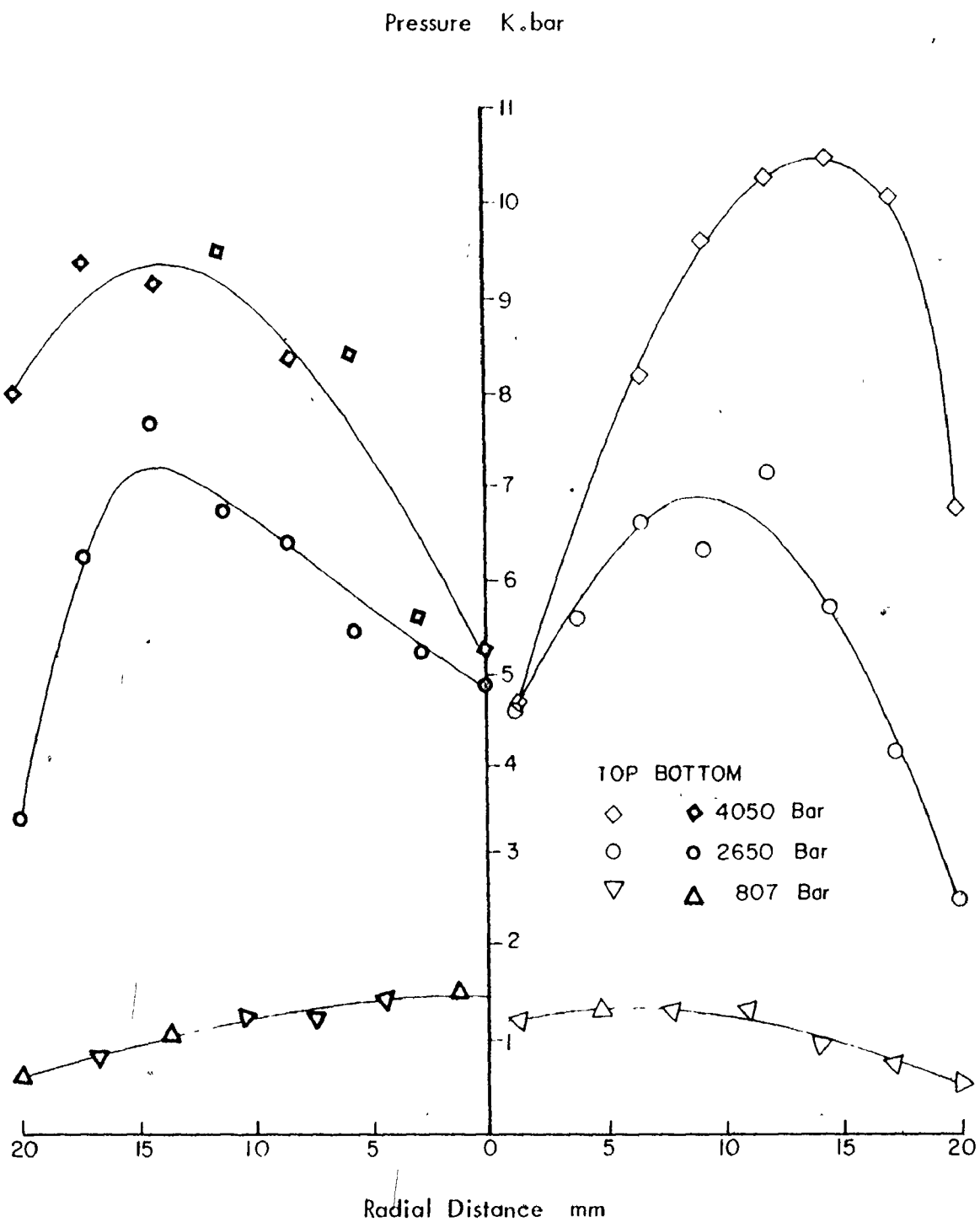
FIGURE 53   PRESSURE DISTRIBUTION ON TOP AND BOTTOM OF OPEN
DIE ALUMINUM COMPACTS
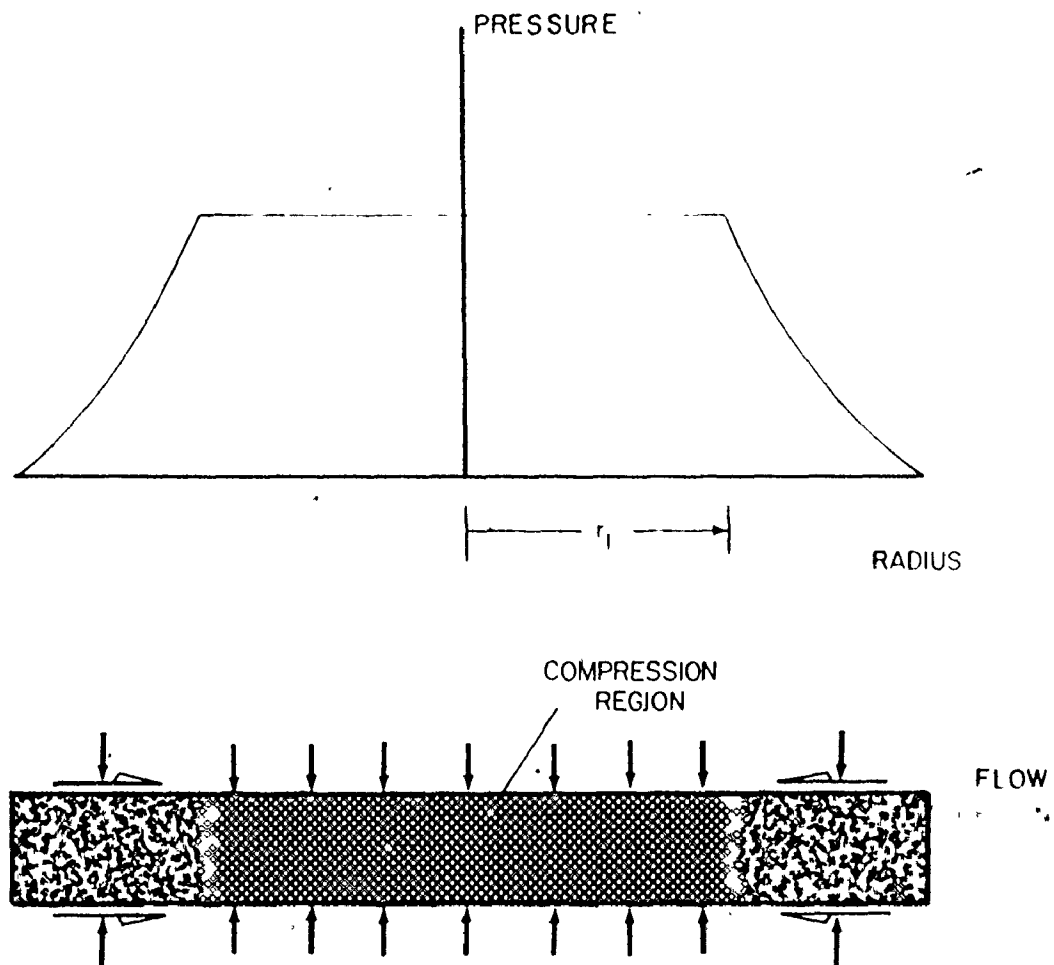
FIGURE 54   SCHEMATIC OPEN DIE COMPACTION BEHAVIOUR OF MATERIAL

Radial Distance   mm
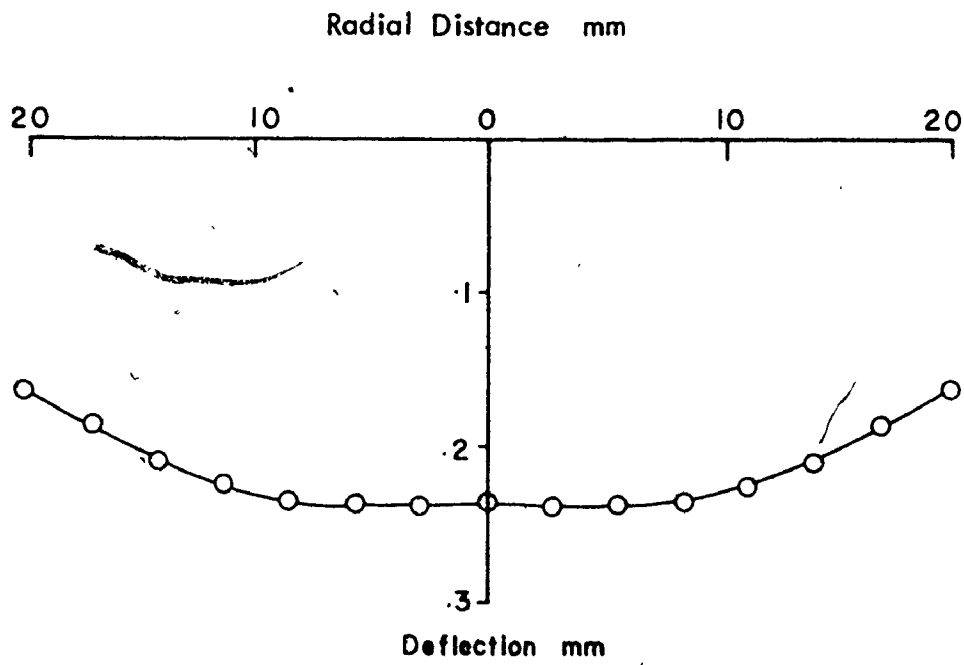
FIGURE 55   ELASTIC DISPLACEMENT OF BOTTOM DIE
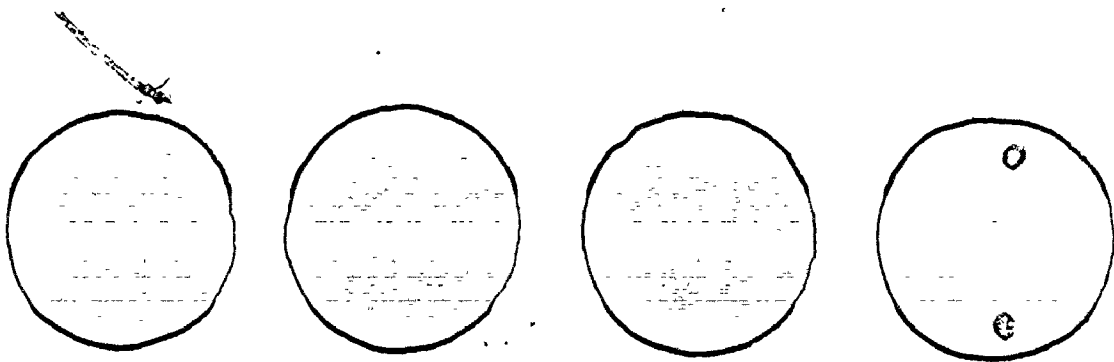
FIGURE 56   OPEN DIE IRON COMPACTS
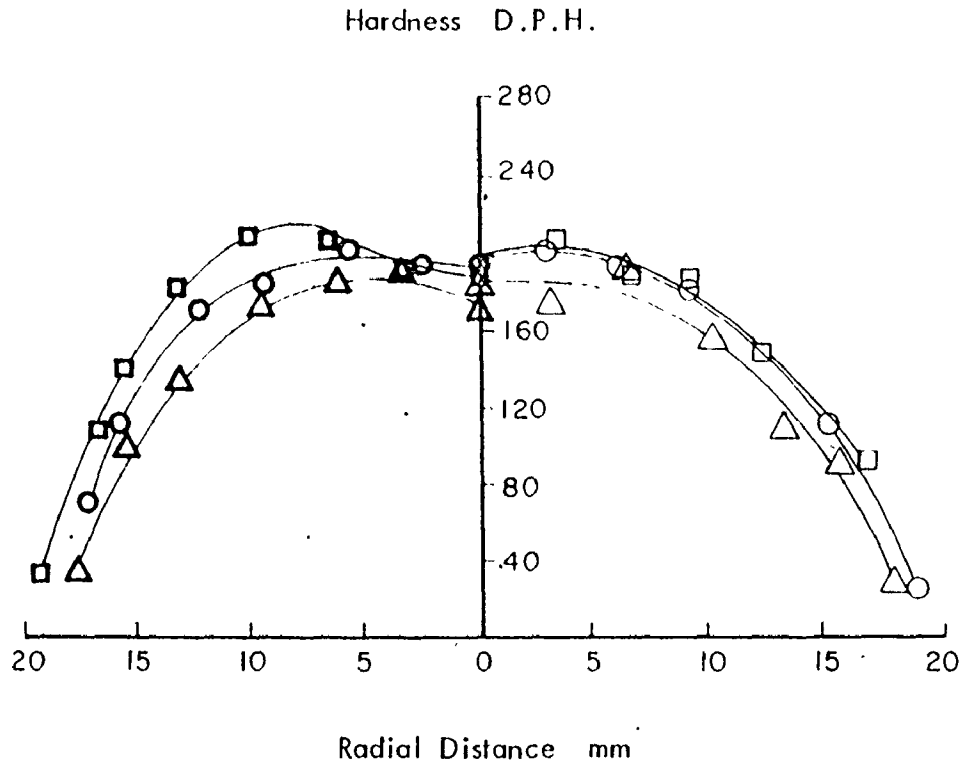
FIGURE 57   HARDNESS DISTRIBUTION ON TOP AND BOTTOM OF
OPEN DIE IRON COMPACTS

BOTTOM	TOP		
◼	☐	10300	Bar
◉	◯	8900	Bar
▲	△	7450	Bar
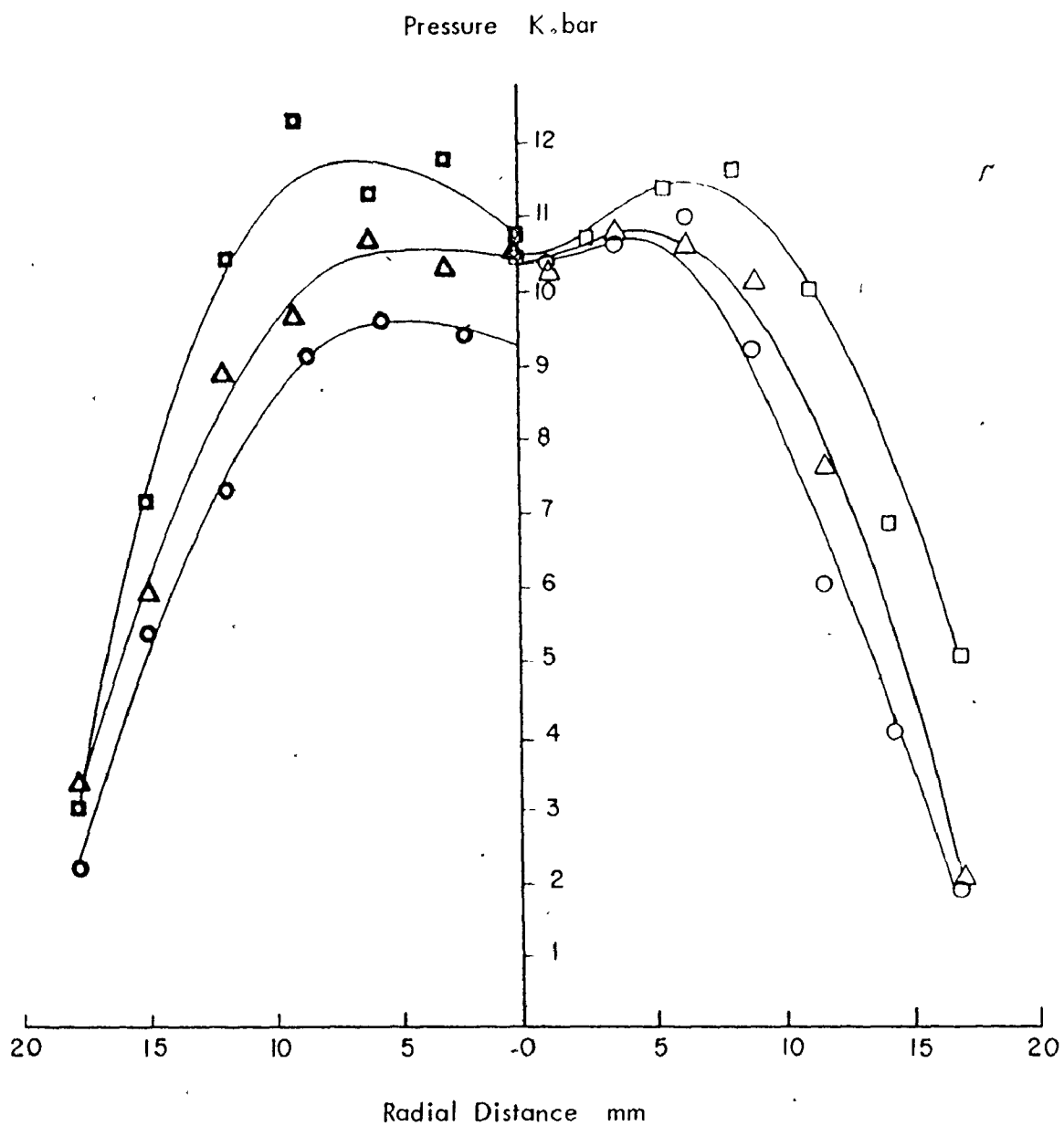
FIGURE 58   PRESSURE DISTRIBUTION ON TOP AND BOTTOM OF OPEN DIE IRON COMPACTS

BOTTOM	TOP	
■	□	10300 Bar
▲	△	8900 Bar
●	○	7450 Bar

TABLES

Distance From Bottom of Vessel (cm)	o/p Per Ksi (mV)	Pressure Vessel Displacement (cm) $\times 10^{-5}$
1.5	0.0	0.0
5.0	1.051	.83
9.0	1.546	1.97
12.0	2.900·	3.69
17.8	5.700	7.26
20.0	6.617	8.42
22.5	7.433	9.46
27.5	8.25	10.50
36.0	8.25	10.50
44.5	8.433	10.75
49.0	8.45	10.76
56.7	8.3125	10.58
60.5	8.4375	10.74
63.7	7.07	9.00
66.0	5.85	7.45
67.2	5.700	7.26
71.0	4.971	3.91
72.5	2.167	2.76
92.0	.24	.31
94.0	0.0	0.0

TABLE 1   RADIAL DISPLACEMENT OF PRESSURE VESSEL

Screen Analysis (U.S.Std.), %		Chemical Analysis, %	
Mesh	Typical Range		
+ 50	Trace	Al	99.4
- 50 + 100	10-20	Al_2O_3	.3
-100 + 200	20-30	Fe	.15
-200 + 325	15-25	Si	.07
- 325	30-40	Other Metallics Each	.0
Particle Size		Density	g/cm^3
Average Particle Diameter APD 23 - 28 Microns		Apparent	1.2
		Tapped	1.5

Ref. 59

TABLE 2   CHEMICAL AND SCREEN ANALYSIS OF ATOMIZED ALUMINUM POWDER

Screen Analysis, %		Chemical Analysis, %	
Mesh	Typical Range		
- 80 + 100	% max.	Total Iron	97.5 98.5
-100 + 150	9-14	Carbon	0.0015-0.0022
-150 +	19-23	Sulfur	0.005
-200 +	6-9	Phosphorus	0.012
-250 -	20-28	Manganese	0.45 - 0.65
-325	28-42	Acid Insoluable	0.20 - 0.45
Apparent Density 2.39 g/cc			

Ref. 60

TABLE 3   CHEMICAL AND SCREEN ANALYSIS OF REDUCED IRON POWDER

Sieve Analysis, Tyler, %		Chemical Analysis, %	
Cu	99.87	+ 140 mesh	Trace
Zn	.020	+ 200	19.1
Sn	.007	+ 325	21.0
Pb	.061	- 325	59.9
Fe	.011		
Mg	.196		
Ni	.0028	Apparent Density	2.98 g/cm^3
P	.026	Tapped	3.66 g/cm^3

Ref. 61

TABLE 4   CHEMICAL AND SCREEN ANALYSIS OF ATOMIZED
COPPER POWDER

Sieve Analysis, Tyler, %		Chemical Analysis, %	
Cu	.0015	+ 200 mesh	3.2
Zn	.0028	+ 325	11.1
Sn	.001	- 325	85.7
Apparent Density	4.95 g/cm^3		
Tapped	7.04 g/cm^3		

Ref. 61

TABLE 5   CHEMICAL AND SCREEN ANALYSIS OF ATOMIZED
LEAD POWDER

Mould No.	Material	I.D. mm	O.D. mm	Length mm	Weight of (gm)			
					Al	Fe	Cu	Pb
1	Latex	30.0	33.0	125.0	100.00	222.00	358.00	492
2	Urethane 50 dur.	13.0	18.0	130.0	21.5			
3	Latex	24.99	28.17	125.4	84.5			
4	Latex	54.99	58.17	125.4	430.6			
5	Urethane 50 dur.	24.99	34.99	125.4	84.5			
6	Urethane 50 dur.	54.99	64.99	125.4	430.6			
7	Urethane 70 dur.	24.99	34.99	125.4	84.5			
8	Urethane 70 dur.	54.99	64.99	125.4	430.6			
9	Urethane 50 dur.	9.98	19.98	125.4	14.00			
10	Urethane 50 dur.	9.98	30.00	125.4	14.00			
11	Urethane 50 dur.	9.98	39.98	125.4	14.00			
12	Urethane 70 dur.	9.98	19.98	125.4	14.00			
13	Urethane 70 dur.	9.98	30.00	125.4	14.00			
14	Urethane 70 dur.	9.98	39.98	125.4	14.00			

TABLE 6   DIMENSIONS OF MOULDS AND POWDER WEIGHTS

Specimen No.	Weight gm	Diameter mm	Length mm	Density g/cc	% Density
1	8.00	19.96	9.97	2.564	94.98
2	8.00	19.97	9.98	2.559	94.79
3	8.01	19.99	9.99	2.555	94.62
4	8.01	20.0	9.97	2.557	94.72
5	7.98	19.96	9.98	2.555	94.65

TABLE 7   DENSITY VARIATION ALONG COMPACT LENGTH

Specimen No.	Weight gm	Diameter mm	Length mm	Density g/cc	% Density
1	3.63	12.66	12 73	2.265	83.90
2	8.37	19.10	12.89	2.265	83.89
3	22.85	31.78	12.68	2.272	84.14
4	45.19	44.48	12.89	2.257	83.59

TABLE 8   DENSITY VARIATION ACROSS COMPACT DIAMETER

Mould Material	Pressure Bar	Small Diameter					Large Diameter				
		Wt. gm	Diam. mm	Length mm	Density g/cc	% T.H. Density	Wt. gm	Diam. mm	Length mm	Density g/cc	% T.H. Density
Rubber(Latex)	1030	13.43	19.00	19.97	2.37	87.78	68.97	43.02	20.03	2.37	87.73
	2070	14.50	19.02	19.99	2.55	94.55	74.32	43.00	20.02	2.56	94.69
	3100	14.83	18.98	19.98	2.63	97.16	76.42	43.02	20.04	2.62	97.22
Urethane 50	1030	13.36	19.02	19.97	2.35	87.21	68.72	42.97	20.01	2.37	87.74
	2070	14.54	19.02	20.03	2.55	94.63	74.32	43.02	20.03	2.55	94.56
	3100	14.93	19.02	20.03	2.62	97.16	76.08	42.98	19.98	2.63	97.24
Urethane 70	1030	13.40	19.00	20.04	2.36	87.35	68.60	42.99	20.02	2.63	87.47
	2070	14.44	19.02	19.97	2.54	94.26	74.19	42.97	20.01	2.56	94.69
	3100	14.81	18.98	19.99	2.62	96.98	76.14	42.95	20.02	2.63	97.23

TABLE 9   RESULTS OF EFFECT OF TOOL MATERIAL AND DIAMETER

A. URETHANE 50

Wall Thickness mm	1030 bar					2070 bar					3100 bar				
	Wt. gm	Diam. mm	Length mm	Density g/cc	%Th. Density	Wt. gm	Diam. mm	Length mm	Density g/cc	%Th. Density	Wt. gm	Diam. mm	Length mm	Density g/cc	%Th. Density
5.0	1.50	8.01	12.72	2.34	86.67	1.61	8.04	12.70	2.48	91.85	1.66	0.03	12.75	2.57	95.22
10.0	1.50	8.02	12.67	2.34	86.81	1.62	8.04	12.67	2.52	93.30	1.66	8.01	12.73	2.59	95.89
15.0	1.50	8.07	12.68	2.33	86.26	1.61	8.03	12.69	2.51	92.79	1.66	8.03	12.70	2.59	95.81

B. URETHANE 70

Wall Thickness mm	1030 bar					2070 bar					3100 bar				
	Wt. gm	Diam. mm	Length mm	Density g/cc	%Th. Density	Wt. gm	Diam. mm	Length mm	Density g/cc	%Th. Density	Wt. gm	Diam. mm	Length mm	Density g/cc	%Th. Density
5.0	1.50	8.02	12.71	2.34	86.63	1.62	8.03	12.75	2.51	92.96	1.65	8.01	12.68	2.58	95.63
10.0	1.50	8.01	12.73	2.34	86.59	1.63	8.05	12.74	2.52	93.30	1.63	7.99	12.69	2.56	94.93
15.0	1.50	8.03	12.75	2.83	86.33	1.62	8.03	12.73	2.44	90.33	1.65	8.02	12.70	2.57	95.26

TABLE 10   RESULTS OF EFFECT OF TOOL THICKNESS

Load Kgf		Load Cell o/p mV	
		Loading (compressive)	unloading (release)
Calibration Setting — **6 Volts**	18140	.80	.80
	36290	1.59	1.596
	54430	2.40	2.38
	72580	3.19	3.19
	·90720	3.98	3.98
12 Volts	18140	1.6	1.6
	27220	2.4	2.4
	36290	3.2	3.2
	43360	4.0	4.01
	54430	4.8	4.8
	72580	6.4	6.4
	90720	7.94	7.94

TABLE 11   LOAD CELL CALIBRATION (HIGH LOADS)

		Loading (compressive)		Unloading (release)	
		Load Kgf	Load Cell o/p mV	Load Kgf	Load Cell o/p mV
		453.6	.0200	3719	.1760
		884.5	.0380	3189	.1520
		1429	.0640	2812	.1360
	6 Volts	1878	.0854	2168	.1064
Calibration Setting		2368	.1080	1315	.0648
		2781	.1280	666.8	.0344
		3280	.1504	394.6	.0200
		4282	.1988		
		476.3	.0440	4069	.3840
		884.5	.0820	3642	.3450
		1470	.1360	3284	.3140
	12 Volts	2109	.1976	2830	.2800
		2767	.2600	2309	.2270
		3184	.3000	1901	.1860
		3674	.3460	1352	.1330
		4173	.3930	625.5	.0804
				385.6	.0380

TABLE 12   LOAD CELL CALIBRATION (LOW LOADS)

Actual Load Kgf	Integrated Load Kgf			Integrated/Actual Load	
	Top	Bottom	Bottom/Top	Top	Bottom
8499	11410	9803	.859	1.342	1.153
16683	16889	15695	.929	1.012	.941
18000	16743	11875	.721	.927	.658

TABLE 13   COMPARISON OF INTEGRATED AND ACTUAL LOADS APPLIED FOR CLOSED DIE ALUMINUM COMPACTS

Actual Load Kgf	Integrated Load Kgf			Integrated/Actual Load	
	Top	Bottom	Bottom/Top	Top	Bottom
21213	29017	25850	.891	1.368	1.219
34753	45292	43313	.956	1.303	1.246
69506	77167	64456	.835	1.11	0.927

TABLE 14   COMPARISON OF INTEGRATED AND ACTUAL LOADS APPLIED FOR CLOSED DIE IRON COMPACTS

Actual Load Kgf	Integrated Load Kgf		Integrated/Actual Load	
	Top	Bottom	Top	Bottom
12818	12378	13396	.966	1.045
41974	67216	78191	1.601	1.863
64090	11672	133488	1.825	2.083

TABLE 15   COMPARISON OF INTEGRATED AND ACTUAL LOADS APPLIED FOR OPEN DIE ALUMINUM COMPACTS

Actual Load Kgf	Integrated Load Kgf		Integrated/Actual Load	
	Top	Bottom	Top	Bottom
118251	76666	86447	.6483	.7310
140818	99010	98418	.6989	.7031
163837	106059	107476	.6473	.6560

TABLE 16   COMPARISON OF INTEGRATED AND ACTUAL LOADS OF OPEN DIE IRON COMPACTS

REFERENCES

1. John McDermott, "Powdered Metals Techology", 1974, New Jersey.

2. E.L.J. Papen, "Automated Isostatic Pressing", British Research Association Proceedings 4th Symposium Special Ceramics,(1967) p.69.

3. Paul J. Gripshover, "A Comparison of Conventional and Hydrostatic Pressing of Metal Powders", Materials Technology, Vol.1, (1970), p.520.

4. P.J. James, "Fundamental Aspects of the Consolidation of Powders", Powder Metallurgy International, Vol.4, (1972).

5. J.K. Beddow, "Initial Stage of Compacting Metal Powders", International Journal of Powder Metallurgy, 9(4), (1973).

6. M. Stromgen, H. Astrom, and K.E. Easterling, "The Effect of Inter-particle Contact Area on the Strength of Cold-Pressed Aluminum Powder Compacts", Powder Metallurgy, (1973), Vol. 16, No.32, p.155.

7. V.P. Bondarenko, S.S. Dzharmarov, and A.A. Baidenko, "Application of Theoretical Pressing Equations to the Hydrostatic Densification of Hard-Alloy Mixtures", Poroshkovaya Metallurgiya, No.1 (133), (1974), p.16.

8. R.L. Hewitt, R. Venter, M.C. deMalherbe, "A Review of Some Equations and Recent Developments in Powder Compaction", South African Mech. Eng., Vol.23, (1973), p.214.

9. M. Yu. Balshin, Poroshkovaya Metallurgia, Mashgiz, Moscow (1948).

10. I. Shapiro and I.M. Kolthoff, "The Compressibility of Silver Bromide Powders", J. Phys. Colloid. Chem., Vol.51, (1947), p.483.

11. K. Konopicky, "Parallelitat der Gesetzmassigkeiten in Keramik und Pulvermetallurgie", Radex-Rundschau, Vol. 141, (1948), p.141.

12. C. Torre, "Theorie und Verhalten der Zussammenge Pressten Pulver", Berg-Huttenmann, Monatsh. Montan. Hochschule Leoben, Vol. 93, (1948), p.62.

13.   R.W. Heckel, "Density-Pressure Relationships in Powder Compaction",
       Trans. Metall. Soc. AIME, Vol.221, (1961), p.671.

14.   N.F. Kunin and B.D. Yurchenko, "Regularities in the Compacting of
       Powders of Different Materials", Poroshkovaya Metallurgiya,
       Vol.18, (1963), p.3.

15.   R.W. Heckel, "Density-Pressure Relationships in Powder Compaction",
       Trans. Metall. Soc. AIME, Vol.221, (1961), p.671.

16.   R.W. Heckel, "A Normalized Density-Pressure Curve for Powder Com-
       paction", Trans. Metall. Soc. AIME, Vol.224, (1962), p.1073.

17.   N.F. Kunin and B.D. Yurchenko, "On a Rational Equation of Pressing
       Metal Powders", Poroshkovaya Metallurgiya, Vol.20 (1964), p.3.

18.   J. Greenspan, "High Pressure Isostatic Pressing and Presureless Sinter-
       ing of Some Metal Powder Compacts", Metals for the Space,
       Age, (ed.F. Benesovsky), p.163, (1964), Vienna (Springer).

19.   V.S. Savin, N.B. Ukhina, and N.A. Fedotov, "Equation of Pressing
       of Nickel Powders", Poroshkovaya Metallurgiya, Vol.74,
       (1969), p.11.

20.   M.Yu. Bal'shin, Powder Metallurgy, Mashgiz, Moscow (1948).

21.   H. Lipson, 'Powder Metallurgy Bull, Vol.5, (1950), p.52.

22.   G.A. Meerson, A.F. Islankina, V.N. Mel'nikov, and L.D. Gol'dman,
       "Hydrostatic Pressing of Steel Powders", Poroshkovaya Metal-
       lurgiya, Vol.79, (1969), p.13.

23.   P.N. Tomilson, R.L. Hewitt, R.D. Venter, "Powder Compaction at
       Very High Pressures", M.T.D.R. Conference, Birmingham, (1974).

24.   R.L. Hewitt, W. Wallace, and M.C. deMalherbe, "The Effects of
       Strain-Hardening in Powder Compaction", Powder Metallurgy,
       Vol.16, (1973), p.88.

25.   R.L. Hewitt, W. Wallace, and M.C. deMalherbe, "Plastic Deformation
       in Metal Powder Compaction", Powder Metallurgy, Vol.17, (1974).

26.   R. Kamm, M. Steinberg and J. Wulff, "Plastic Deformation in Metal-
       Powder Compacts", Metals Technology, (1947), p.439.

27. R. Kamm, M. Steinberg, Junior Members, and J. Wulff, "Lead-Grid Study of Metal Powder Compaction", Metals Technology, (1949), p.694.

28. G.C. Kuczynski and I. Zaplatynskyj, "Density Distribution in Metal Powder Compacts", Journal of Metals, (1956), p.215.

29. G.M. Zhdanovich, "Pressure and Density Distribution in the Single and Double-Ended Pressing of Axially-Symmetric Compacts", Poroshkovaya Metallurgiya, Vol. (78), (1969), p.24.

30. I.D. Radomysel'skii and E.L. Pechentkovskii, "Effect of Pressing Tool Design on Density Distribution in Bushing-Type Sintered Parts", Poroshkovaya Metallurgiya, Vol.(88),(1970), p.277.

31. I.M. Fedorchenko, R.A. Kovyney, and O.F. Polukhin, "Use of Pin Sensors for Studying the Pressures Exerted on the Working Parts of Die Sets", Poroshkovaya Metallurgiya, Vol.(91), (1970),p.26.

32. I.M. Fedorchenko et al., R.A. Kovynev, and O.F. Polukhin, "Stresses Set Up in the Working Parts of Die Sets During the Pressing of Metal Powders", Poroshkovaya Metallurgiya, Vol.(92), (1970),p.17.

33. G.A. Meerson, N.I. Rasskazov, and V.P. Chulkov, "Experimental Investigation of the Compaction Process of Powder Materials", Poroshkovaya Metallurgiya, Vol.(85), (1970), p.21.

34. S.E. Vinogradov, "Variation of the Lateral Pressure in the Compaction of Metal Powders", Poroshkovskaya Metallurgiya, Vol.(92), (1970), p.13.

35. V.P. Katashinskii and N.V. Rukhailo, "Deformation Process of Metal Powders in an Open Volume", Poroshkovaya Metallurgiya, Vol. (87), (1970), p.28.

36. H.F. Fischmeister, B. Aren, and K.E. Easterling, "Deformation and Densification of Porous Preforms in Hot Forging", Powder Metallurgy, Vol.(12), (1971), p.144.

37. M. Wakatsuki, K. Ichinose, and T. Aoki, "Notes on Compressible Gasket and Bridgman-Anvil Type High Pressure Apparatus", Japanese Journal of Applied Physics, Vol.(11), (1972), p.578.

38. G.A. Meerson, V.A. Ivensen, F.I. Sapronov, and V.B. Vissarionov, "Lateral Pressure Distribution in the Compaction of Tungsten Carbide-Cobalt Mixtures", Poroshkovaya Metallurgiya, Vol.(110), (1972), p.15.

39. O.V. Roman, V.E. Perel'man, and E.A. Doroshkevich, "Distribution of Density in Metal Powder Compacts", Poroshkovaya Metallurgiya, Vol. (116), (1972), p.14.

40. O.I. Shulishova and I.A. Shcherbak, "Investigation of Density Distribution in Porous Parts", Poroshkovaya Metallurgiya, Vol.(121), (1973), p.93.

41. I.V. Vlasyuk, V.N. Klimenko, I.D. Radomysel'skii, V.Z. Spuskanyuk, and Yu. F. Chernyi, "Methods of Cold Pressing Powder Mixtures for the Production of High-Speed Steels", Poroshkovaya Metallurgiya, Vol.(126), (1973), p.16.

42. B.G.A. Aren, "Optimizing the Preform Shape in Powder Forging of Linear Gear Profile", Powder Metallurgy International, Vol.(7), (1975), p.12.

43. K. Marshall, "Some Observations on the Elucidation and Control of Die Compaction Processes", Proc. 1st Int. Conf. on the Compaction and Consolidation of Particular Matter.

44. "Blue Strand Wire Rope Catalogue" Wire Rope Industries of Canada, Publication No. WRI 681, Montreal (1968).

45. T.E. Davidson and D.P. Kendall, "The Design of High Pressure Containers and Associated Equipment", ed. Pugh H.Li.D., Elsevier, London, (1970), p.148.

46. S.J. Paprocki and E.S. Hodge, "The Compaction of Powders by Isostatic Pressure","Mechanical Behaviour of Materials under Pressure" ed. Pugh H. Li.D., Elsevier, London, (1970),p.613.

47. Private Communication, Autoclave Engineers Inc., Box 4007 - Erie, Pa., U.S.A.

48. I.K. Bloor, R.D. Brett, and P. Popper, "Isostatic Pressing of Articles from Powders, with Particular Reference to Tooling Design and Behaviour", Proc. 1st. Int. Conf. on The Compaction and Consolidation of Particular Matter, Brighton, England, (1972), p.251.

49.   R.L. Hewitt, "The Isostatic Compaction and Hydrostatic Extrusion of Some Metal Powders", Ph.D. Thesis, McMaster University, (1973).

50.   I.L. Roikh, N.A. Litovchenko, S.G. Belitskaya, L.G. Engorova, and A.S. Sakhiev, "Application of the Scanning Electron Microscope in the Examination of Powders", Poroshkovaya Metallurgiya, Vol. (118), (1972), p.6.

51.   W. Hofmann, "Lead and Lead Alloys Properties and Technology", London, (1970), p.197.

52.   F.V. Warnock and P.P. Benham, "Mechanics of Solids and Strength of Materials", Pitman Paperbacks, London, (1967), p.455.

53.   "Carboloy Grades/Properties Handbook", General Electric, U.S.A., (1970).

54.   I.M. Fedorchenko, R.A. Kovynev, and O.F. Polukhin, Poroshkovaya Metallurgiya, No.11, (1968).

55.   P.J. James, "Fundamental Aspects of the Consolidation of Powders", Powder Metallurgy International, Vol. (4), (1972), p.145.

56.   Technical Data, Atlas Selectalloy Steels, Atlas Steel Company, Ontario, p.27.

57.   J.S. Hirschorn and M.W. Gray, International Journal of Powder Metallurgy, Vol. (1), (1969), p.35.

58.   M.F. Burr and M.J. Donachie, "Effects of Pressing on Metal Powders", Trans. ASM., Vol. (56), (1963), p.863.

59.   "Alcoa Aluminum Powder and Pigments Review", Aluminum Company of America, Review No.6, Pittsburgh, (1971), p.5.

60.   "AMAX Metal Powders Laboratory Data Sheet", Niagara Falls, (1975).

61.   "Metal Powder Quality Control Data Sheet", The Canada Metal Company Limited, Oakville, Ontario, (1975).